universität wien

MASTERARBEIT / MASTER'S THESIS

Titel der Masterarbeit / Title of the Master's Thesis

„The kinetic isotope effect in the hydroamination reaction“

verfasst von / submitted by

Alexandra Dworzak, BSc

angestrebter akademischer Grad / in partial fulfilment of the requirements for the degree of

Master of Science (MSc)

Wien, 2018 / Vienna 2018

Studienkennzahl lt. Studienblatt / degree programme code as it appears on the student record sheet:	A 066 862
Studienrichtung lt. Studienblatt / degree programme as it appears on the student record sheet:	Masterstudium Chemie (Chemistry)
Betreut von / Supervisor:	Univ.-Prof. Dr. Kai Carsten Hultzsch
Mitbetreut von / Co-Supervisor:	

Table of contents

1. Abstract (deutsch)

Die Arbeit hatte zum Ziel einen Einblick in den Reaktionsmechansimus sowohl der (intramolekularen) Hydroaminierung als auch der (intramolekularen) Hydroaminierung-Carbocyclisierung zu geben.
Um dies zu bewerkstelligen wurde der kinetische Isotopeneffekt genutzt.

Die Reaktionen von sekundären Aminen (*N*-methylpent-4-en-1-amin (**3**), *N*-benzylpent-4-en-1-amin (**4**), *N*-allylpent-4-en-1-amine (**5**) sowie *N*,2,2-trimethylpent-4-en-1-amin (**6**)) und den korrespondierenden am Stickstoff deuterierten Substrate mit den Katalysatoren $Cp^*_2SmCH(TMS)_2$ (**1**) und BINO-TPS-Y(BDMA*)* (**2**) wurden untersucht.

Die Reaktionen wurden im NMR – Maßstab durchgeführt und mittels NMR Spektroskopie untersucht. Ferrocen wurde als interner Standard verwendet. Aus den durch diese Messungen erhaltenen Daten wurden die Reaktionsgeschwindigkeiten und der kinetische Isotopeneffekt berechnet. Außerdem wurden noch Vergleiche zwischen den zwei Katalysatoren angestellt und für *N*-methylpent-4-en-1-amin (**3**) sowie für *N*-allylpent-4-en-1-amin (**5**) die Aktivierungsparameter bestimmt.

Ein Vorschlag für die Mechanismen dieser Reaktionen wurde aus den erhaltenen Daten sowie vorherigen Studien für die Hydroaminierung sowie die Hydroaminierung-Carbocyclisierung erstellt.

2. Abstract

The aim of the work was to gain insight into the mechanism of the reaction of the (intramolecular) hydroamination as well as the (intramolecular) hydroamination/carbocyclization, utilizing the kinetic isotope effect.

The reaction of secondary amines as well as the corresponding *N*-deuterated secondary amines (*N*-methylpent-4-en-1-amine (**3**), *N*-benzylpent-4-en-1-amine (**4**)**,** *N*-allylpent-4-en-1-amine (**5**), as well as *N*,2,2-trimethylpent-4-en-1-amine (**6**)) were studied using $Cp^*_2SmCH(TMS)_2$ (**1**) and BINO-TPS-Y(BDMA) (**2**) as catalyst.

The reactions were performed on an NMR-scale and monitored by NMR-spectroscopy using ferrocene as internal standard. From these measurements the reaction rates and the kinetic isotope effects were calculated.
Furthermore, a comparison of the two catalysts was performed and the activation parameters were obtained for *N*-methylpent-4-en-1-amine (**3**) as well as for *N*-allylpent-4-en-1-amine (**5**).

A suggestion for the reaction mechanism is given, using this data and prior studies of the hydroamination as well as the hydroamination/carbocyclization.

3. Abbreviations

BINO-TPS-Y(BDMA)	bis(2-((dimethylamino)methyl)phenyl)bis((3-(triphenylsilyl) naphthalen-2-yl)oxy)yttrium
BINO-TPS	triphenylsilyl-binaphthol
cat.	catalyst
Cp^*_2	bis(pentamethylcyclopentadienyl)
$Cp^*_2NdCH(TMS)_2$	bis(trimethylsilyl)methyl)bis(1,2,3,4,5-pentamethylcyclopenta-2,4-dien-1-yl)neodymium
$Cp^*_2SmCH(TMS)_2$	bis(trimethylsilyl)methyl)bis(1,2,3,4,5-pentamethylcyclopenta-2,4-dien-1-yl)samarium
h	Planck constant, $6.626\ 10^{-34}$ J s
k	reaction constant
k_b	Boltzmann constant, $1.381\ 10^{-23}$ J K^{-1}
k_D	reaction constant of deuterated reactions
k_H	reaction constant of non-deuterated reactions
k_{obs}	observed reaction constant
KIE	kinetic isotope effect
Ln	lanthanides; mostly La, Nd, Sm, Y, Lu
m_r	reduced mass
NMR	nuclear magnetic resonance
N_t	turn over frequency
R	gas constant, 8.314 J K^{-1} mol^{-1}
RDS	rate-determining step
subst.	substrate
T	temperature
TS	transition state
$Y(BDMA)_3$	tris[N,N-(dimethylbenzyl)amine]yttrium
$\Delta H^‡$	activation enthalpy
$\Delta S^‡$	activation entropy

4. Theoretical Background

4.1 Kinetic isotope effect (KIE)

There are many ways in physical organic chemistry to reveal the mechanism of an organic reaction, e.g. crossover experiments or isotope labelling. Because of the increasing interest in organometallic reactions, these tools have also been applied in the studies for reaction mechanisms in organometallic reactions.[1]

One of these tools is the so called kinetic isotope effect. The difficulty in the studies of organometallic reactions is, that the steps are often fast and complex and the rate-determining step (RDS) is not always easily found. Although isotope labelling and crossover experiments are essential devices in physical organic chemistry, they are of little use in this specific problem.

However, the KIE is useful in the clarification of certain reaction mechanisms in organometallic chemistry. Through the KIE it can be determined if the RDS contains breaking, forming or rehybridizing of a specific bond and a proposed mechanism can be confirmed or declined.

To measure the KIE an atom of the substrate is replaced by an isotope. In most of the cases the replaced atom is hydrogen and the used isotope is deuterium. Isotope effects with other elements can also be obtained, but they are smaller than the H/D KIEs and more difficult to measure.[1]

This can be explained through the origin of the KIEs, which can be found in the difference of zero-point energies between X – H and X – D bonds. This difference comes from the different stretching bond vibrations of the isomers.

The stretching vibration of a bond is related to the reduced mass (m_r) of the participating atoms, as shown in equation 1.[1]

$$\nu = \frac{1}{2\pi}\sqrt{\frac{k}{m_r}} \text{ with } m_r = \frac{m_1 * m_2}{m_1 + m_2}$$

Equation 1 – Stretching vibration frequency

$$e_n = \left(n + \frac{1}{2}\right) hv$$

$$with\ n = 0\ for\ the\ zero\ point\ energies$$

Equation 2 – Energy dependency of stretching frequency

Since the zero point energies – as well as all energies – are depend on the stretching frequency – as shown in Equation 2 – they are in relation to the reduced mass.
This connection can be seen in the Morse potential shown in Figure 1.

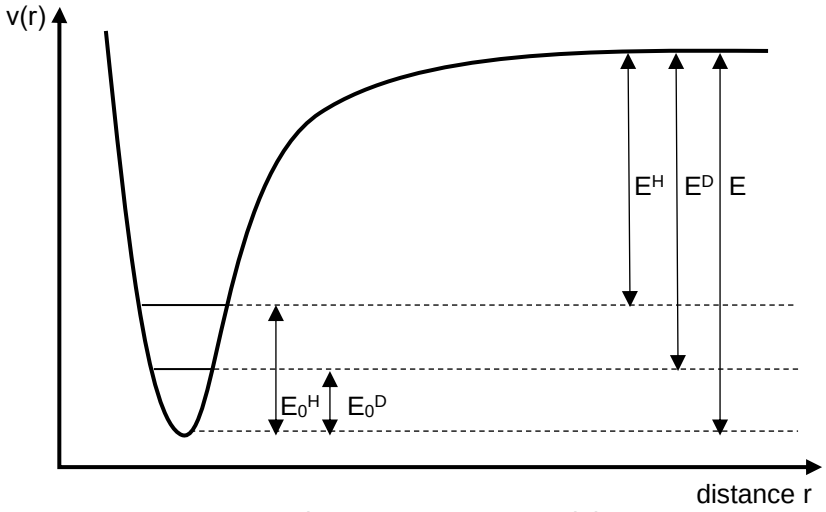

Figure 1 – Morse potential

In Table 1 the reduced masses of some example bonds are shown. The ratio of the reduced masses between C – D/C – H bonds is 1.86, the ratio between N – D/N – H bonds is even a little bit higher with 1.88, whereas the ratio between ^{13}C – H/^{12}C – H and the one between ^{15}N – H/^{14}N – H bonds is below 1.01.
Therefore, the difference in the zero-point energies is higher between hydrogen and deuterium as it is between any other atom and one of its isotopes.

Table 1 – Calculated examples of reduced masses

	C-H	**C-D**	**N-H**	**N-D**	**^{12}C-H**	**^{13}C-H**	**^{14}N -H**	**^{15}N-H**
m_r	0.923	1.715	0.933	1.750	0.930	0.935	0.940	0.945

Since the zero-point energy of a C – H bond is higher than the one of a C – D bond, the activation energy that is needed to break the C – H bond is lower, as Figure 1 shows.

The KIE of a reaction is determined from the difference in the reaction constants k_H and k_D. k_H/k_D of 1 would mean, that there is no isotope effect and therefore, no change in the X – H/X – D bond – where X is C or N – within the RDS.
When the X – H/X – D bond is broken in the RDS a k_H/k_D value >> 1 would be obtained (primary KIE). In the example of the C – H/C – D bond the k_H/k_D ratio of a complete cleavage of the bond would lead to a theoretically KIE of 6.5–7. But since in most transition states (TS) the bond is only broken partly, while a new bond is being formed, the practically obtained KIEs are somewhere between the theoretically obtained value and 1.

If the bond is not broken, but rather there is a change in the hybridization between the substrate and the TS, the value of the KIE is either between 1.1 and 1.2 (normal KIE) or between 0.8 and 0.9 (inverse KIE). The inverse KIE can for example be obtained if there is a change from a C-atom with sp^2-hybridization to the much stiffer C-atom with sp^3-hybridization.[1]

4.2 Hydroamination reactions

Nitrogen containing compounds are of significant importance in biological systems and therefore of relevance in the synthesis of pharmaceuticals and pesticides.
An approach to synthesize these compounds is the catalytic hydroamination – the addition of primary or secondary amino functionalities to unsaturated carbon–carbon bonds. These reactions can be performed either intra- (Equation 3) or inter-molecular (Equation 4), but in both cases in a waste free manner from rather simple starting materials.[2,3,4,5]

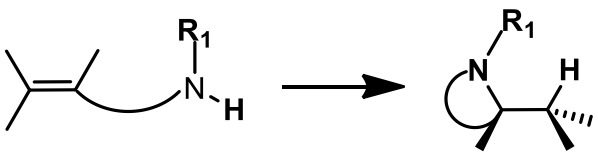

Equation 3 – Intramolecular hydroamination

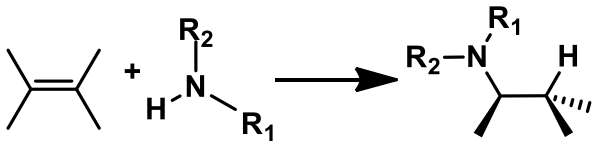

Equation 4 – Intermolecular hydroamination

Until now there have been different catalyst systems found for this reaction – based on either alkali, alkaline earth or transition metals.
However, many of these catalytic systems can only be used with activated alkenes and alkynes as well as with certain types of amines. In spite of this rare earth metal catalyst are reactive towards simple substrates.[2]
Such catalysts – using lanthanides (Ln = La, Nd, Sm, Y, Lu) as metal centre – have been first reported by Marks *et al.* in 1989. They were found as an alternative to the industrial-scale synthesis of alkylamines which were accomplished by the dehydration of alcohols in the presence of amines or other alternative reactions.[6]

Marks *et al*. also studied the kinetics of the reaction to look into its mechanism. These studies showed, that in the case of the intramolecular reaction of 5-pentenamine the 5-exo product is favoured over the 6-endo product and exclusively formed. Thus they proposed a four centred ring in the transition state for the insertion/cyclization step of the catalytic cycle (**III** in Scheme 1).

A general mechanism of this catalytic cycle is shown in Scheme 1. The first step of the reaction is the ligand substitution of an alkyl or amido ligand of the precatalyst against the amine (**I**) leading to (**II**). A rapid proton transfer from the amine (**I**) to the alkyl/amido ligand takes place *via* a four-centered protonolysis transition state. Afterwards the insertion/cyclization step *via* the four-centered transition state (**III**) gives compound (**IV**). Then another ligand substitution *via* protonolysis takes place where the product (**V**) is substituted by another substrate. Since the protonolysis steps have been found to proceed rapidly (within a few seconds), the rate determining step was thought to be the insertion/cyclization step of the catalytic cycle.

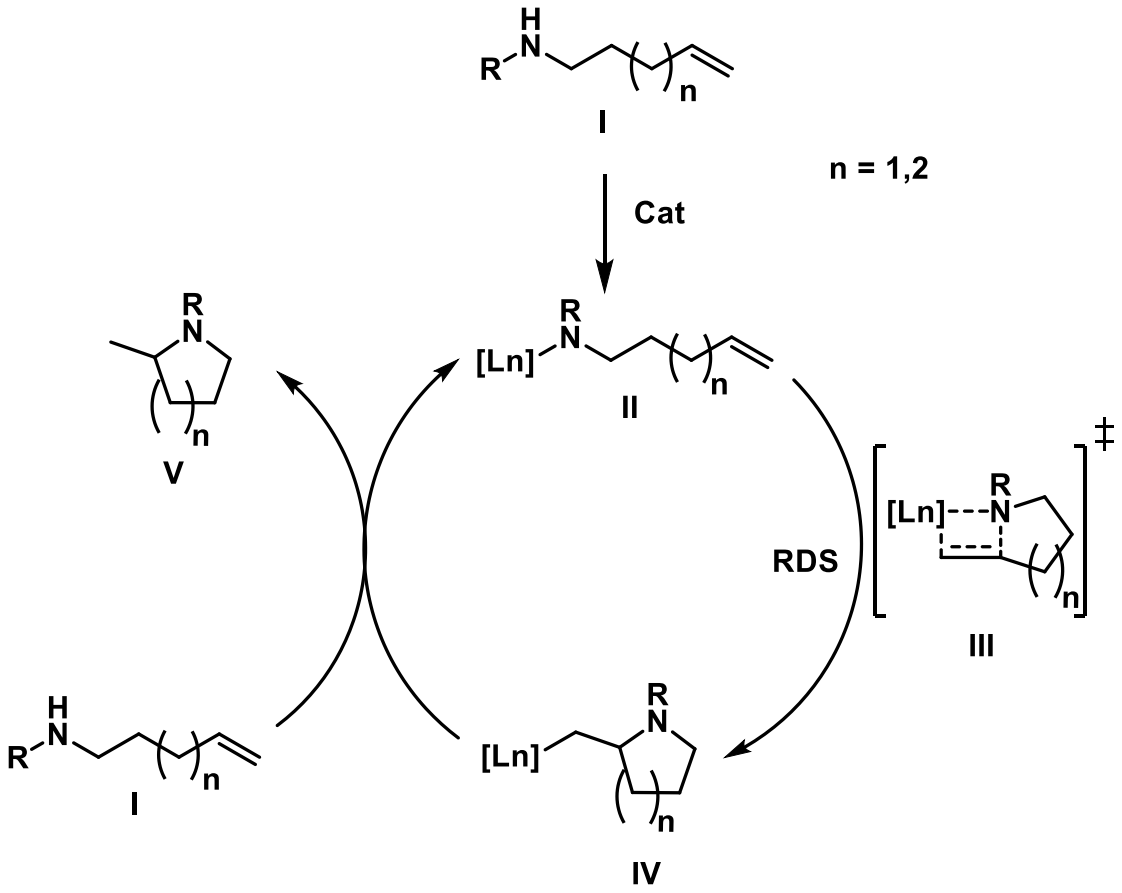

Scheme 1 – Proposed mechanism of intramolecular hydroamination

Marks *et al.* found that the shown mechanism, with the insertion/cyclization step as rate determining step seemed to be in agreement with the measured kinetic data. Furthermore, the mechanism was analysed by a computational study, which confirmed, that the cyclization step is the RDS.[6,7]

The group of Marks also looked into the kinetic isotope effect of the reaction. These investigations showed rather high KIEs for various reactions that suggested a primary effect. The KIEs were investigated for the cyclization reactions of 1-aminopent-4-ene (k_H/k_D = 2.7), 2-aminohex-5-ene (k_H/k_D = 5.2) and 2,2-dimethyl-1-aminopent-4-ene (k_H/k_D = 4.1). Therefore, a N – H bond must be broken or formed within the rate determining step. A concerted mechanism, which includes another amine that is coordinated to the metal center and delivers the proton for the hydroamination (Scheme 2) could explain the primary kinetic isotope effect.[6]

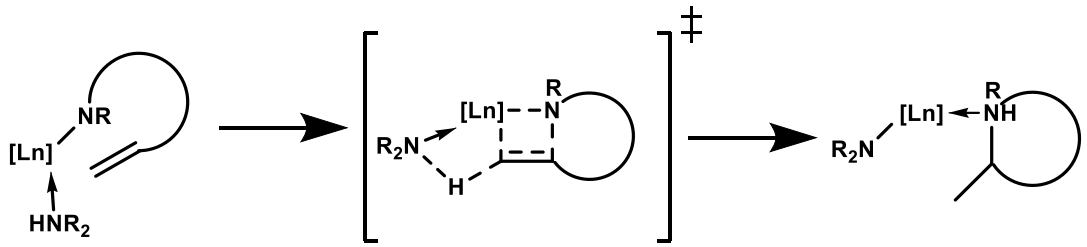

Scheme 2 – Possible source of the N – H/N – D – kinetic isotope effect

A primary KIE that indicates a similar mechanism than the one shown in Scheme 2 has not only been found for achiral catalyst systems in the studies of Marks et al. in 1992. A KIE of k_H/k_D = 4.2 is reported at 40°C by Hultzsch *et al.* for chiral binapthol systems.[2] This indicates that the chiral catalysts follow a similar concerted mechanism as the suggested one.

Similar concerted mechanisms have also been found for other catalyst systems. These include catalysts based on zirconium, magnesium or yttrium. Experimental studies for concerted C-N/C-H bond formation with zirconium catalysts have been made by Sadow *et al.* as well as Schafer *et al.*.[8–10] Furthermore Sadow *et al*. also did studies on this concerted mechanism with yttrium and magnesium catalysts.[11,12] These experimental studies have been supplemented by computational studies by Sven Tobisch.[13–17]

4.3 Hydroamination/carbocyclization reactions

Beside the hydroamination to form carbon–nitrogen bonds, also the formation of carbon–carbon bonds *via* catalytic reactions is of great interest. It has been shown, that lanthanide – alkyl and – heteroatom bonds can undergo insertion with unsaturated carbon – carbon bonds in the right chemical environment. This environment is provided by a catalyst with bis(pentamethylcyclopentadienyl) (=Cp^*_2) ligands, e.g. the ones shown in Equation 5.[4,18]

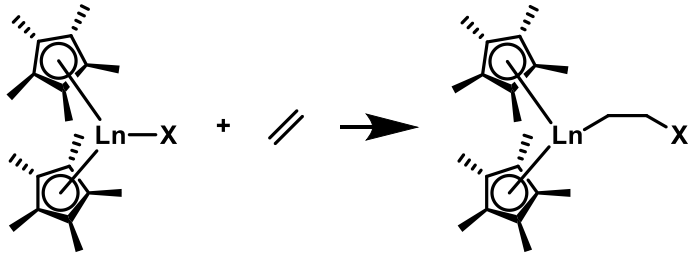

X = alkyl, NR_2, PR_2, SR, OR (for alkynes)

Equation 5 - Scheme of olefine insertion

Therefore, these types of catalysts can be used to achieve olefin insertion instead of the protonolysis after the hydroamination step, achieving additional C – C bond formation. Tandem reactions of C – N and C – C forming processes have been established through the usage of lanthanide-catalysts.
Sequential hydroamination/carbocyclization can be used to synthesize polycyclic, heteroatom skeletons, e.g. pyrroles, pyrolizidines, indolizidines and pyrazines, as well as polycyclic aromatic nitrogen heterocycles, like the quinolizine ring system.[19–21]

Marks *et al.* furthermore suggested the mechanism for the intramolecular hydroamination/carbocyclization shown in Scheme 3, with the insertion of an unsaturated carbon-carbon bond in the Ln – N bond being the rate determining step. This insertion seems to set the overall rate of the bicyclization and is followed by the more rapid insertion of an unsaturated carbon–carbon bond in the resulting Ln – C bond and therefore the second ring closure.[19]

Similar to the hydroamination, the first step of the reaction is the ligand substitution via protonolysis. First the migratory insertion of one olefin in the Ln–amide bond takes place to give species (**IX**). Then another migratory insertion/cyclization step takes place in the carbocyclization part of the reaction, which yields species (**XI**). Protonolysis by the substrate completes the catalytic cycle and gives the product (**XII**).

This proposed mechanism of the hydroamination/carbocyclization however is in contradiction to the former mentioned possible source of the kinetic isotope effect (Scheme 2), because then the catalytic cycle would have to include only the hydroamination step.

Therefore, it wouldn't be possible to explain a potential KIE in the hydroamination/carbocyclization in the same way.

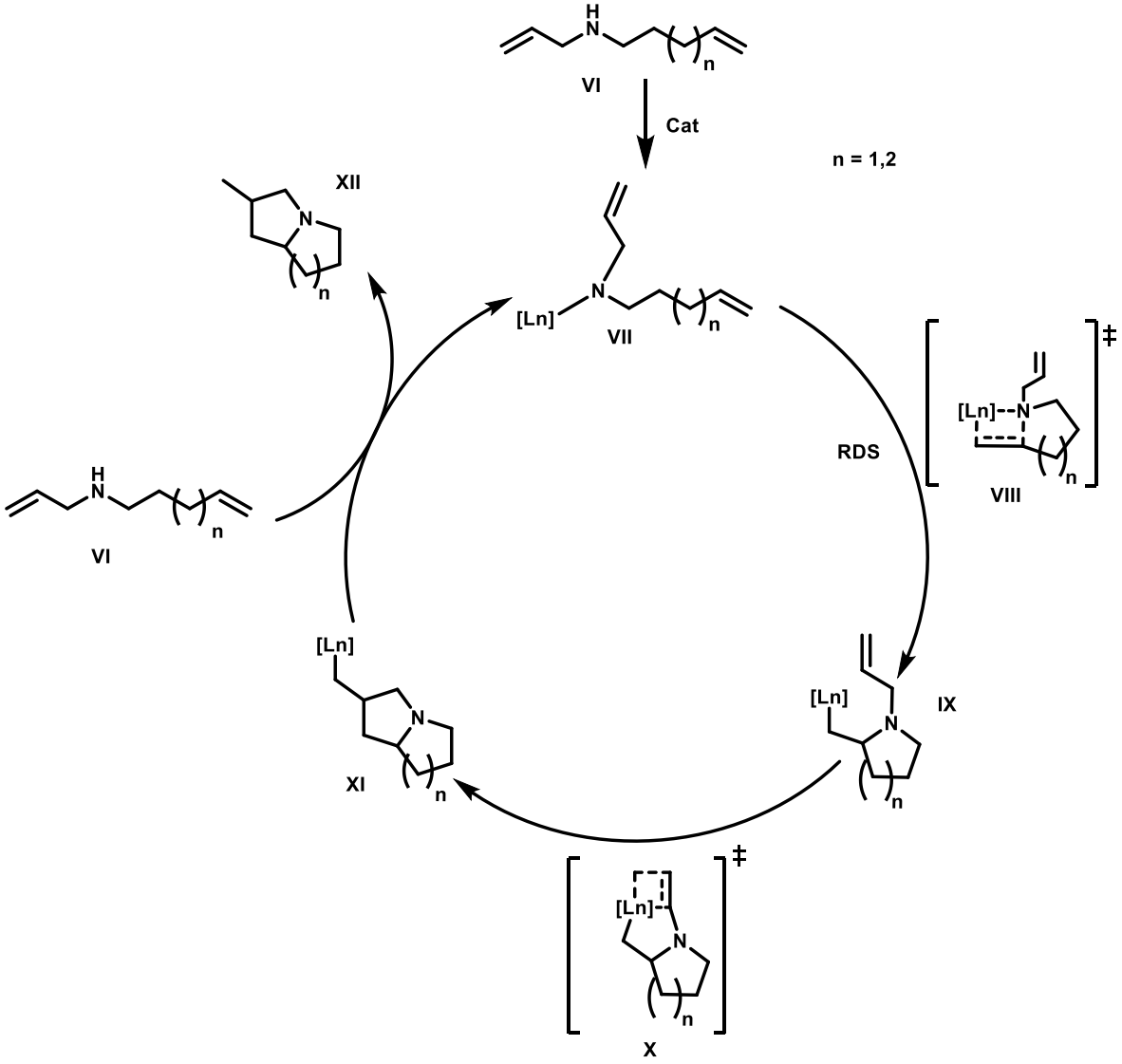

Scheme 3 – Proposed mechanism of the intramolecular hydroamination/carbocyclization

There is an intermolecular reaction as well as an intramolecular one. It is possible to synthesize five-five and six-five membered rings through the intramolecular reaction; the second ring closure only undergoes a five or six-membered cyclization with significant yield. If the second ring would be bigger, the ring closure is sterically less favoured and therefore not as rapid, as the competitive Ln – C bond protonolysis.[19]

Molander *et al.* have found that catalyst with different lanthanide metals prefer to form different ring sizes.[21] The $Cp^*_2NdCH(TMS)_2$ precatalyst is more reactive for the formation of 6-membered rings as they can be found in the quinolizidine ring system (Equation 6), than the corresponding samarium catalyst.

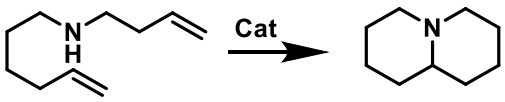

Equation 6 – Exemplary formation of a quinolizidine ring system

On the other hand, the samarium – catalyst proceeds the formation of 5-membered pyrrolizidine systems, which can be seen in Equation 7, faster than the neodymium catalyst.

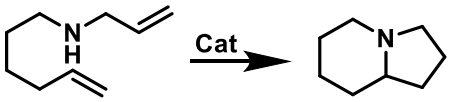

Equation 7 – Exemplary formation of a pyrrolizidine ring system

An explanation for this might be found in the ionic radius of the catalysts. The neodymium catalyst has a larger ionic radius (1.109 Å) than the samarium catalyst (1.079 Å) and therefore favours the formation of the larger six membered rings.[6,21]

5 Objectives

The Objectives of this study is to verify the proposed mechanism of the hydroamination as well as the proposed mechanism of the hydroamination carbocyclization. In order to do this, the kinetic isotope effect of both the hydroamination and the hydroamination carbocyclization reactions should be determined for some substrates. Furthermore the activation parameters for both reactions should be determined and compared to literature results.

The obtained information should be compared to the proposed mechanism of the reactions and if necessary the mechanism should be revised.

6 Results and Discussion

Lanthanide-based complexes have successfully been utilized as catalysts for the hydroamination.[3,4,6,18,20] Since the $Cp^*_2SmCH(TMS)_2$ (**1**) precatalyst – which is shown in Figure 2 – also readily undergoes hydroamination/carbocyclization reactions, that gain five-five membered – pyrrolizidine like – rings, this was the catalyst of choice for the kinetic examinations.[6,21]

For comparison an yttrium-precatalyst with a triphenylsilyl binaphtholate-ligand (BINO-TPS-Y(BDMA) (**2**)), that was reported earlier by Hultzsch *et al.* was used.[2]

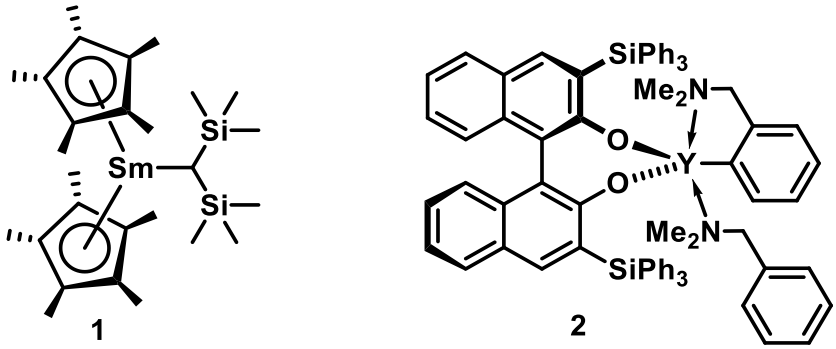

*Figure 2 – $Cp^*_2SmCH(TMS)_2$ **(1)** and BINO-TPS-Y(BDMA) **(2)** precatalyst*

6.1 Substrate Synthesis

Table 2 – General table for the synthesis of pent-4-en-1-amine substrates

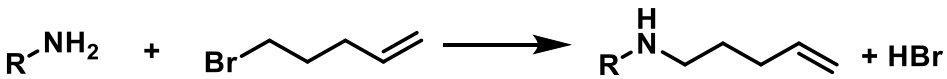

R	solvent	cat.	T [°C]	time [h]	yield %	product
CH_3	EtOH	NaI	60°C	15h	50	**3**
CH_2Ph	EtOH	NaI	75°C	15h	60	**4**
$CH_2CH{=}CH_2$	–	–	70°C	4d	58	**5**

The synthesis of ***N*-methylpent-4-en-1-amine** (**3**) gave the best yield, when it was performed according to the literature procedure.[22] The progress of the reaction could be seen in a colour shift from a very light yellow to orange. The general conditions for the reaction are shown in Table 2. The methylamine was used as an aqueous solution and in 10 times excess. It was also tried to use less excess (2 times) of Methylamine,

but this led to *N*-methyldipent-4-en-1-amine and only little of the desired *N*-methylpent-4-en-1-amine.

Like the other reactions, the synthesis of ***N*-benzylpent-4-en-1-amine** (**4**) was performed after the literature procedure.[22] During the reaction the solution turned yellow. After the first distillation there was still ethanol in the product. Therefore, another fractionary distillation was done to obtain a pure product.

The synthesis of ***N*-allylpent-4-en-1-amine** (**5**) was performed according to the literature procedure according to conditions shown in Table 2.[19] In contrast to the other two reactions neither a solvent nor a catalyst was used for this reaction. The reaction was performed in a pressure tube. Similar to the other reactions the colour of the solution turned orange during the progress of the reaction.

In all three of the S_N reactions HBr protonates the more basic products rather than the amine substrates.

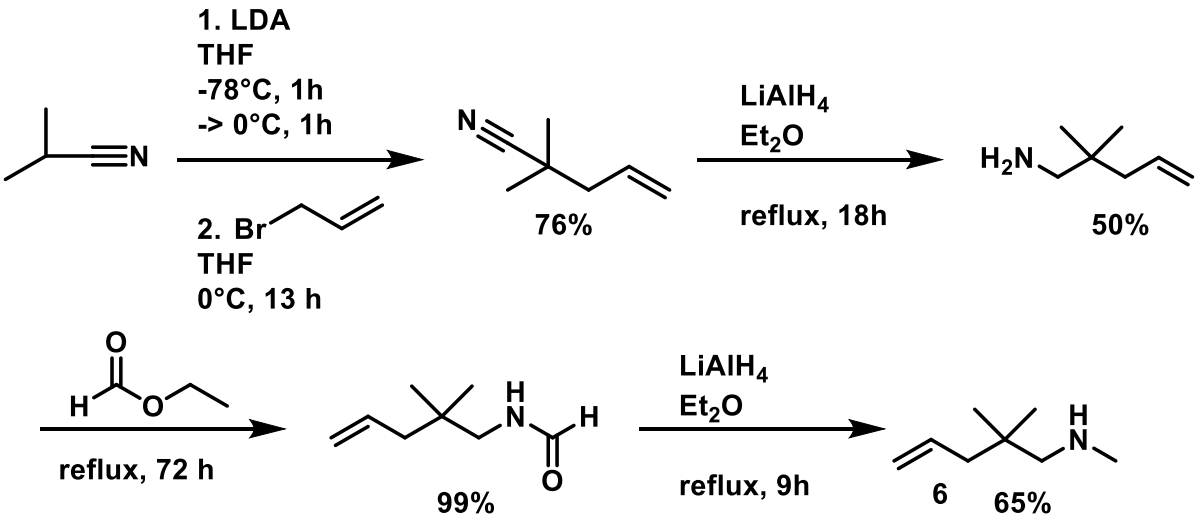

*Scheme 4 – Reaction scheme for the syntheis of N,2,2-trimethylpent-4-en-1-amine (**6**)*

The synthesis of ***N*,2,2-trimethylpent-4-en-1-amine** (**6**) – shown in Scheme 4 – was performed according to the literature procedure.[23,24]

Since the first crude NMR spectrum of the reddish 2,2-dimethylpent-4-enenitrile showed that still some of the solvent and some impurities remained, the mixture was again dissolved in Et_2O, washed another time with brine and dried again. After the reaction of 2,2-dimethylpent-4-en-1-amine with ethylformate and the following removal

of the excess ethylformate, an NMR spectrum was recorded, which showed that there was approximately a third of the initial unreacted starting material left. Therefore, ethylformate was added again and the reaction was set to reflux for two more days. Both reductions with $LiAlH_4$ were performed without any remarkable difficulties.

Table 3 – Deuteration of pent-4-en-1-amines

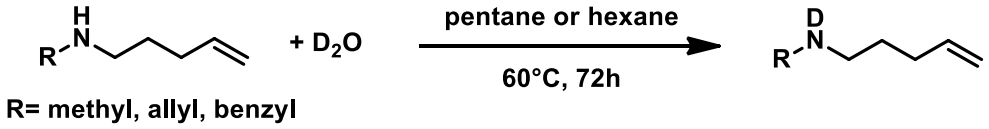

R= methyl, allyl, benzyl

R	solvent	product	yield %
CH_3	pentane	**3-*d***	14
CH_2Ph	hexane	**4-*d***	67
$CH_2CH=CH_2$	hexane	**5-*d***	67

The N-deuteration of the amine substrates was performed according to a literature procedure for related aminoalkene substrates, the general condition for these reactions are provided in Table 3.[25]

In the first attempt the reaction of N-methylpent-4-en-1-amine (**3**) was performed in a normal flask with hexane as solvent. But because of the rather low boiling point (108.3 ± 9.0°C – distillation at 75°C at 350 mbar), some of the product was lost while removing the solvent by rotary evaporation. Therefore, pentane was used as solvent at the next attempt to obtain more of the product. Since the boiling point of pentane at room pressure is 36°C and therefore far below the temperature used as reaction condition, the reaction was carried out in a pressure tube, to prevent the solvent from completely vaporizing.

Since the pressure tube proved to be a good choice as a flask – preventing the solvent as well as the substrate from boiling of – the reactions of N-benzylpent-4-en-1-amine (**4**) and of N-allylpent-4-en-1-amine (**5**) were both carried out in such flasks. Both reactions used hexane as solvent.

6.2 Catalyst synthesis

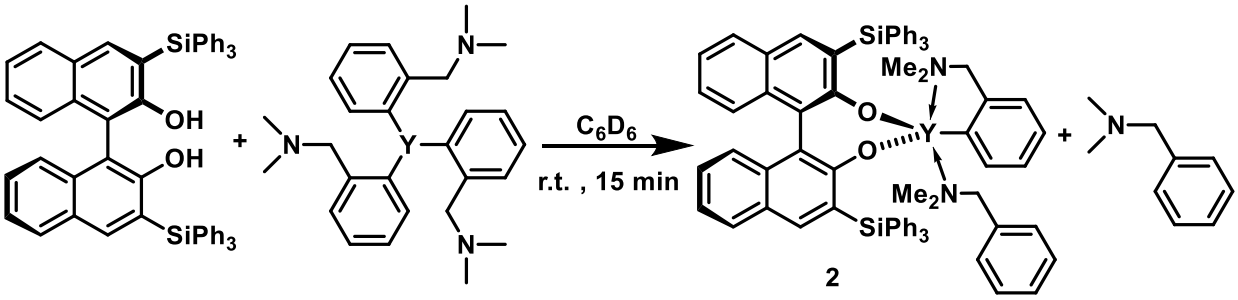

Equation 8 – Synthesis of BINO-TPS-Y(BDMA)

The BINO-TPS-Y(BDMA) **(2)** precatalyst was obtained from the already synthesized triphenylsilyl-binaphthol-ligand (BINO-TPS) and tri[N,N-(dimethylbenzyl)amine]yttrium ($Y(BDMA)_3$) in a 1:1 ratio in C_6D_6 at room temperature as shown in Equation 8.

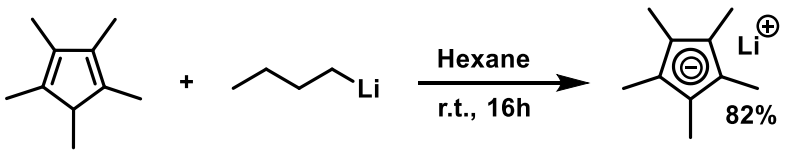

Equation 9 – Synthesis of Cp-Li*

The synthesis of Cp*-Li – shown in Equation 9 - followed the literature procedure.[26] To obtain the product, the solution was washed with hexane and afterwards dried *in vacuo* which led to a white to slightly yellowish powder.

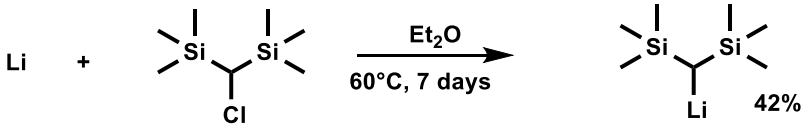

Equation 10 –Synthesis of (bis(trimethylsilyl)methyl)lithium

The synthesis of (bis(trimethylsilyl)methyl)lithium with pure lithium following the literature procedure[27] shown in Equation 10 didn't work every time. Using Li granulate with 0.5% sodium led to a higher yield and a faster reaction, because the sodium impurity activates the lithium.

Synthesis of (bis(trimethylsilyl)methyl)bis(1,2,3,4,5-pentamethylcyclopenta-2,4-dien-1-yl)samarium (Cp*Sm CH(TMS)$_2$) (1)

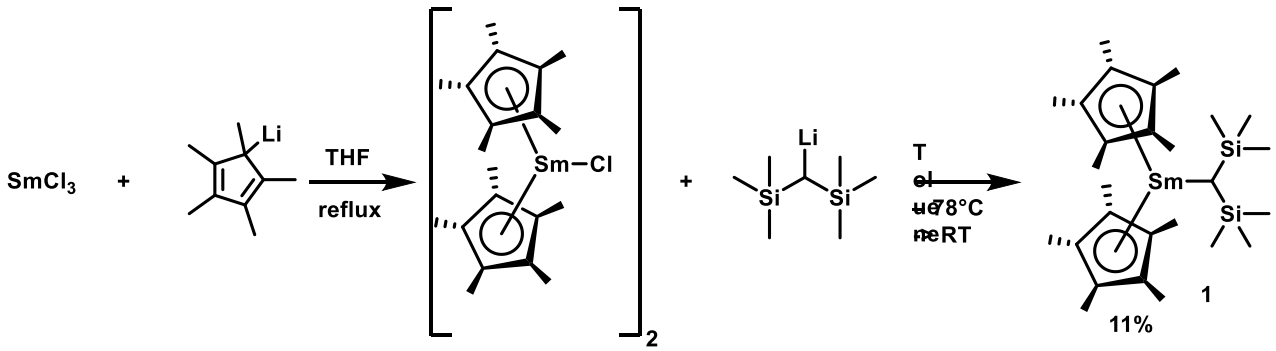

*Scheme 5 – Synthesis of (Cp*SmCH(TMS)$_2$) (**1**)*

The Cp*$_2$SmCH(TMS)$_2$ (**1**) precatalyst was obtained from $SmCl_3$, Cp*-Li and (bis(trimethylsilyl)methyl)lithium, following Scheme 5.[28]
In contrast to the literature procedure the $SmCl_3$ was stirred in THF overnight at room temperature to make sure that the $SmCl_3$ had formed the THF adduct.

6.3 Hydroamination

6.3.1 Reaction kinetics and Activation parameters

Cyclization of N-methylpent-4-en-1-amine (3)

The first reaction that was examined was the intramolecular hydroamination of *N*-methylpent-4-ene-1-amine (**3**) to 1,2-dimethylpyrrolidine (**7**).

As shown in Table 4 the reaction was examined with different substrate to catalyst ratios and for 5 mol% of Cp*$_2$SmCH(TMS)$_2$ (**1**) precatalyst at different temperatures. The reaction was performed on an NMR-scale in deuterated benzene and the reaction control was monitored by ^{1}H-NMR spectroscopy.

The reaction with 3 mol% of catalyst took over 24 hours. The reaction showed only little conversion after 2 hours at room temperature and was then heated to 60°C for 22

hours. The reason for this might be some little impurities in the substrate, which interfere with the reaction if the catalyst concentration is too little.
Therefore, the catalyst concentration was increased to 5 mol%. The reaction at 5 mol% proceeded with a better time range of about 4 hours until complete conversion at room temperature.

*Table 4 – Catalytic hydroamination of N-methylpent-4-en-1-amine (**3**) with an initial substrate concentration of 0.5 mol L^{-1}*

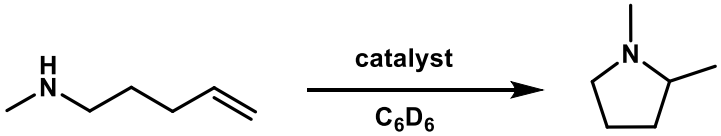

3 **7**

Entry	catalyst	T [°C]	[cat.] [subst.]$^{-1}$ [%]	N_t [h^{-1}]	k_{obs} [mol L^{-1} h^{-1}]
1	**1**	21→60	3	–	–
2	**1**	25	5	5.0 ± 0.1	0.12 ± 0.003
3	**1**	30	5	5.8 ± 0.2	0.15 ± 0.004
4	**1**	40	5	16.1 ± 0.4	0.40 ± 0.010
5	**1**	45	5	21.2 ± 0.5	0.53 ± 0.011
6	**1**	21	10	7.0 ± 0.1	0.35 ± 0.005
7	**2**	21	5	1.2 ± 0.05	0.03 ± 0.001
8	**2**	25	5	1.2 ± 0.005	0.03 ± 0.0001
9	**2**	50	5	10.4 ± 0.2	0.26 ± 0.004

The reaction was monitored *via* ^{1}H–NMR spectroscopy with ferrocene as internal standard. The conversion was measured through the disappearance of the significant signals of the olefinic protons at 5.82 – 5.73 ppm and at 4.99 – 4.89 ppm as well as the appearance of the signal of the methane group of the product at 2.98 – 2.95 ppm – shown in Figure 3.

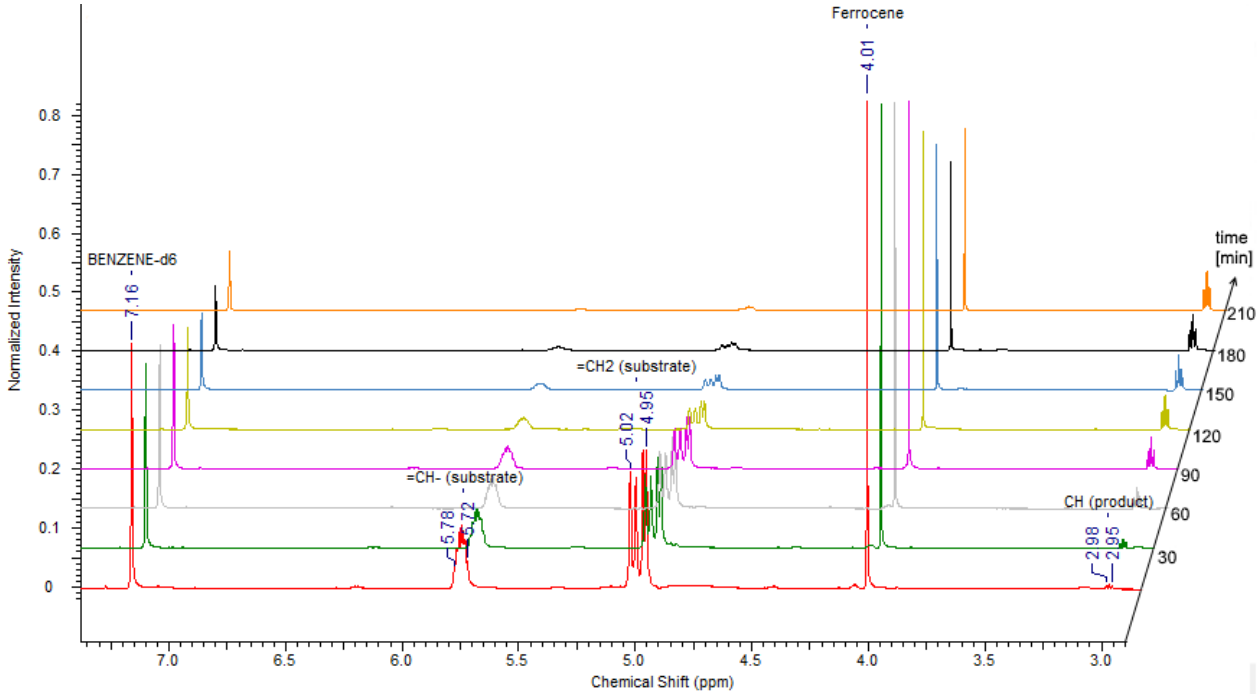

*Figure 3 – ^{1}H - NMR spectra of the samarium-catalyzed cyclization of N-methylpent-4-en-1-amine (**3**) to give 1,2-dimethylpyrrolidine (**7**)*

Through the measurement of the conversion, the concentration of the substrate could be monitored over time and the reaction order determined.

The reaction with 5 mol% of the $Cp^*_2SmCH(TMS)_2$ (**1**) appeared to be zeroth order in substrate until full conversion, shown in Figure 4.

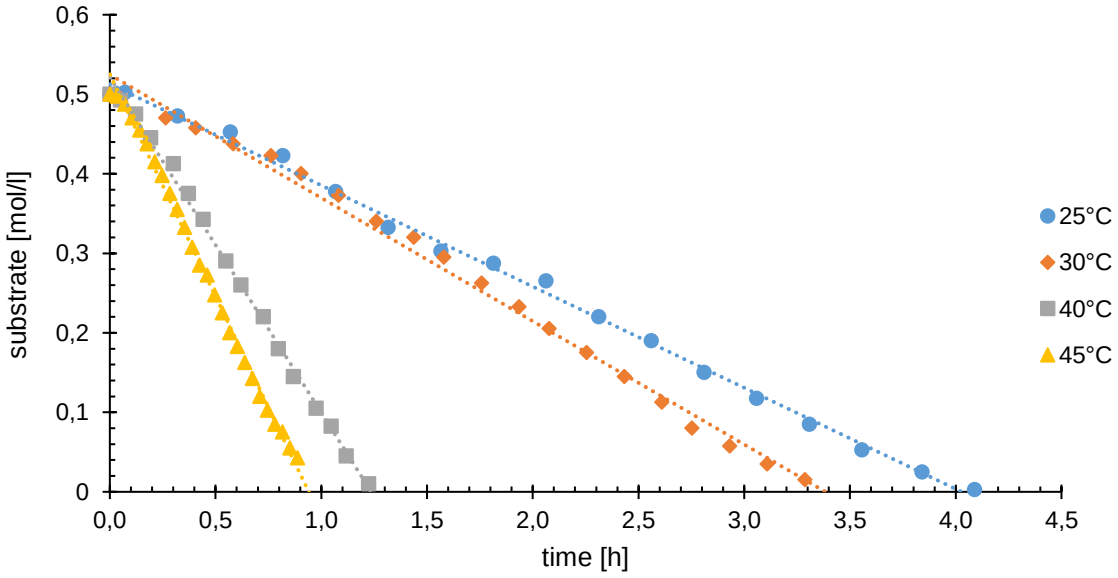

*Figure 4 – Comparison of the time dependence of substrate concentration at different temperatures with 5 mol% of Sm – catalyst (**1**)*

The reaction was performed at different temperatures, showing that the time to full conversion was decreasing with increasing temperature. As can be seen in Figure 4, the time to full conversion at room temperature was approximately 4 hours and at 45°C only one hour.

From this data the turnover frequency N_t (Equation 12) and the reaction rate *r* as well as the observed reaction constant k_{obs} (Equation 11) were calculated and are shown in Table 4.

$$r = \frac{d[subst]}{dt} = -\,k\,[cat]\,[subst.]^0 = -\,k_{obs}\,[subst]^0$$

Equation 11 – Reaction constant

$$N_t = \frac{k_{obs}}{[cat.]} = k$$

Equation 12 – Turn over frequency

The activation entropy $\Delta S^{\ddagger}$ and the activation enthalpy $\Delta H^{\ddagger}$ were obtained from the Eyring plot (Figure 5).

$$\ln\left(\frac{k}{T}\right) = \frac{-\Delta H^{\neq}}{R \times T} + \ln\left(\frac{k_b}{h}\right) + \frac{\Delta S^{\neq}}{R}$$

Equation 13 – Eyring equation

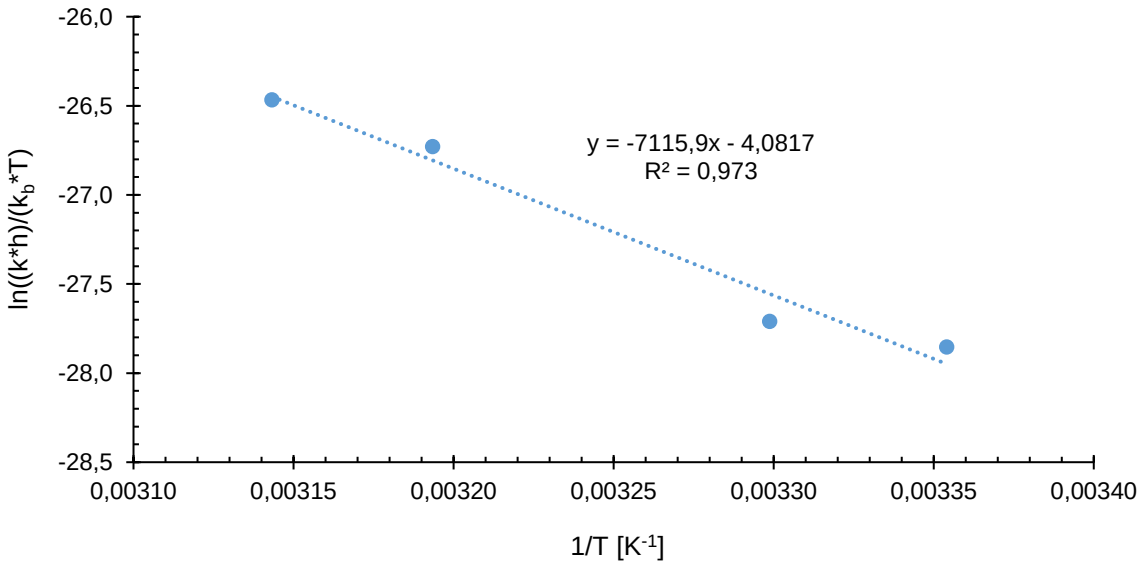

*Figure 5 – Eyring plot for the hydroamination of (**3**) with an initial substrate concentration of 0.5 mol L^{-1} and 5 mol% of Sm – catalyst (**1**)*

The activation parameters could be directly obtained from the Eyring plot shown in Figure 5. The y-intercept is proportional to the entropy (Equation 14) while the incline is in proportion to the enthalpy (Equation 15).

Table 5 – Value and Deviation derived by regression analysis

	Value	Deviation
y-intercept	-4.0817	2.7253
incline	-7115.9	838.96

The activation parameters $\Delta H^{\ddagger} = 59 \pm 7$ kJ mol^{-1} and $\Delta S^{\ddagger} = -34 \pm 23$ J K^{-1} mol^{-1} were obtained from the linear regression of the Eyring plot (Table 5) for 0.5 mol L^{-1} initial substrate concentration and 5 mol% of Cp*$_2$SmCH(TMS)$_2$ (**1**).

$$\ln\left(\frac{k\,h}{k_b\,T}\right) = \frac{\Delta S^{\neq}}{R}$$

Equation 14 – Activation entropy

$$\ln\left(\frac{k\,h}{k_b\,T}\right) T = \frac{\Delta H^{\neq}}{R}$$

Equation 15 – Activation enthalpy

Marks *et al*. reported the activation parameters for the reaction from pent-4-en-1-amine to 2-methylpyrrolidine with Cp*$_2$LaCH(TMS)$_2$. The activation enthalpy $\Delta H^{\ddagger}$ for this reaction was 12.7 ± 1.4 kcal mol^{-1}, which equals approximately 53 ± 6 kJ mol^{-1} and the activation entropy $\Delta S^{\ddagger}$ was –27.0 ± 4.6 eu, which equals approximately –113 ± 19 J K^{-1} mol^{-1}.[6]

Therefore, the enthalpy is in a similar range as the found activation parameters for the reaction from *N*-methylpent-4-en-1-amine to 1,2-dimethylpyrrolidine with Cp*$_2$SmCH(TMS)$_2$ (**1**), whereas the entropy differs from the literature. On the other hand the percentage of the deviation of the entropy is higher (33%) than the one of the enthalpy (11%). Therefore, the entropy seems to be more delicate for uncertainties of measurements and the difference between the literature and the obtained data might result out of these.

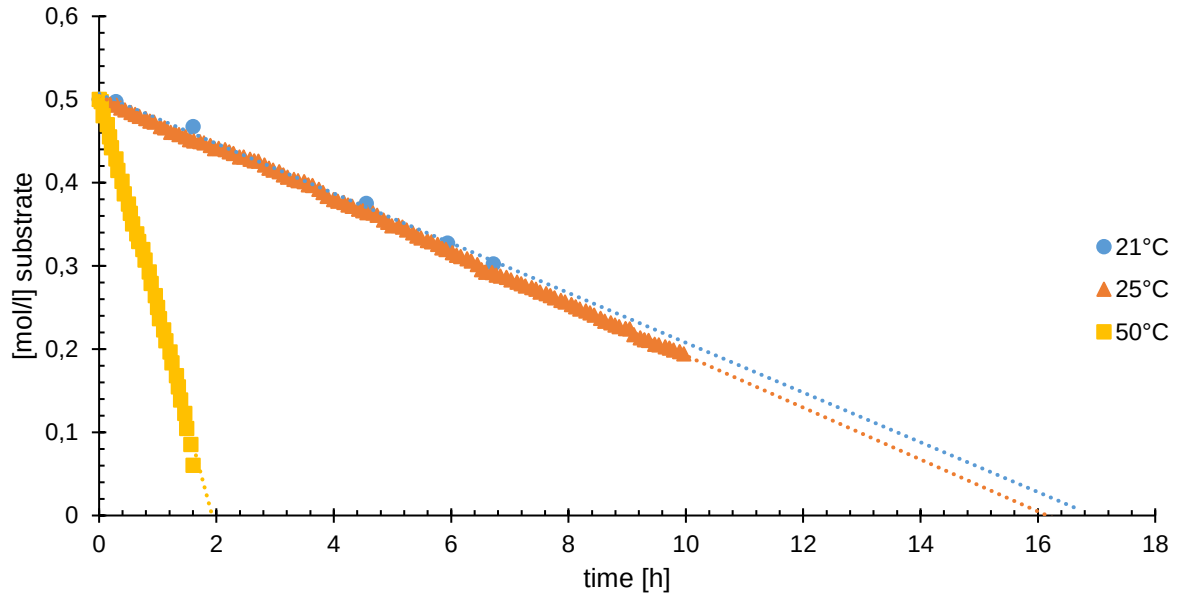

*Figure 6 – Comparison of the time dependence of substrate concentration at different temperatures with 5 mol% of BINO-TPS-Y(BDMA) as catalyst **(2)***

Cyclization of *N*-methylpent-4-ene-1-amine (**3**) was then investigated with the BINO-TPS-Y(BDMA)-catalyst (**2**), as shown in Table 4.

Again, the reaction was carried out at different temperatures. The reaction seemed to be zeroth order in substrate concentration again and the time to full conversion was decreasing with increasing reaction temperature, as shown in Figure 6.

The time to full conversion at 25°C was approximately 16 hours, compared to approximately 2 hours at 50°C.

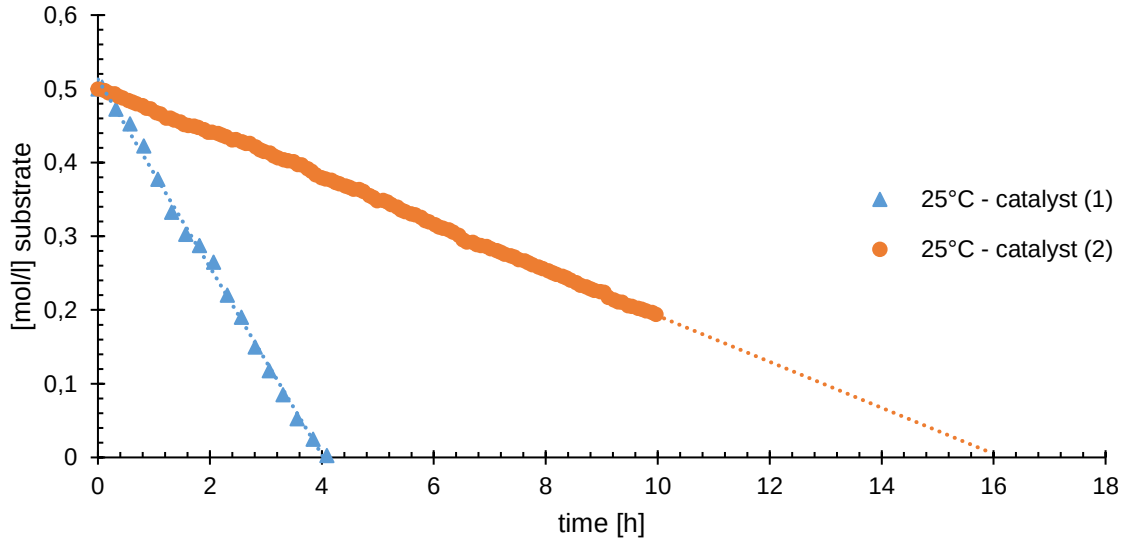

*Figure 7 – Comparison of the time dependence of substrate concentration with either 5 mol% of Sm – catalyst (**1**) or BINO-TPS-Y(BDMA) - catalyst (**2**)*

Furthermore, the reaction was significantly faster with $Cp^*_2SmCH(TMS)_2$ (**1**) than with the BINO-TPS-Y(BDMA)-catalyst (**2**) (Figure 7). This is not so surprising as the larger lanthanides are commonly more reactive in the intramolecular hydroamination reaction.[6]

While the reaction with $Cp^*_2SmCH(TMS)_2$ (**1**) took 4 hours with 5 mol% of catalyst at 25°C, the BINO-TPS-Y(BDMA) complex (**2**) took 16 hours under the same circumstances, as shown in Figure 7. Therefore, the reaction with $Cp^*_2SmCH(TMS)_2$ (**1**) was 4 times faster than the reaction with the BINO-TPS-Y(BDMA)-catalyst (**2**).

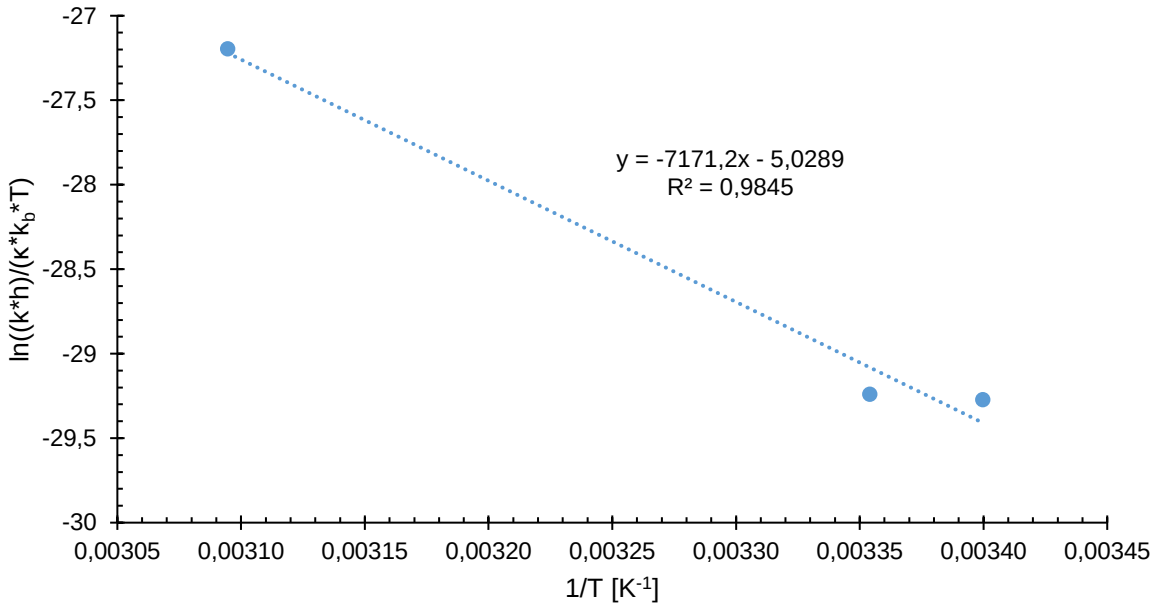

*Figure 8 – Eyring – Plot for the hydroamination of (**3**) with an initial substrate concentration of 0.5 mol L^{-1} and 5 mol% of BINO-TPS-Y(BDMA) – catalyst (**2**)*

The activation enthalpy $\Delta H^{\ddagger}$ and the activation entropy $\Delta S^{\ddagger}$ were obtained from the Eyring plot (Figure 8).

Table 6 – Value and Deviation derived by regression analysis

	Value	Deviation
y-intercept	-5.0289	2.9955
incline	-7171.2	899.43

The activation parameters were determined as $\Delta H^{\ddagger} = 60 \pm 7$ kJ mol^{-1} and $\Delta S^{\ddagger} = -42 \pm 25$ J K^{-1} mol^{-1} for 0,5 mol L^{-1} initial substrate concentration and 5 mol% of the BINO-TPS-Y(BDMA) yttrium (**2**) catalyst.

Prior studies of the Hultzsch group were made concerning the activation parameters for the reaction from pent-4-en-1-amine to 2-methylpyrrolidine with this catalyst.
The activation enthalpy $\Delta H^{\ddagger}$ for this reaction was 57.4 ± 0.8 kJ mol^{-1} for *(S)*-2-methylpyrrolidine and 61.5 ± 0.7 kJ mol^{-1} for *(R)*-2-methylpyrrolidine and the activation entropy $\Delta S^{\ddagger}$ was –102 ± 3 J K^{-1} mol^{-1} for *(S)*-2-methylpyrrolidine and –103 ± 3 J K^{-1} mol^{-1} for *(R)*-2-methylpyrrolidine.[2]
Like before, the activation enthalpy is in a similar range as the activation parameters for the reaction of N-methylpent-4-en-1-amine to 1,2-dimethylpyrrolidine with $Cp^*_2SmCH(TMS)_2$ (**1**), but again the activation entropy differs.

Cyclization of N-Benzylpent-4-en-1-amine (4)

*Table 7 – Catalytic hydroamination of N-benzylpent-4-en-1-amine **(4)** with an initial substrate concentration of 0,5 mol L^{-1}*

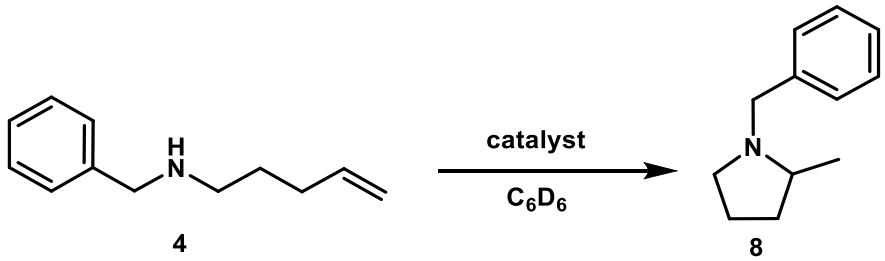

4 **8**

Entry	catalyst	T [°C]	[cat.] [subst.]$^{-1}$ [%]	N_t [h^{-1}]	k_{obs} [mol L^{-1} h^{-1}]
1	**1**	21	10	-	-
2	**1**	150	10	-	-
3	**2**	21	10	5.5 ± 0.7	0.28 ± 0.03
4	**2**	21	5	0.7 ± 0.03[a]	0.04 ± 0.002[a]

[a]*data derived from the linear part of the reaction*

The conversion was measured through the disappearance of the signals of the olefinic protons at 5.77 – 5.67 ppm and at 5.00 – 4.93 ppm as well as the appearance of the signal of the methine group of the product at 3.96 – 3.93 ppm – as can be seen in Figure 9.

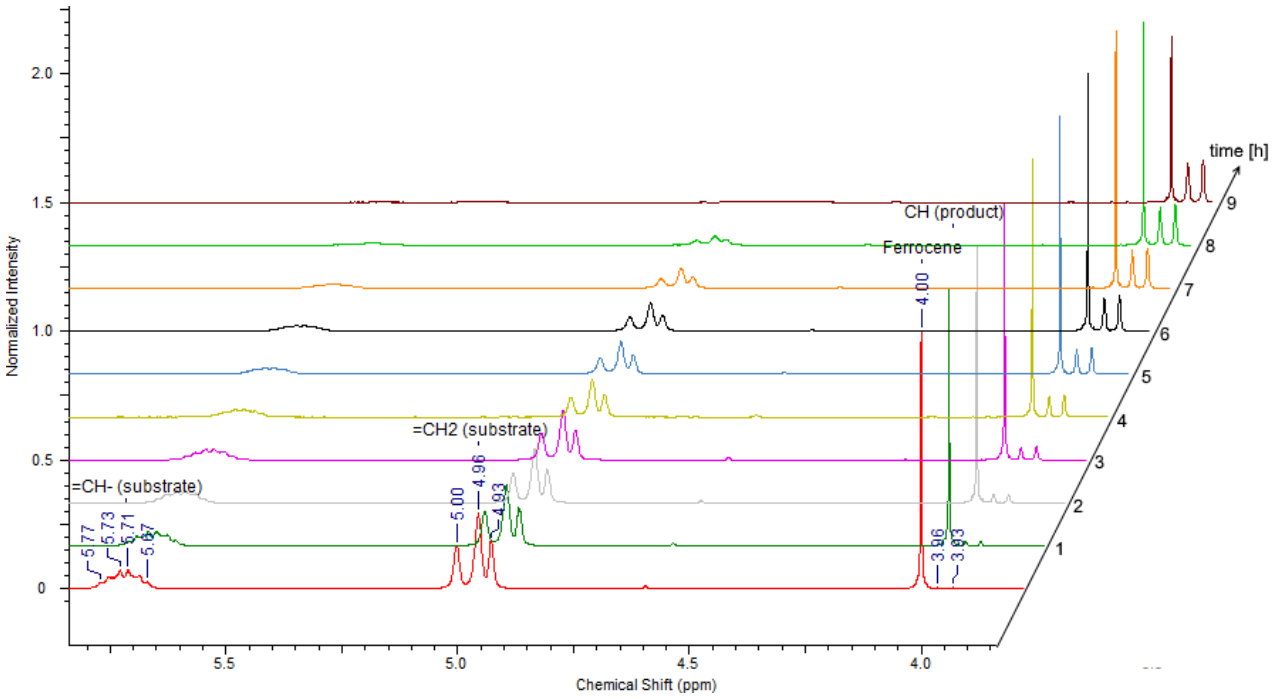

*Figure 9 – ^{1}H - NMR spectra of the samarium-catalyzed cyclization of N-benzylpent-4-en-1-amine (**4**) to give 1-benzyl-2-methylpyrrolidine (**8**)*

The reaction of *N*-benzylpent-4-en-1-amine (**4**) to 1-benzyl-2-methylpyrrolidine (**8**) was unsuccessful with Cp*$_2$SmCH(TMS)$_2$ as precatalyst, as entry 1 and 2 of Table 7 show.

The reaction at 21°C showed not even 10% conversion after 10 hours. The reaction at 150°C started with a rather good reaction rate, but stopped at around 20% conversion, shown in Figure 10.

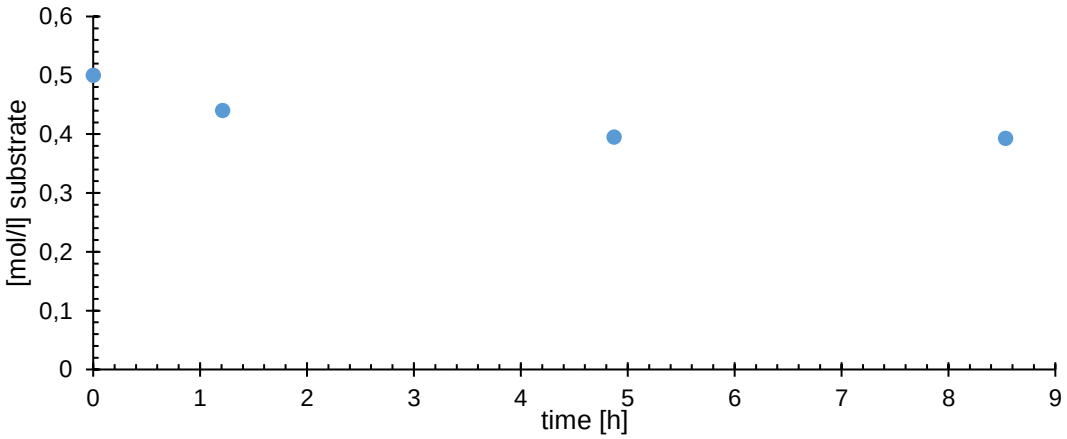

Figure 10 – Time dependence of substrate concentration at 150°C with 10 mol% Cp$_2$SmCH(TMS)$_2$ **(1)***

The reaction with the BINO-TPS-Y(BDMA) (**2**) precatalyst showed a better reaction rate on the other hand. Table 7 and Figure 11 show, that the reaction with 10 mol% catalyst took 1.83 hours at room temperature and a N_t of 5.5 h^{-1} as well as a reaction rate constant of 0.28 mol L^{-1} h^{-1}. Furthermore, the reaction showed a linear dependence between substrate concentration and time and is therefore zeroth order in substrate concentration.

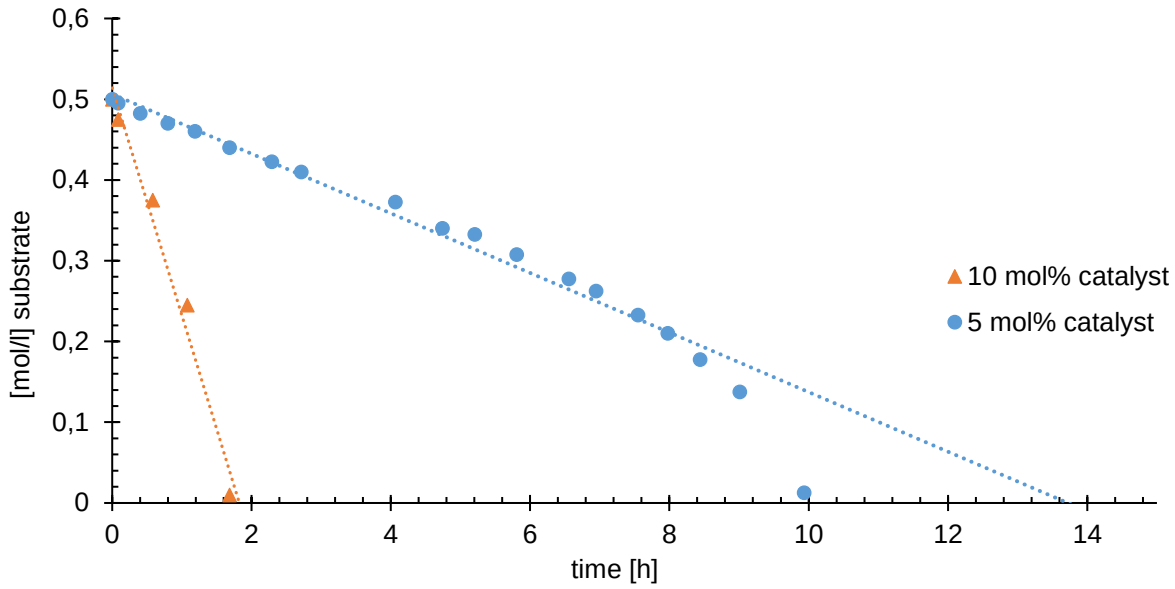

*Figure 11 – Comparison of the time dependence of substrate concentration with different concentrations of BINO-TPS-Y(BDMA) - catalyst (**2**)*

The reaction with 5 mol% of catalyst started with a linear dependency between substrate concentration and time, but around 25% conversion the reaction began to proceed faster. Figure 11 shows, that the reaction was finished after around 10 hours, while it should take 13.72 hours with the initial reaction rate.

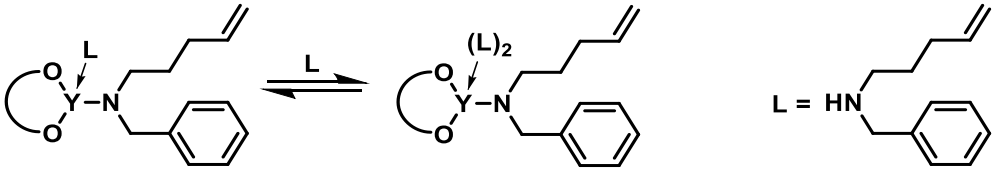

Equation 16 – Equilibrium between active and inactive catalytic species

An explanation for this behaviour was proposed.[2] The catalytic active binaphtholate amido amine species is in equilibrium with an inactive binaptholate amide diamine species shown in Equation 16. During the reaction this equilibrium is shifted to the active species due to the decreasing concentration of the substrate, needed to form the inactive species. Therefore a self-activation takes place during the reaction.[2]

Furthermore, the reaction with 10 mol% of catalyst is approximately 7 times faster than the reaction with 5 mol% of catalyst.

Cyclization of N,2,2-trimethylpent-4-en-1-amine (6)

*Table 8 – Catalytic hydroamination of N,2,2-trimethylpent-4-en-1-amine (**6**) with an initial substrate concentration of 0.5 mol L^{-1}*

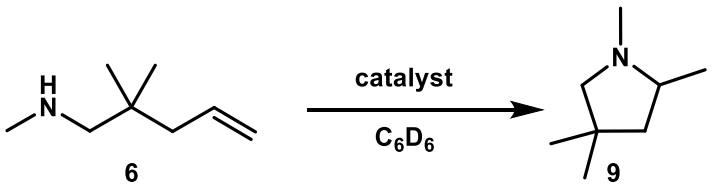

Entry	catalyst	T [°C]	[cat.] [subst.]$^{-1}$ [%]	N_t [h^{-1}]	k_{obs} [mol L^{-1} h^{-1}]
1	**1**	21	5	7.5 ± 0.7	0.19 ± 0.02
2	**2**	21	5	>124	>3.10

The conversion of the reaction of *N*,2,2-trimethylpent-4-en-1-amine (**6**) to 1,2,4,4-Tetramethylpyrrolidine (**9**) was measured through the disappearance of the signals of the olefinic protons at 5.84 – 5.76 ppm and at 5.05 – 5.00 ppm as well as the appearance of the signal of the methine group of the product at 2.70 – 2.68 ppm – as can be seen in Figure 12.

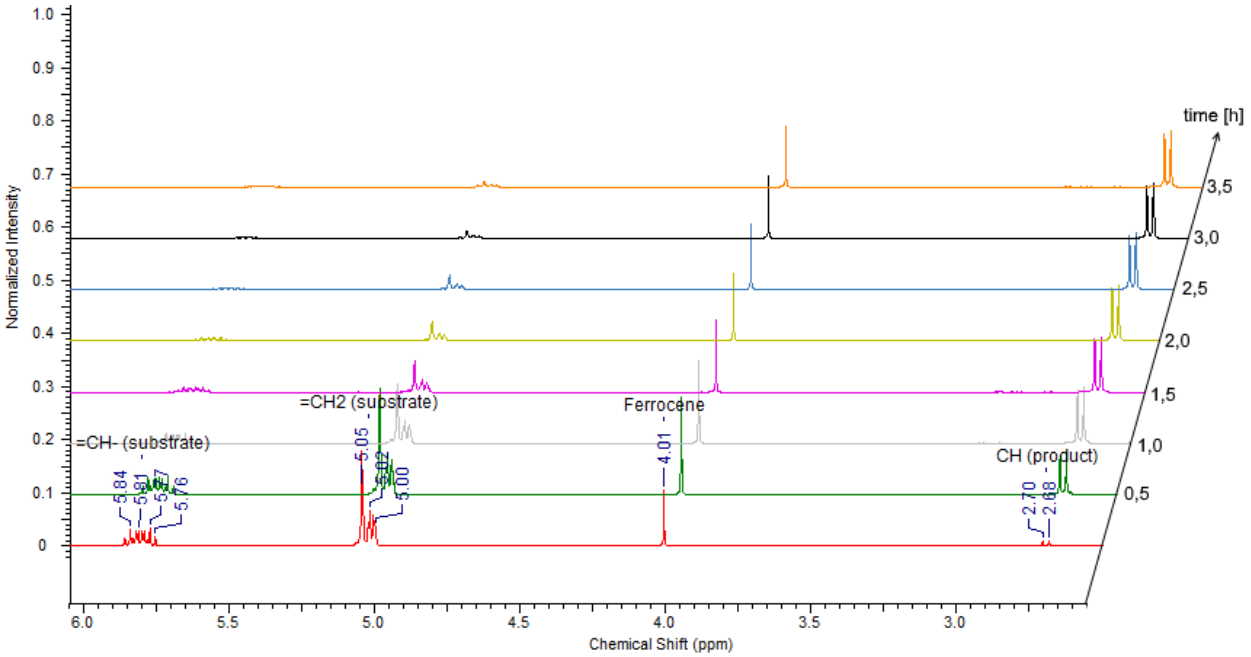

*Figure 12 – ^1H – NMR spectra of the samarium-catalyzed cyclization of N,2,2-trimethylpent-4-en-1-amine (**6**) to give 1,2,4,4-Tetramethylpyrrolidine (**9**)*

The reaction of *N*,2,2-trimethylpent-4-en-1-amine (**6**) with $Cp^*_2SmCH(TMS)_2$ (**1**) showed a linear dependency between substrate concentration and time until 70% conversion, as shown in Figure 13. Afterwards the reaction began to slow down. Reaction time, turnover frequency and reaction rate constant – which are shown in Table 8 – were determined by extrapolation of the linear part of the reaction curve.

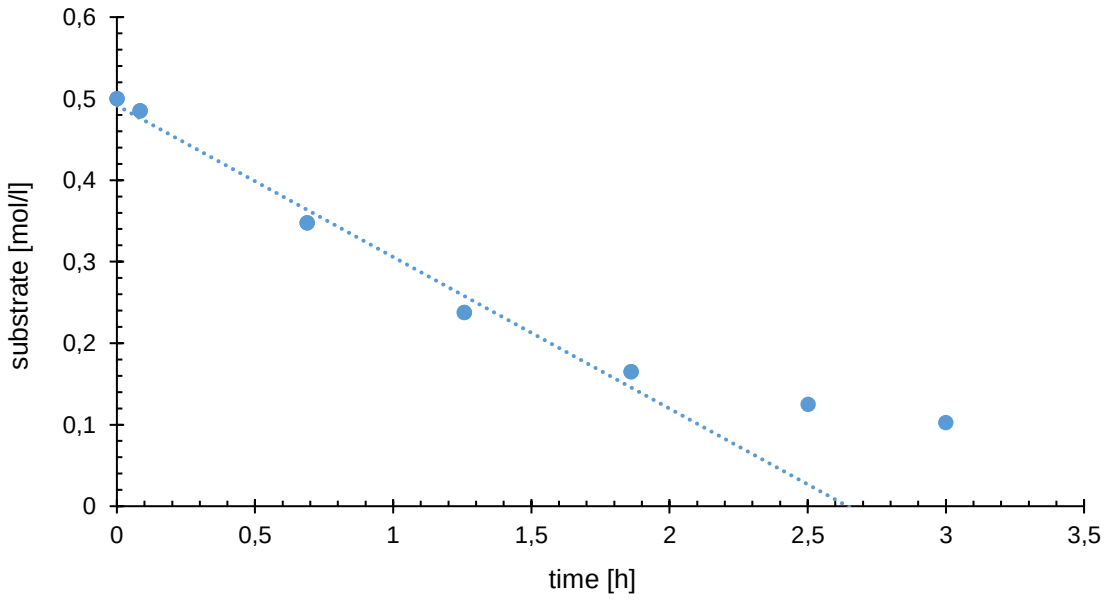

*Figure 13 – Time dependence of substrate (**6**) concentration at 21°C with 5 mol% $Cp^*_2SmCH(TMS)_2$ (**1**)*

The reaction shown in Figure 13 with 5 mol% $Cp^*_2SmCH(TMS)_2$ (**1**) took 2.64 hours and had a N_t of 7.5 h^{-1} and a reaction rate constant of 0.19 mol L^{-1} h^{-1}.
The reaction with 5 mol% BINO-TPS-Y(BDMA) (**2**) catalyst on the other hand was already finished when the first NMR was measured after 0.16 hours and therefore had a turnover rate of over 124 h^{-1} and a reaction rate constant of over 3.10.
Therefore, the reaction with the BINO-TPS-Y(BDMA) (**2**) catalyst was over 16 times faster than the reaction with $Cp^*_2SmCH(TMS)_2$ (**1**) under the same conditions.

Cyclization of N-allylpent-4-en-1-amine (5)

The hydroamination/carbocyclization reaction of N-allylpent-4-en-1-amine (**5**) to 2-methylhexahydro-1H-pyrrolizine (**10**) was attempted first with the BINO-TPS-Y(BDMA) (**2**) precatalyst.
As shown in Table 9 the reaction only undergoes the hydroamination step leading to 1-ally-2-methylpyrrolidine (**11**). It was examined for 5 mol% as well as for 10 mol% of precatalyst at room temperature.

*Table 9 – Catalytic hydroamination of N-allylpent-4-en-1-amine (**13**) with an initial substrate concentration of 0,5 mol L^{-1} and BINO-TPS-Y(BDMA (**2**) – catalyst*

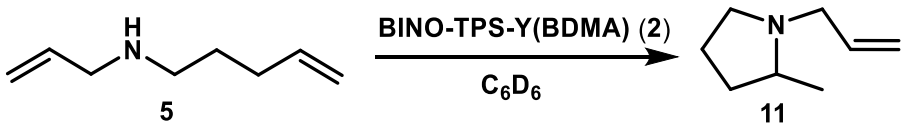

Entry	T [°C]	[cat.] [subst.]$^{-1}$ [%]	N_t [h^{-1}]	k_{obs} [mol L^{-1} h^{-1}]
1	21	5	2.3 ± 0.1	0.06 ± 0.003
2	21	10	4.5 ± 0.3	0.22 ± 0.01

Like the other reactions, this reaction was monitored by ^{1}H–NMR spectroscopy using ferrocene as internal standard, as well. The conversion was measured through the decrease of the signals of the olefinic protons at 5.95 – 5.73 ppm and at 5.20 – 4.94 ppm as well as the appearance of the signal of the methine group of the product at 3.43 – 3.39 ppm – as shown in Figure 14.

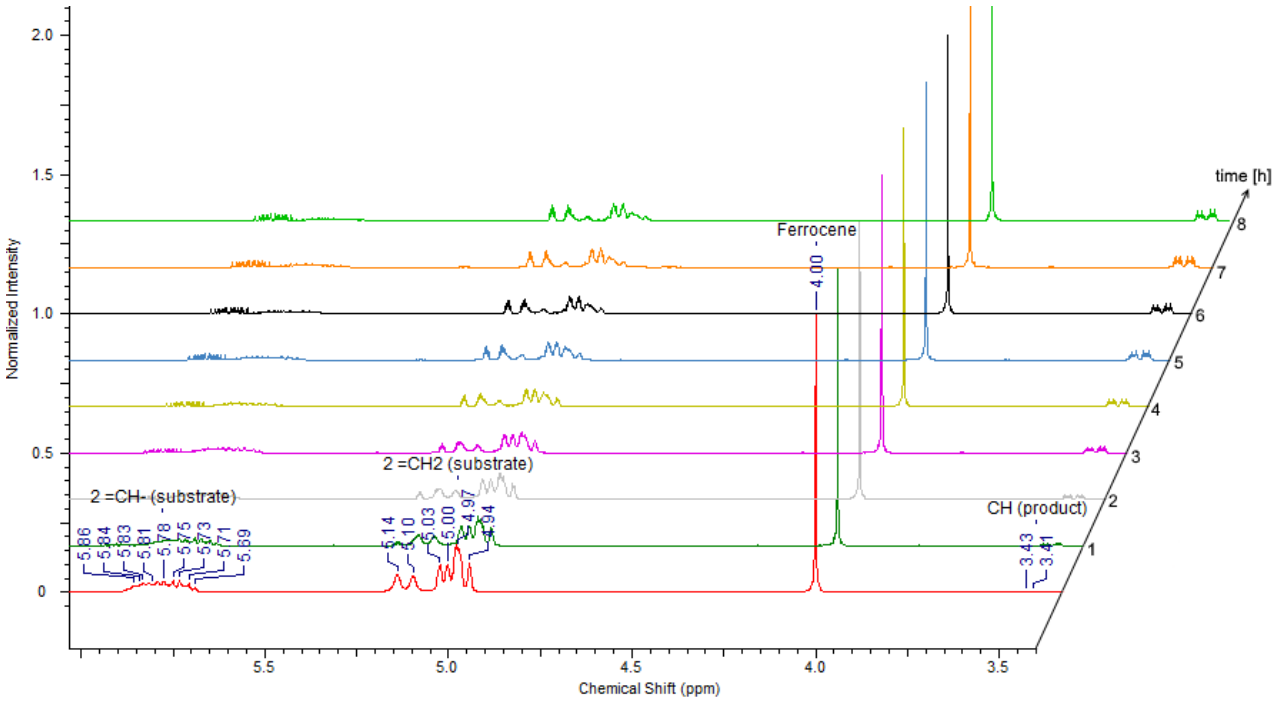

*Figure 14 – ^{1}H - NMR spectra of the yttrium-catalyzed cyclization of N-allylpent-4-en-1-amine (**5**) to give 1-ally-2-methylpyrrolidine (**11**)*

The reaction with 10 mol% of the BINO-TPS-Y(BDMA) (**2**) catalyst appears to be zeroth order in substrate until full conversion. Figure 15 shows that the reaction with 5 mol% of catalyst on the other hand gets slower after around 60% conversion.

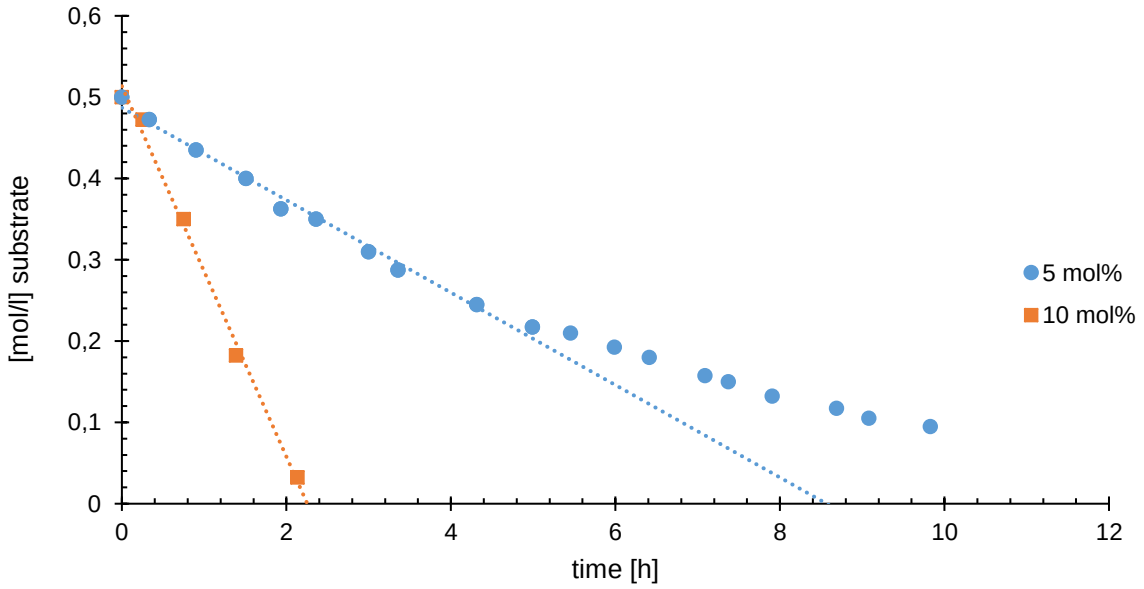

*Figure 15 - Comparison of the time dependence of substrate concentration with different concentrations of BINO-TPS-Y(BDMA) – catalyst (**2**)*

Reaction kinetics and activation parameters - discussion

The kinetic data shows that the reaction of *N*-methylpent-4-en-1-amine **(3)** with 5 mol% of $Cp^*_2SmCH(TMS)_2$ **(1)** appears to be zeroth order in substrate concentration until full conversion at different temperatures.

Marks *et al.* suggested a zeroth order reaction in substrate concentration and a first order reaction in catalyst concentration for lanthanide catalysts with Cp* ligands.[6]
The obtained data seemed to be in agreement with the proposed mechanism of the hydroamination with the RDS being the insertion/cyclization step, as shown in Figure 16.

The reaction of *N*-methylpent-4-en-1-amine (**3**) with the BINO-TPS-Y(BDMA) (**2**) also appeares to be zero order in substrate concentration, being in agreement with the suggested mechanism from Marks *et al.*

Furthermore, the data suggests, that the BINO-TPS-Y(BDMA) catalyst (**2**) proceeds better with sterically more hindered substrates, than $Cp^*_2SmCH(TMS)_2$ (**1**), as can be seen in the reaction of *N*,2,2-trimethylpent-4-en-1-amine (**6**) or the reaction of *N*-benzylpent-4-en-1-amine (**4**)

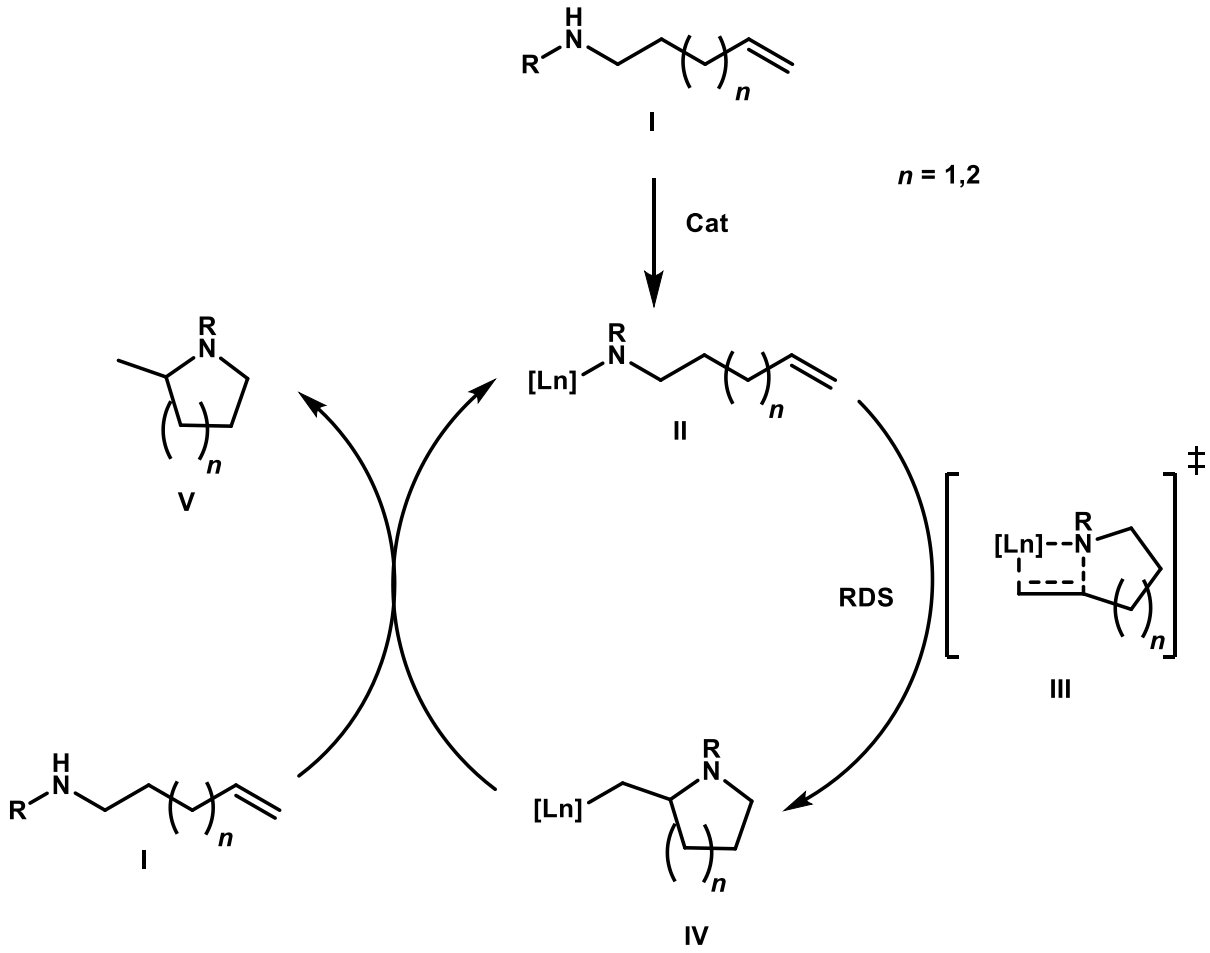

Figure 16 – Proposed mechanism of intramolecular hydroamination

The activation parameters were obtained only for the reaction of *N*-methylpent-4-ene-1-amine **(3).**

For both reactions – with $Cp^*_2SmCH(TMS)_2$ (**1**) and with BINO-TPS-Y(BDMA) yttrium (**2**) as catalyst – the enthalpy was very similar to the enthalpy found in the literature, whereas the entropy differed from the comparison reactions. As stated before, the entropy seems to be more delicate for uncertainties of measurements and the difference between the literature and the obtained data might therefore result out of these.

6.3.2 Kinetic isotope effect

Cyclization of *N*-methylpent-4-en-1-amine-*d* (3-*d*)

*Table 10 – Catalytic hydroamination of N-methylpent-4-en-1-amine-d (**3**-d) with an initial substrate concentration of 0.5 mol L^{-1}*

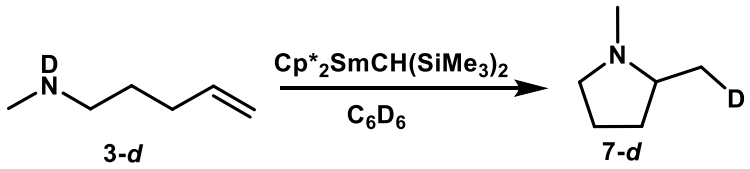

Entry	T [°C]	[cat.] [subst.]$^{-1}$ [%]	N_t [h^{-1}]	k_{obs} [mol L^{-1} h^{-1}]
1	25	5	1.2 ± 0.05	0.03 ± 0.001
2	40	5	5.4 ± 0.42	0.13 ± 0.010
3	60	5	6.6 ± 0.36	0.17 ± 0.009
4	21	10	1.2 ± 0.06	0.06 ± 0.003

The results of the reaction with the *N*-deuterated *N*-methylpent-4-en-1-amine (**3-*d***) are stated in Table 10. The conversion was measured through the same signals as the conversion of the reactions with N-mehtylpent-4-en-1-amine (**3**).

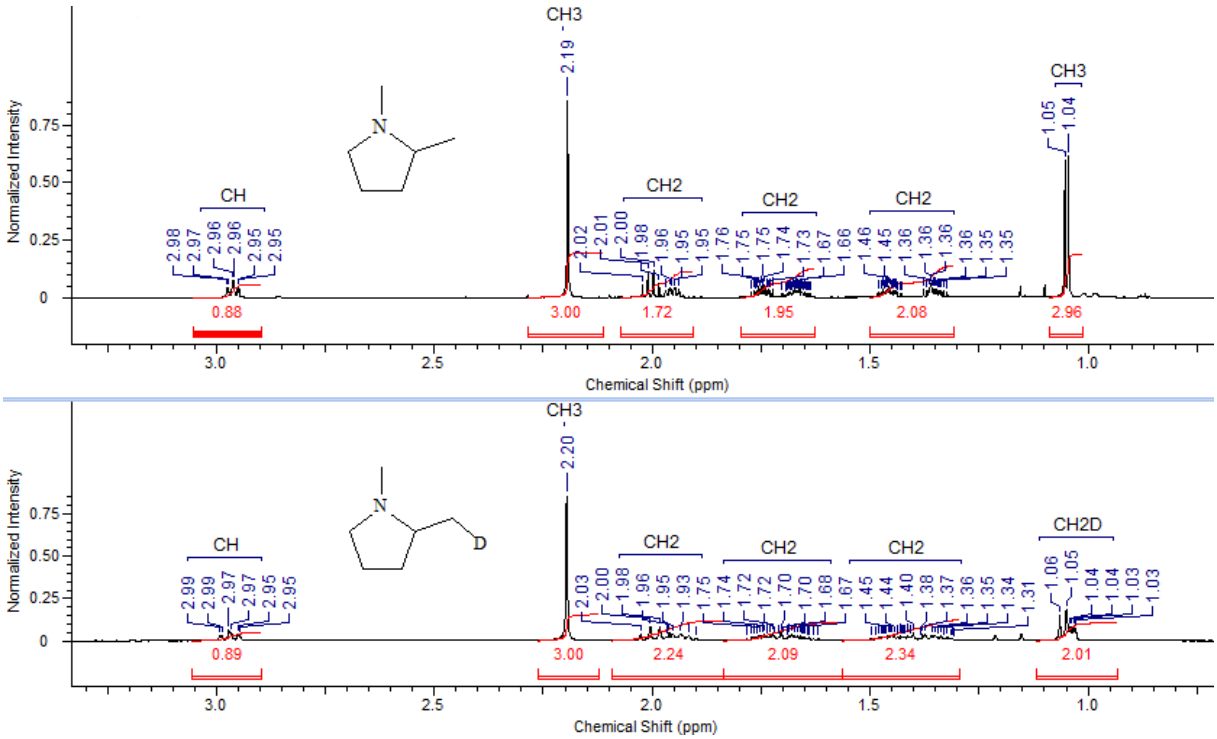

*Figure 17 – ^{1}H-NMR spectra of 1,2-dimethylpyrrolidine (**7**) and 1-methyl-2-(methyl-d)-pyrrolidine (**7-d**)*

Figure 17 and Figure 18 suggest that 1,2-dimethylpyrrolidine (**7**) is mostly – but not thoroughly deuterated at the 2-methyl group, indicating 1-methyl-2-(methyl-d)-pyrrolidine (**7-*d***) as main product of the cyclization of *N*-deutero-*N*-methylpent-4-en-1-amine (**3-*d***).

Whilst the integration of the ^{1}H-NMR spectra of **7** and **7-*d*** indicates, that the deuterium mainly can be found at this group, the $^{13}C\{^{1}H\}$ – NMR spectrum shows four peaks rather than a triplet which indicates a mixture of deuterated and non-deuterated product. Therefore the methyl-group seems to be not completely deuterated. Through integration of the ^{1}H-NMR of the substrate **3-*d*** the amount of not deuterated amine was calculated to approximately 1%.

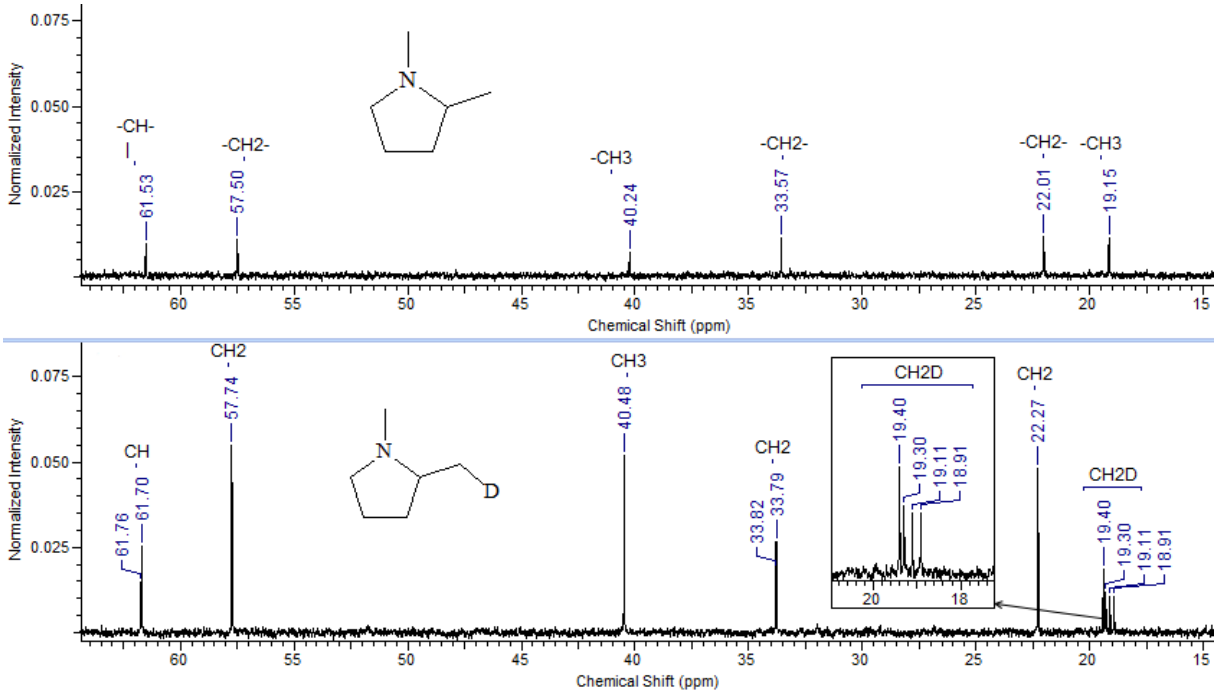

*Figure 18 – $^{13}C\{^{1}H\}$-NMR spectra of 1,2-dimethylpyrrolidine (**7**) and 1-methyl-2-(methyl-d)-pyrrolidine (**7-*d***)*

The reaction with 5 mol% of $Cp^*_2SmCH(TMS)_2$ (**1**) starts zeroth order but gets slower or stops after some time, as Figure 19 shows.

Furthermore, it can be seen, that the slowing in the reaction rate seems to have some kind of temperature dependence since the reaction at 60°C stopped at 30% conversion, whereas the reaction at 40°C proceeded until 60% conversion linearly. The observed reaction constant k_{obs} and the turn over frequency N_t were determined for the linear part of the reaction.

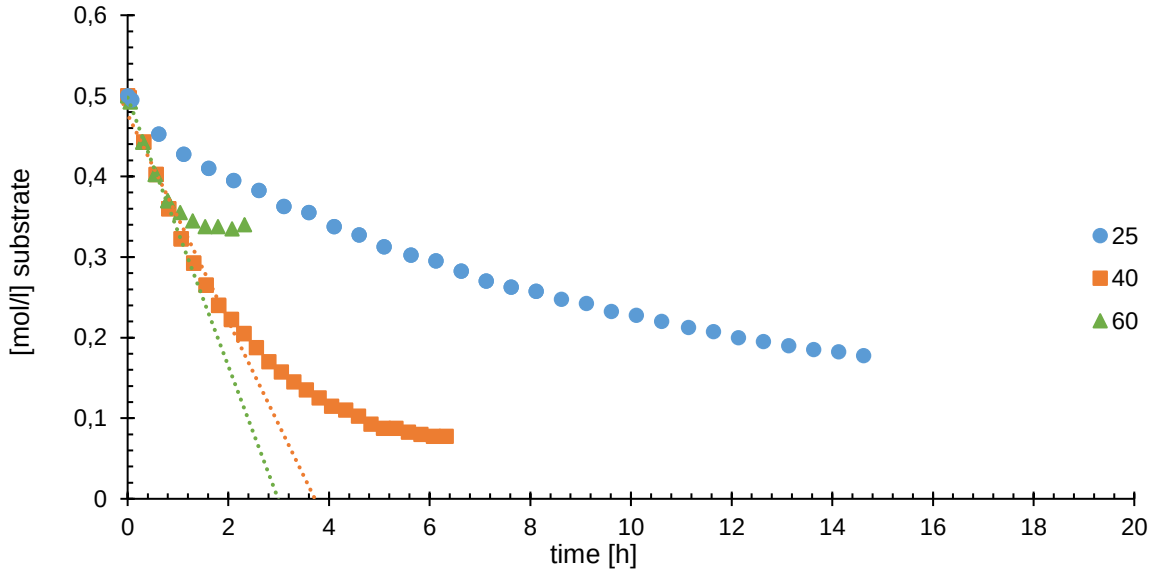

*Figure 19 – Comparison of the time dependence of concentration of **3**-d at different temperatures with 5 mol% of Sm – catalyst (**1**)*

It was also investigated if the reaction was of higher order, but neither the logarithmic first order plot nor a second order plot yielded a linear time dependency. Furthermore, non-deuterated *N*-mehtylpent-4-en-1-amine (**3**) was added to see whether the catalyst was completely quenched.

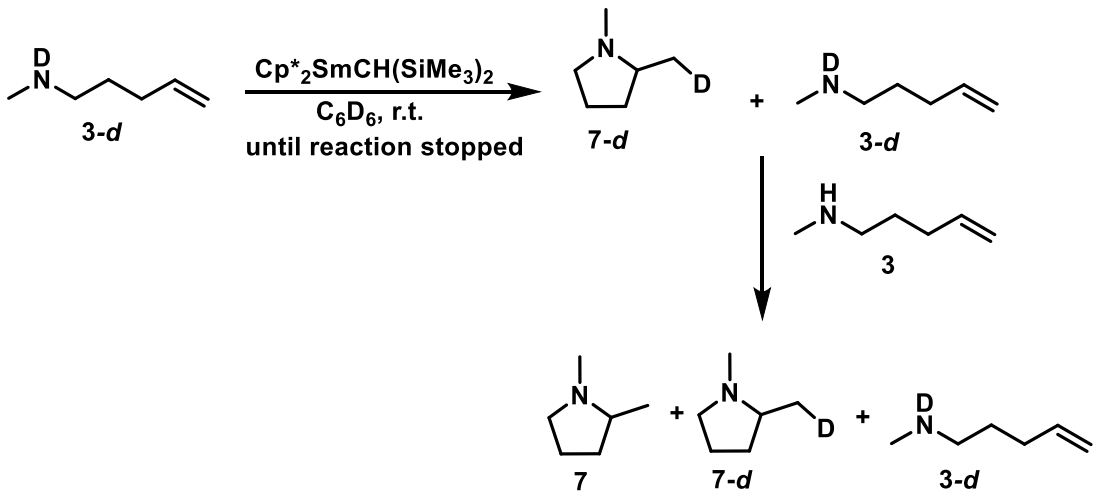

*Scheme 6 – Procedure of the reaction to test whether the catalyst gets completely quenched during the reaction of (**3**-d)*

Said reaction was performed as shown in Scheme 6. First the hydroamination of the deuterated amine (**3-*d***) was performed with 5 mol% of $Cp^*_2SmCH(TMS)_2$ and after the

reaction stopped, 1 equivalent of the non-deuterated amine **3** was added. The non-deuterated amine started to react, therefore the catalyst couldn't have been completely quenched, as can be seen in Figure 20 and Figure 21.

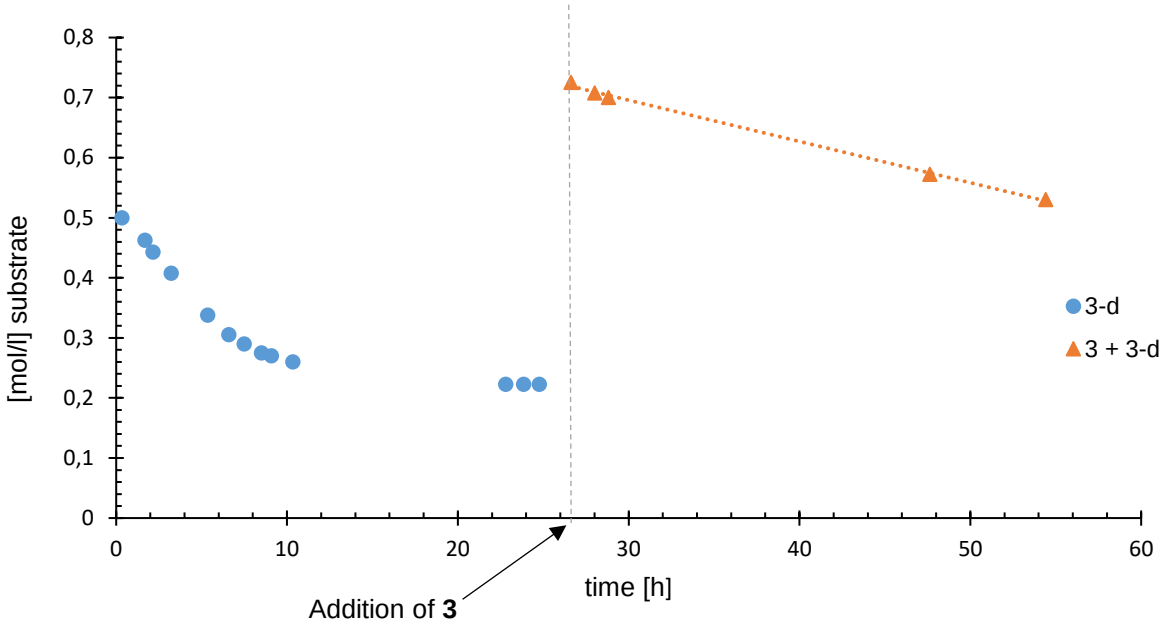

*Figure 20 – Time dependence of the concentration of the substrates of the test reaction to see whether the catalyst gets completely quenched during the reaction of **3**-d*

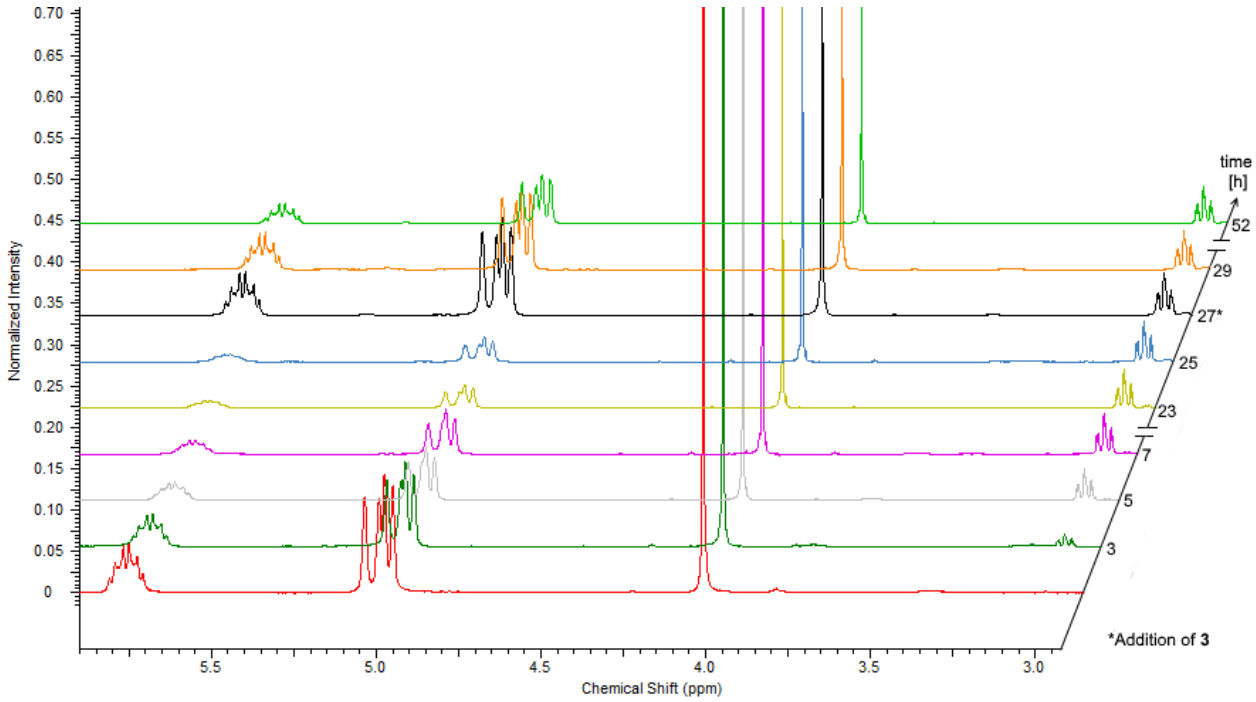

*Figure 21 – ^{1}H-NMR spectra of the test reaction to see whether the catalyst gets completely quenched during the reaction of **3**-d*

To get more accurate data the reaction of *N*-deutero-*N*-mehtylpent-4-en-1-amine (**3-*d***) was performed with 10 mol% of $Cp^*_2SmCH(TMS)_2$ (**1**). This reaction proceeded to 70% conversion with zeroth order as can be seen in Figure 22.

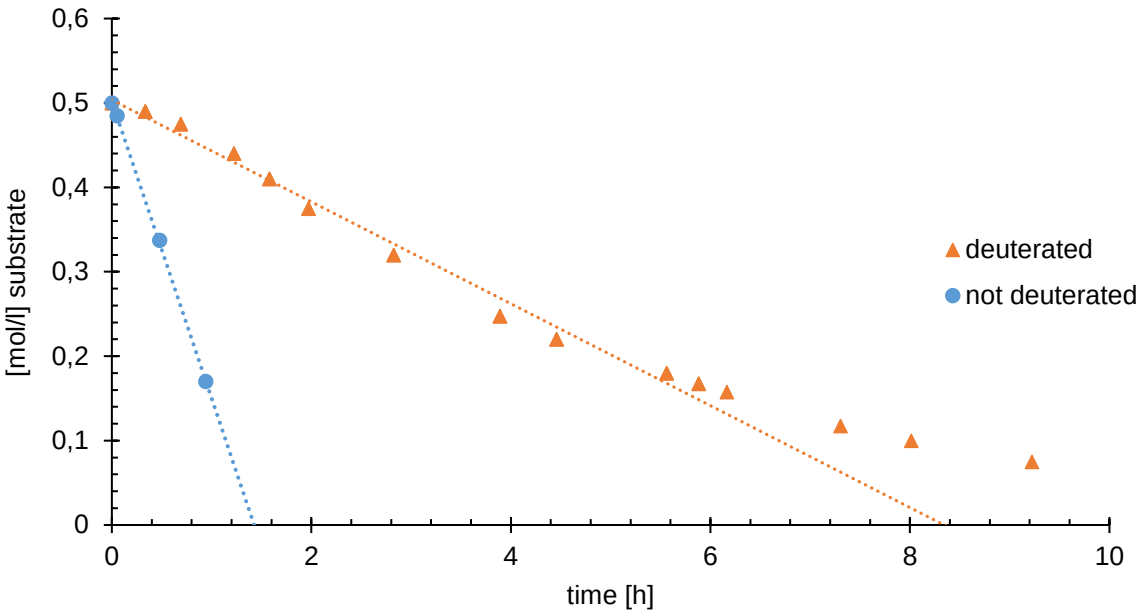

*Figure 22 – Comparison of the time dependence of substrate concentration with either N-methylpent-4-en-1-amine (**3**) or N-deutero-N-methylpent-4-en-1-amine (**3**-d) as substrate using 10 mol% $Cp^*_2SmCH(TMS)_2$ (**1**) as catalyst.*

To determine the kinetic isotope effect, the time to completion was compared with the time to completion of the non-deuterated amine **3**. While the reaction of **3-*d*** took 8.34 hours and had a N_t of 1.2 h^{-1} and a reaction constant of 0.06; the reaction of **3** was finished after 1.43 hours and had an N_t of 7.0 h^{-1} and a reaction constant of 0.35. The ratio of k_H/k_D therefore yielded to 5.8 indicating a significant kinetic primary isotope effect.

Attempted cyclization of *N*-Benzyl-*N*-deutero-pentan-4-enamine (4-*d*)

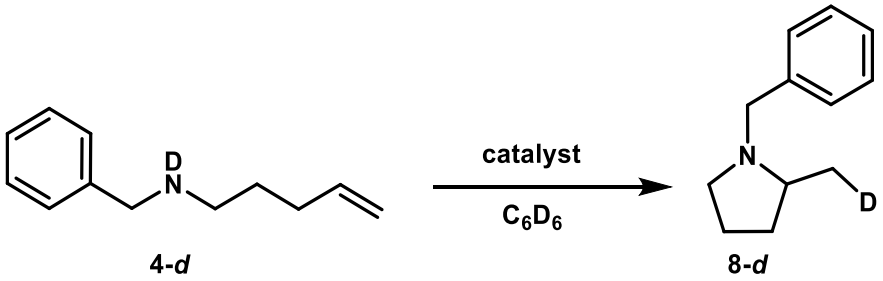

*Figure 23 – Reaction scheme for the synthesis of 1-Benzyl-2-(methyl-d)-pyrrolidine (8-**d**)*

The reaction of *N*-deutero-*N*-benzylpent-4-en-1-amine (**4-*d***) to 1-benzyl-2-(methyl-*d*)pyrrolidine (**8-*d***) neither proceeded with $Cp^*_2SmCH(TMS)_2$ (**1**) nor with the BINO-TPS-Y(BDMA) (**2**) precatalyst. Although the substrate had been distilled and dried over CaH_2 twice, the reason might be, that maybe still some D_2O or another impurity was left, since there was also no reaction with a mixture of deuterated and non-deuterated amine. The reaction was attempted with 10 mol% of the catalysts and also at higher temperature (150°C).

Cyclization of *N*-allylpent-4-en-1-amine-*d* (5-*d*)

*Table 11 – Catalytic Hydroamination of N-allylpent-4-en-1-amine-d (**5-d**) with an initial substrate concentration of 0.5 mol L^{-1} using BINO-TPS-Y(BDMA) (**2**) as catalyst*

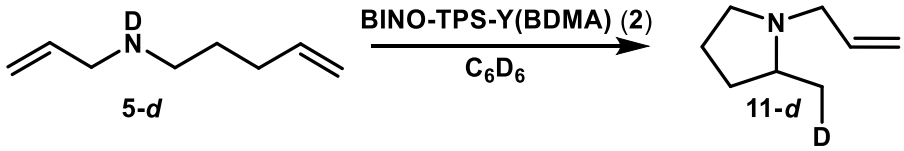

Entry	T [°C]	[cat.] [subst.]$^{-1}$ [%]	N_t [h^{-1}]	k_{obs} [mol L^{-1} h^{-1}]
1	21	10	0.6 ± 0.2	0.03 ± 0.001

The result of the reaction of the *N*-deuterated *N*-allylpent-4-en-1-amine (**5-*d***) with 10 mol% of BINO-TPS-Y(BDMA) (**2**) catalyst is stated in Table 11. The conversion was measured through the same signals as the conversion of the reactions with *N*-allylpent-4-en-1-amine (**5**).

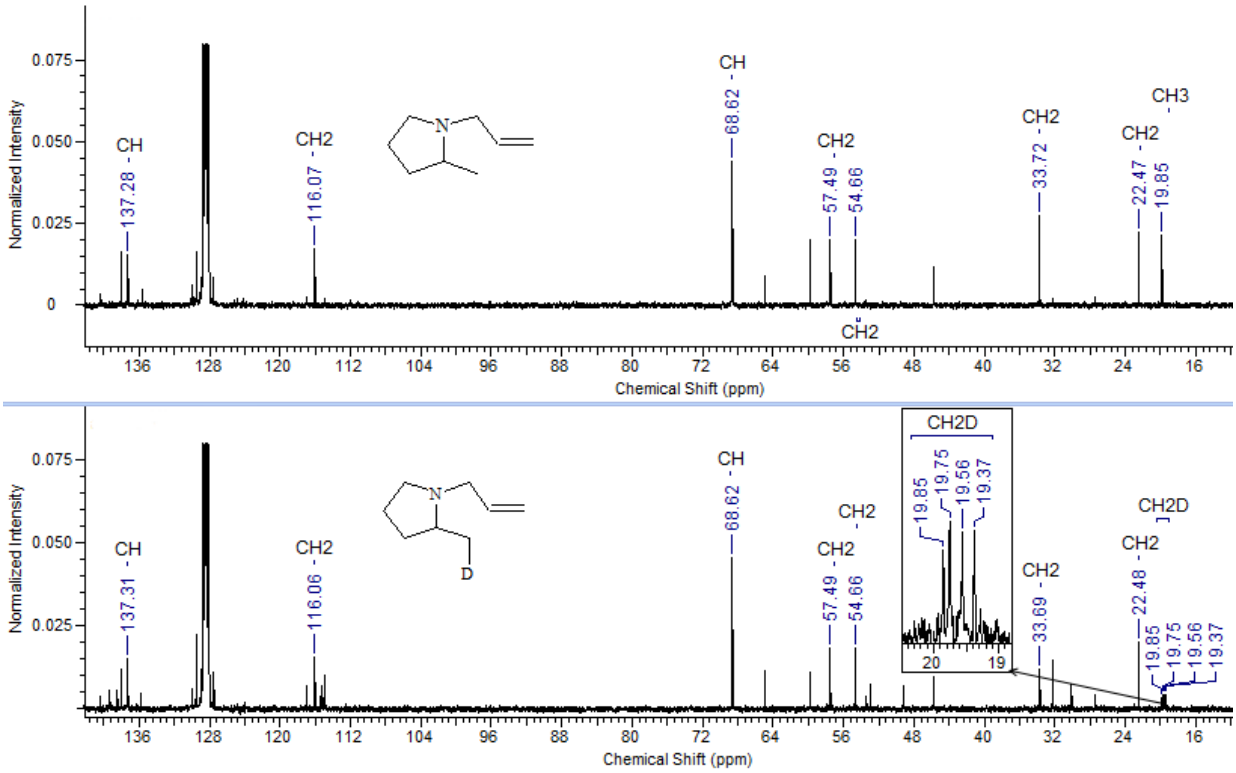

*Figure 24 – $^{13}C\{^1H\}$-NMR spectra of 1-allyl-2-methylpyrrolidine (**11**) and 1-allyl-2-(methyl-d)pyrrolidine (**11-d**)*

Although the $^{13}C\{^1H\}$ – NMR spectrum (Figure 24) shows four peaks rather than a triplet at the methyl group which indicates a mixture of deuterated and non-deuterated product. Nevertheless this seems to be the only signal showing a C – D coupling. This indicates, that the methyl group gets deuterated during the reaction leading to 1-allyl-2-(methyl-d)pyrrolidine (**11-*d***) as the main product. Through integration of the ^1H-NMR of the substrate **5-*d*** the amount of not deuterated amine was calculated to approximately 6%.

The cyclization of *N*-deutero-*N*-allylpent-4-en-1-amine (**5-*d***) with BINO-TPS-Y(BDMA) (**2**) appears to be zeroth order in substrate, as shown in Figure 25.

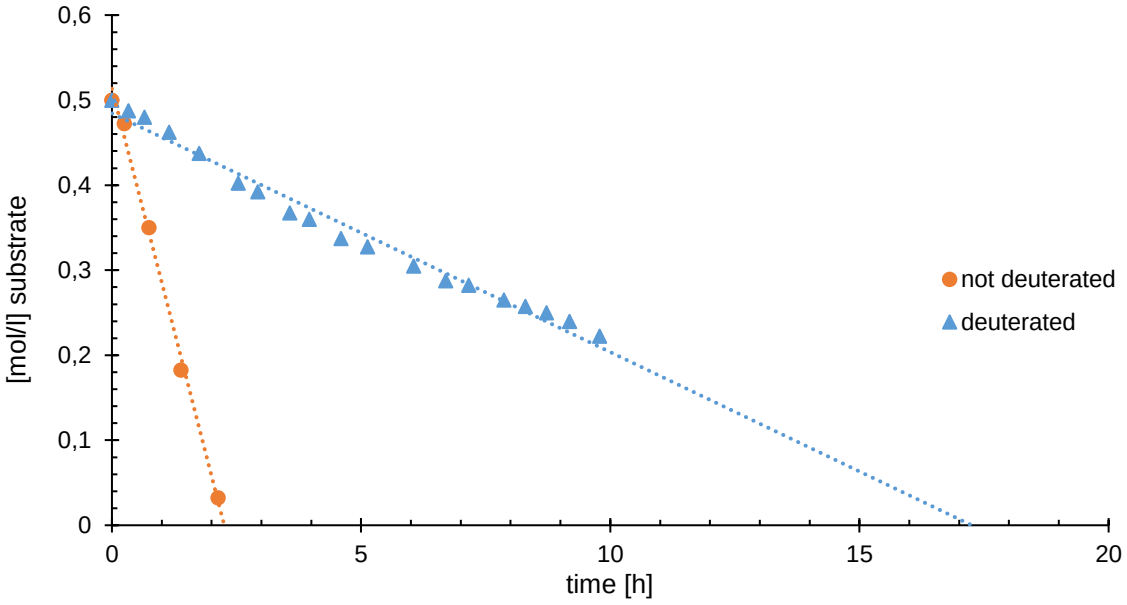

*Figure 25 – Comparison of the time dependence of substrate concentration with either N-allylpent-4-en-1-amine (**5**) or N-deutero-N-allylpent-4-en-1-amine (**5-d**) as substrate using 10 mol% BINO-TPS-Y(BDMA) (**2**) as catalyst*

Comparison of the time to full conversion of the non-deuterated with the deuterated amine showed, that the reaction of **5-*d*** with 10 mol% of BINO-TPS-Y(BDMA) (**2**) precatalyst took 17.25 hours and had a N_t of 0.6 h^{-1} and a rate constant of 0.03 mol L^{-1} h^{-1}; the reaction of **5** was finished after 2.25 hours and had an N_t of 4.5 h^{-1} and a rate constant of 0.22 mol L^{-1} h^{-1}. The ratio of k_H/k_D therefore yielded in 7.5, a significant primary kinetic isotope effect.

The kinetic isotope effect is even higher than the one of the intramolecular hydroamination reaction of *N*-methylpent-4-en-1-amine (**3**).

Kinetic isotope effect - discussion

The kinetic isotope effect was measured for the reaction of *N*-methylpent-4-ene-1-amine (**3**) with $Cp^*_2SmCH(TMS)_2$ (**1**) as well as for the hydroamination reaction of *N*-allylpent-4-en-1-amine with BINO-TPS-Y(BDMA)-$Y(BDMA)_2$ (**2**) as precatalyst.

The comparison of the reactions of the deuterated amines with the non-deuterated amines showed a significant primary kinetic isotope effect. This effect is too high to be yielded from a secondary kinetic isotope effect and therefore the data suggest a primary KIE.

This is in agreement to the investigations of Marks *et al.* who also found a primary KIE for primary aminoalkenes.[6]

But it is also in contradiction to the mechanism shown in Figure 16, since a primary KIE means that a bond formation (or bond breaking) should take place in the rate determining step. The group of Marks proposed an explanation for this effect, using a concerted mechanism.[6]

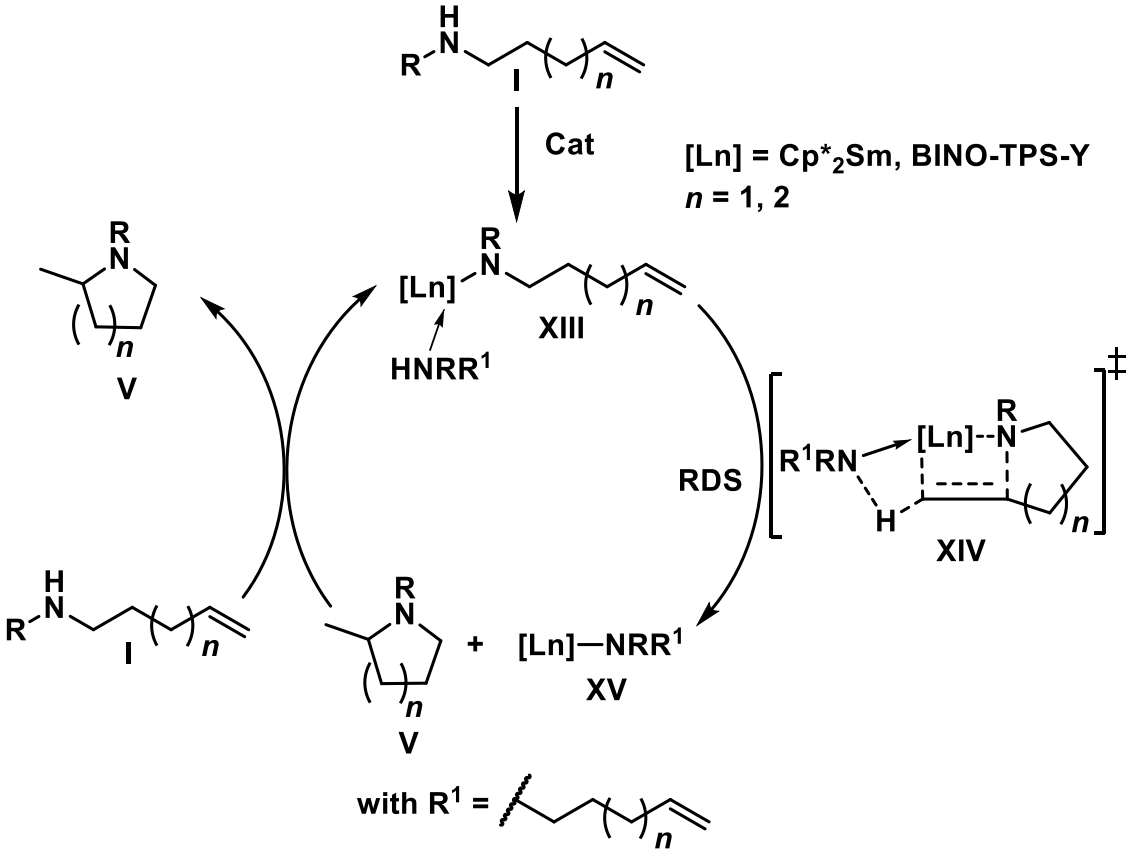

Figure 26 – Possible mechanism for the intramolecular hydroamination

This interpretation together with the general mechanism of the hydroamination led to the proposed mechanism depicted in
Figure *26*.

In this mechanism another amine molecule coordinates to the lanthanide. In the substitution/insertion step, the hydrogen of this amine is transferred to the carbon-atom of the other amine, causing the primary kinetic isotope effect. Afterwards the product is substituted by another substrate, to complete the catalytic cycle.

6.4 Hydroamination Carbocyclization

6.4.1 Reaction Kinetics and Activation Parameters

Cyclization of *N*-allylpent-4-en-1-amine (5)

To examine the hydroamination/carbocyclization the reaction of *N*-allylpent-4-en-1-amine (**5**) to 2-methylhexahydro-1H-pyrrolizine (**10**) was tested with $Cp^*_2SmCH(TMS)_2$ (**1**) as precatalyst.

As shown in Table 12 the reaction was examined for 5 mol% of the $Cp^*_2SmCH(TMS)_2$ (**1**) precatalyst at different temperatures.

*Table 12 – Catalytic Hydroamination of N-allylpent-4-en-1-amine (**5**) with an initial substrate concentration of 0.5 mol L^{-1} and $Cp^*_2SmCH(TMS)_2$ **(1)** as precatalyst*

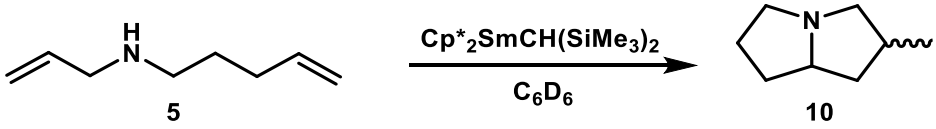

Entry	T [°C]	[cat.] [subst.]$^{-1}$ [%]	N_t [h^{-1}]	k_{obs} [mol L^{-1} h^{-1}]
1	20	5	3.9 ± 0.06	0.10 ± 0.002
2	25	5	4.7 ± 0.08	0.12 ± 0.002
3	30	5	6.7 ± 0.27	0.17 ± 0.007
4	40	5	15.0 ± 0.45	0.37 ± 0.011
5	45	5	18.0 ± 0.65	0.45 ± 0.016
6	21	10	1.9 ± 0.05	0.09 ± 0.002

This reaction was monitored by ^{1}H–NMR spectroscopy with ferrocene as internal standard, as well. The conversion was measured through the disappearance of the significant signals of the olefinic protons at 5.88 – 5.73 ppm and at 5.15 – 4.95 ppm as well as the appearance of the signal of the methine group of the product at 3.61 – 3.54 ppm – as can be seen in Figure 27.

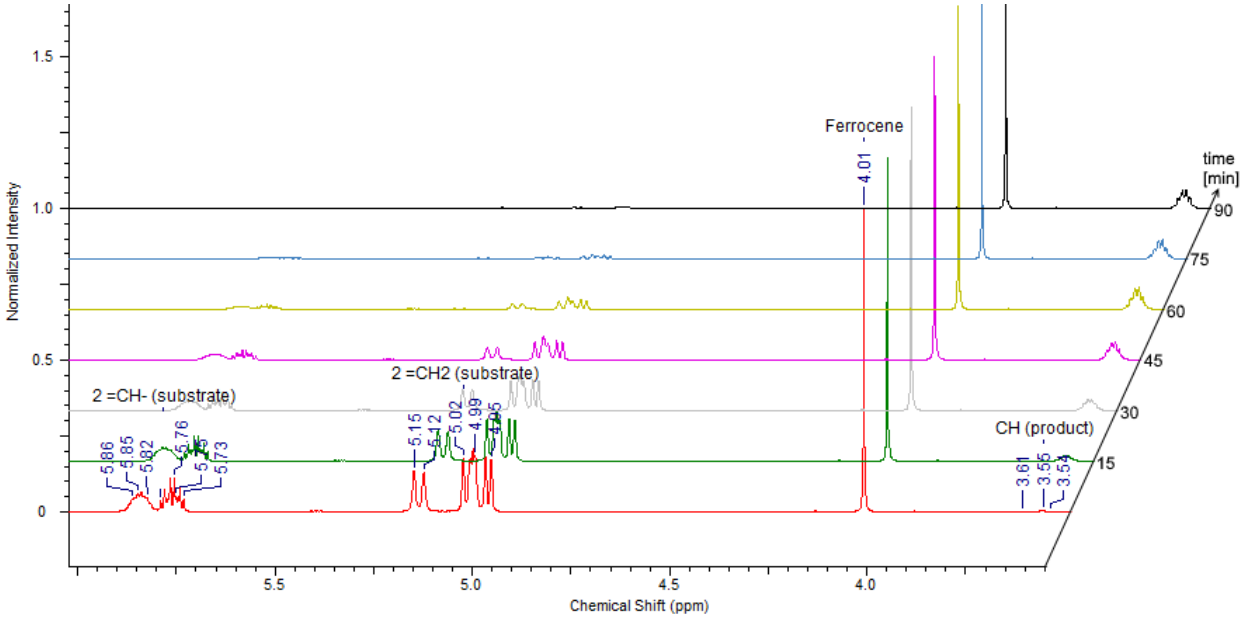

*Figure 27 – ^{1}H - NMR spectra of the samarium-catalyzed cyclication of N-allylpent-4-en-1-amine (**5**) to give 2-methylhexahydro-1H-pyrrolizine (**10**)*

Again the concentration of the substrate was monitored over time using the conversion measurement to determine the reaction order.

The reaction with 5 mol% of the $Cp^*_2SmCH(TMS)_2$ (**1**) appears to be zeroth order in substrate although the reaction gets slower, between 70 and 80% conversion, as can be seen in Figure 28.

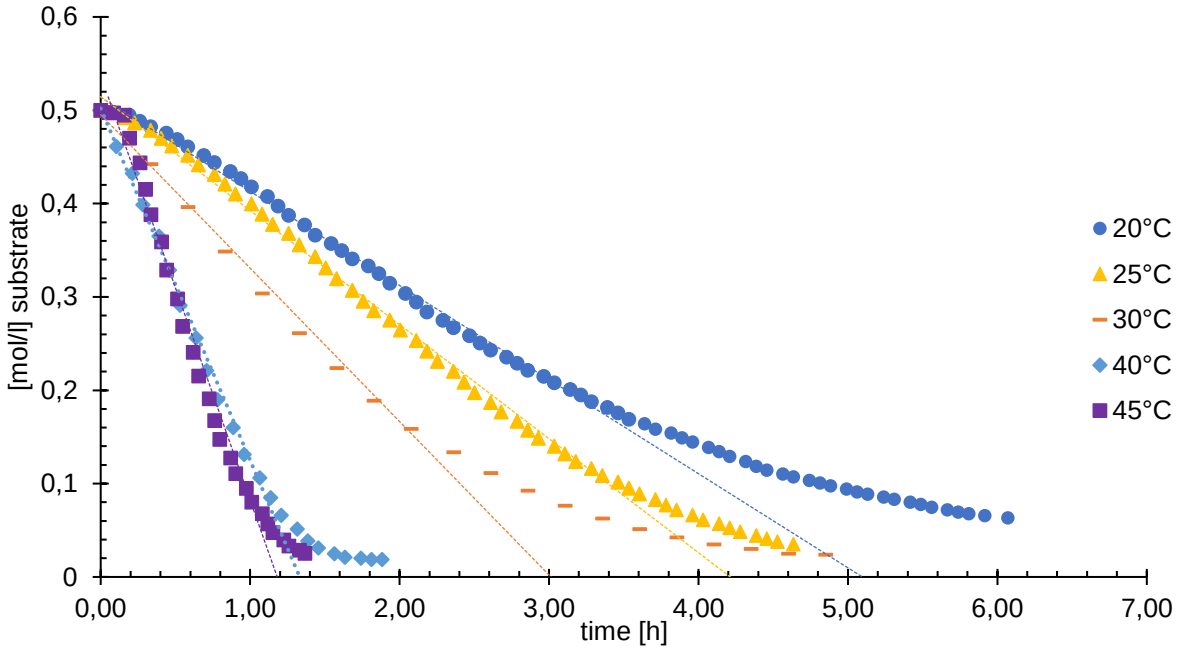

*Figure 28 – Comparison of the time dependence of the concentration of substrate **5** at different temperatures with 5 mol% of Sm - catalyst (**1**)*

Similar to the hydroamination reactions the time to full conversion also decreases with increasing temperature of the hydroamination/carbocyclization.

While the reaction at 20°C took 5.12 hours to complete and had a turnover frequency of 3.9 h^{-1} as well as a reaction rate constant of 0.10 mol L^{-1} h^{-1} while the reaction at 45°C only took 1.11 hours with an N_t of 18.0 h^{-1} and a reaction rate constant of 0.45 mol L^{-1} h^{-1}.

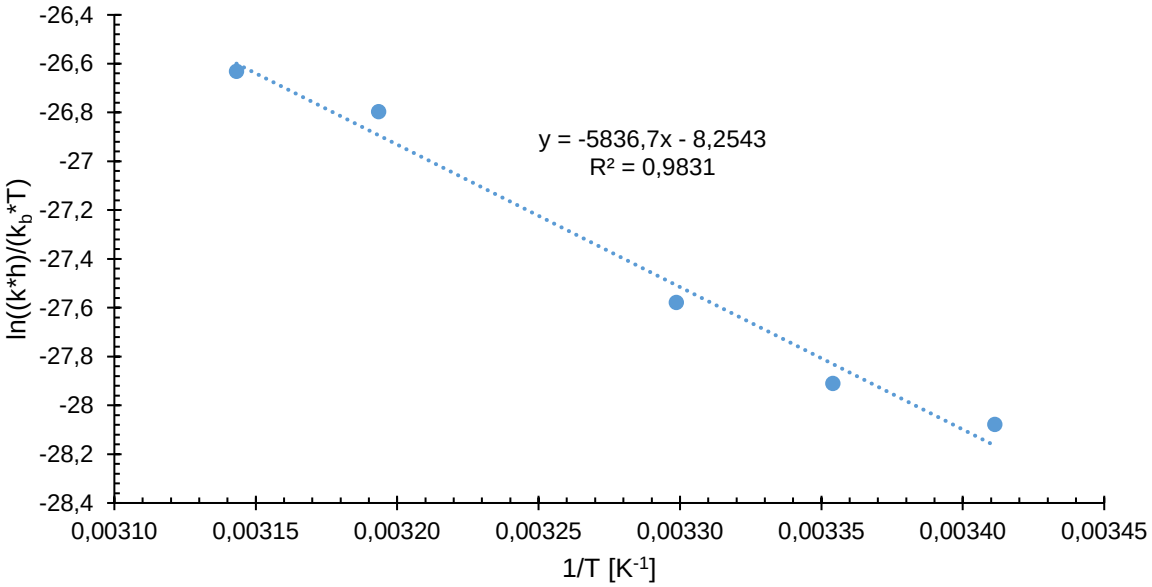

*Figure 29 – Eyring – Plot for the hydroamination of **5** with an initial substrate concentration of 0.5 mol L^{-1} and 5 mol% of $Cp^*_2SmCH(TMS)_2$ - catalyst (**1**)*

Like before the activation parameters could be directly obtained from the Eyring Plot given in Figure 29.

Table 13 – Value and Deviation derived by regression analysis

	Value	Deviation
y-intercept	-8.2543	1.4486
incline	-58136.7	441.41

The linear regression (Table 13) determined the activation enthalpy as $\Delta H^{\ddagger} = 49 \pm 4$ kJ mol^{-1} and activation entropy $\Delta S^{\ddagger} = -69 \pm 12$ J K^{-1} mol^{-1} for 0.5 mol L^{-1} initial substrate concentration and 5 mol% of $Cp^*_2SmCH(TMS)_2$ (**1**).

The values should be compared to the activation parameters of the hydroamination/cyclication of *N*-methylpent-4-en-1-amine (**3**) ($\Delta H^{\ddagger}$ = 59 ± 7 kJ mol^{-1}, $\Delta S^{\ddagger}$ = – 34 ± 23 J K^{-1} mol^{-1}) using $Cp^*_2SmCH(TMS)_2$ (**1**).

Marks *et al*. reported $\Delta H^{\ddagger}$ = 53 ± 6 kJ*mol^{-1} and $\Delta S^{\ddagger}$ = – 113 ± 19 J*K^{-1}*mol^{-1} for the activation parameters for the cyclization of pent-4-en-1-amine to 2-methylpyrrolidine with $Cp^*_2LaCH(TMS)_2$.[6]

Therefore, the data for the hydroamination reactions are in a similar range as the measured activation parameters for the reaction of *N*-allylpent-4-en-1-amine (**5**) to 2-methylhexahydro-1H-pyrrolizine (**10**) with 5 mol% $Cp^*_2SmCH(TMS)_2$ **(1)**.

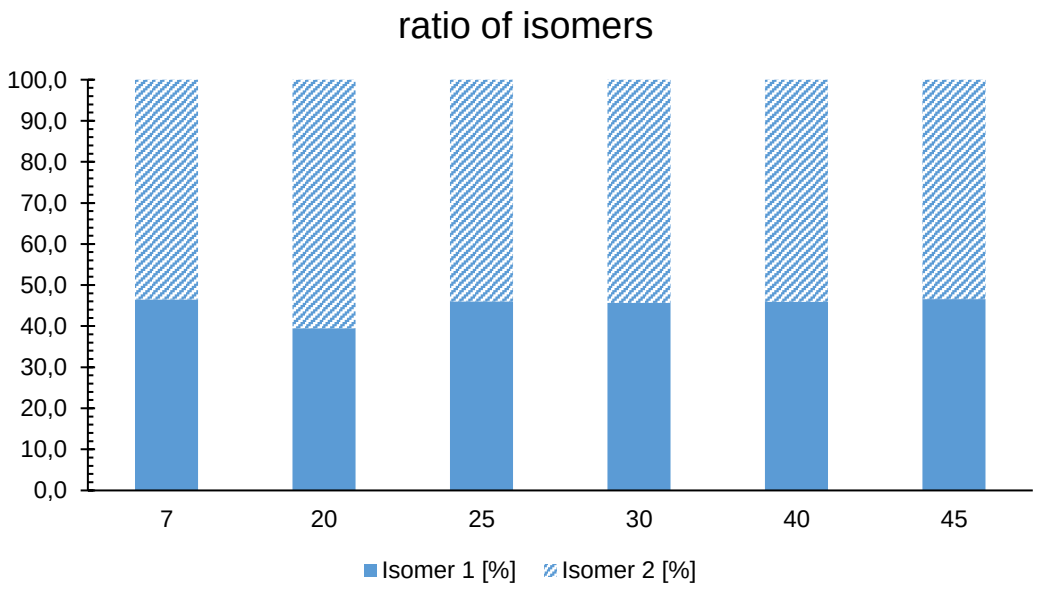

Figure 30 – Comparison of the ratio of the two diastereomers at different reaction temperatures

Furthermore, the ratio of the two diastereomers was determined to see whether the catalyst favours one isomer over the other.
The ratio between the two isomers is in most cases around 45% to 55%, as can be seen in Figure 30. Only for the reaction at 20°C a slightly different ratio of around 40% to 60% was observed. Therefore, another reaction at 7°C was performed, to see whether there is a trend between temperature and ratio. But with this measurement, the ratio was again 45% to 55% for the 2 isomers.
So overall the catalyst doesn't seem to strongly favour one isomer as product. The only derivation was the measurement at 20°C with a ratio of 40:60.

Reaction kinetics and activation parameters - discussion

As stated before, the kinetic data showed, that the reaction of *N*-allylpent-4-en-1-amine (**5**) with 5 mol% of $Cp^*_2SmCH(TMS)_2$ (**1**) appeared to be zeroth order in substrate concentration until around 90% conversion at higher temperature (40 and 45°C), but only until between 60 and 70% conversion at temperatures between 20 and 30°C.

Marks *et al.* suggested a zeroth order dependency on substrate concentration, as well as a first order dependency on catalyst concentration for the hydroamination/carbocyclization,[18] which is in agreement with the obtained experimental data of the present study.

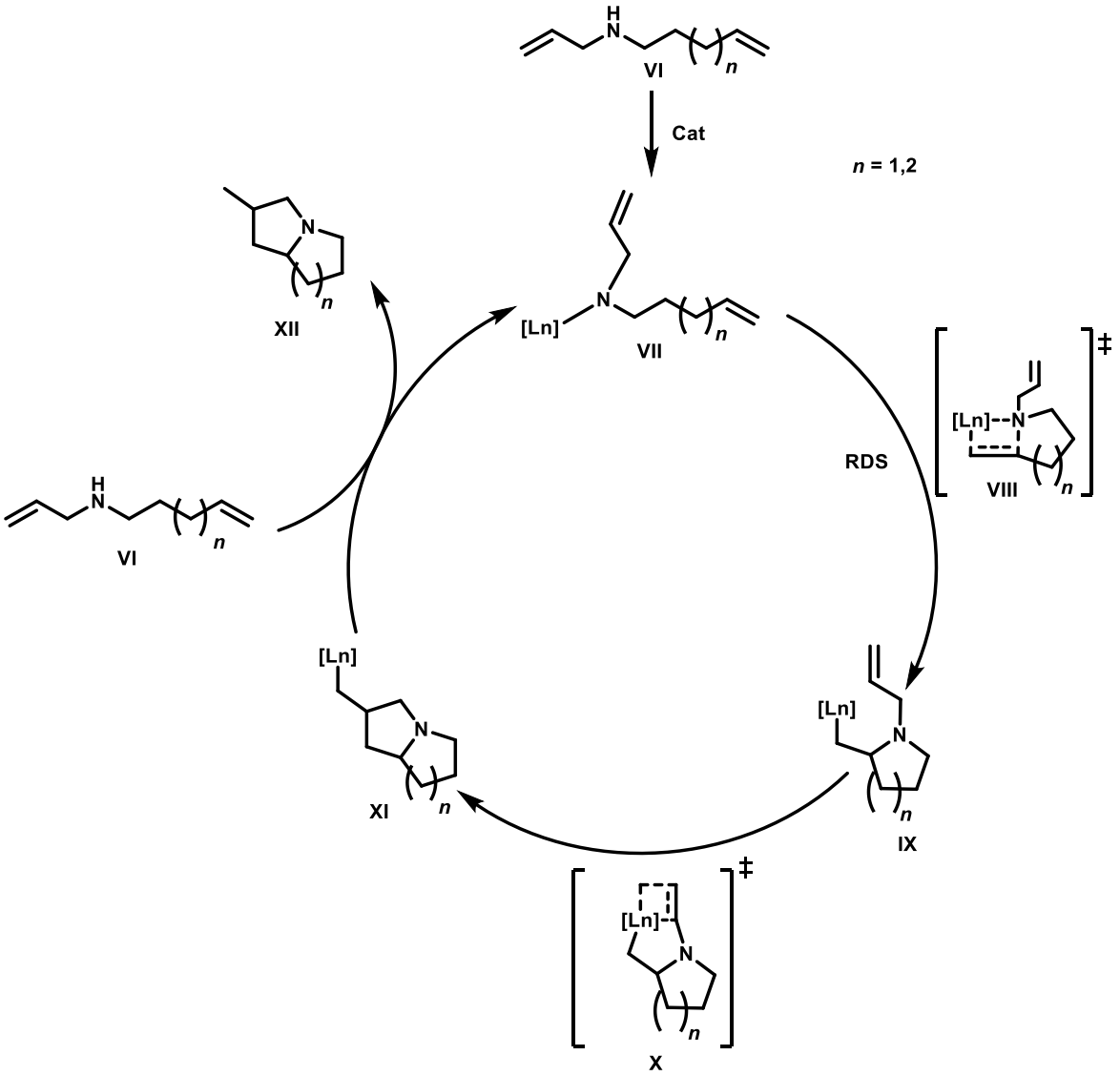

Figure 31 – Proposed mechanism of the intramolecular hydroamination/carbocyclization

The activation parameters of the reaction of *N*-allylpent-4-en-1-amine (**5**) with 5 mol% of $Cp^*_2SmCH(TMS)_2$ (**1**) are in a similar range as the activation parameters found for the hydroamination reaction. This suggests, that the rate determining step of the reaction is in the hydroamination reaction, which is in agreement with the mechanism proposed by Marks *et al.* shown in Figure 31.[19]

The reaction of *N*-allylpent-4-en-1-amine (**5**) with the BINO-TPS-Y(BDMA) catalyst (**2**) only underwent the hydroamination step of the reaction, probably because the carbocyclization wasn't as fast as the competing protonolysis.

6.4.2 Kinetic isotope effect

Cyclization of *N*-allylpent-4-en-1-amine-*d* (5-*d*)

*Table 14 – Catalytic hydroamination/carbocyclozation of N-allylpent-4-en-1-amine-d (**5-d**) with an initial substrate concentration of 0.5 mol L^{-1} and $Cp^*_2SmCH(TMS)_2$ (**1**) as precatalyst*

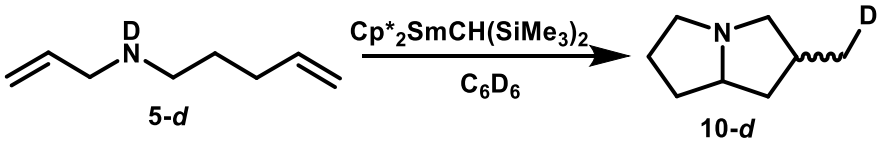

Entry	T [°C]	[cat.] [subst.]$^{-1}$ [%]	N_t [h^{-1}]	k_{obs} [mol L^{-1} h^{-1}]
1	21	5	0.9 ± 0.05	0.02 ± 0.001
2	21	10	0.8 ± 0.02	0.04 ± 0.001

The results of the reaction with the *N*-deuterated *N*-allylpent-4-en-1-amine (**5-*d***) are tabulated in Table 14. The conversion was measured using the same signals as the conversion of the reactions with *N*-allylpent-4-en-1-amine **(5)**.

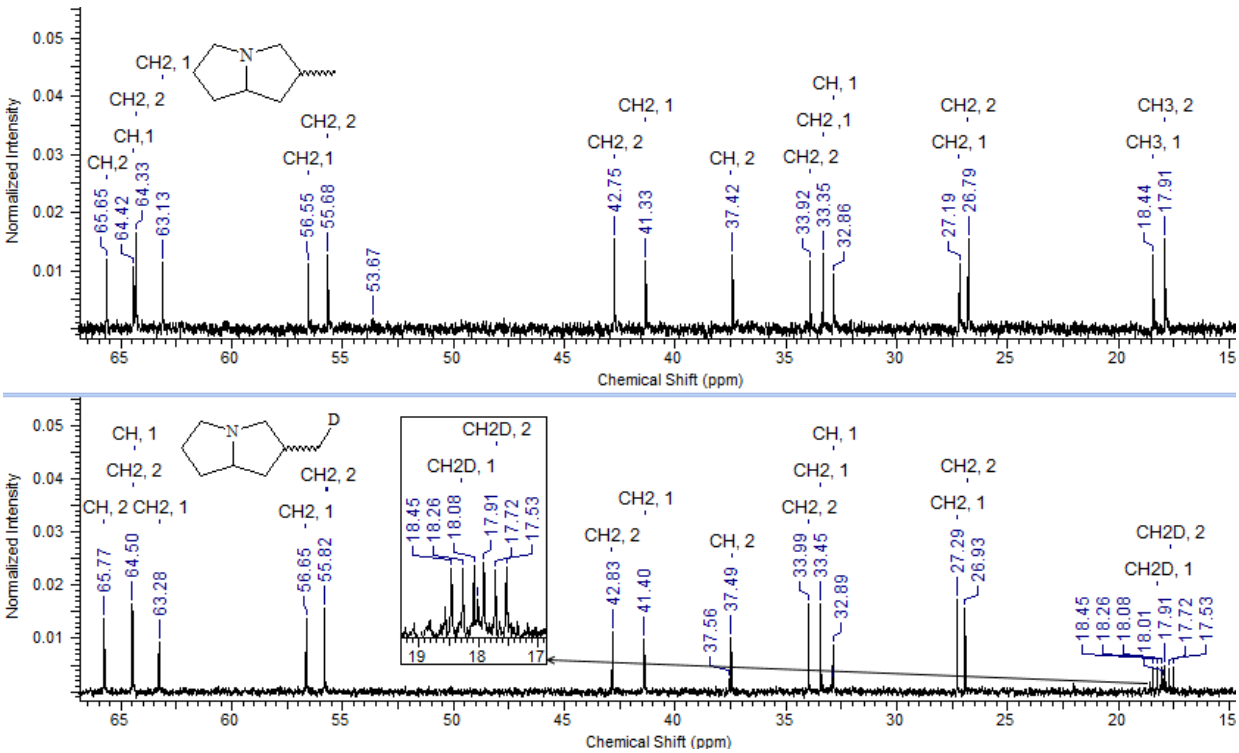

*Figure 32 – $^{13}C\{^1H\}$-NMR spectra of 1-allyl-2-methylpyrrolidine (**10**) and 2-(Methyl-d)hexahydro-1H-pyrrolizine (**10-d**)*

Figure 32 shows that the product of the samarium-catalysed cyclization of N-allylpent-4-en-1-amine-*d* (**5-*d***) is deuterated at the 2-methyl-group. As before the amount of peaks indicate, that the deuteration hasn't been complete. Since the same patch of substrate has been used as for the hydroamination reaction with **2** the amount of not deuterated amine is around approximately 6%.

The reaction with both 5 and 10 mol% of $Cp^*_2SmCH(TMS)_2$ (**1**) seem to be zeroth order, as shown in Figure 33.

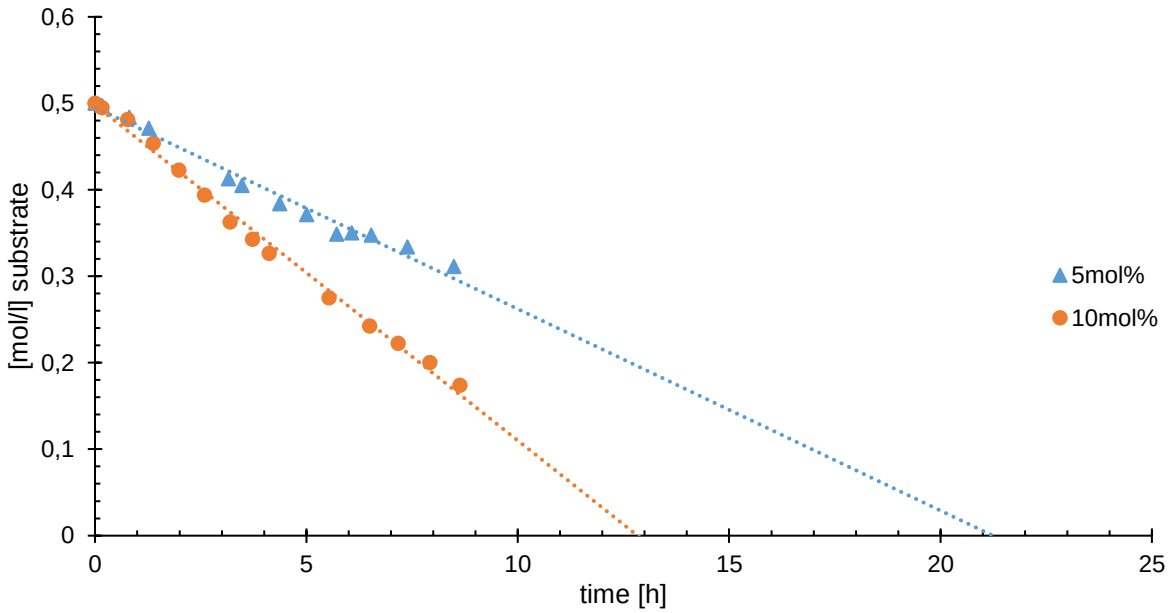

*Figure 33 – Comparison of the time dependence of the concentration of **5-d** with different catalyst loadings of $Cp^*_2SmCH(TMS)_2$ (**1**)*

Furthermore, the reaction with 5 mol% of catalyst should theoretically take 21.24 h, therefore the reaction was complete with 10 mol% of $Cp^*_2SmCH(TMS)_2$ (**1**) to see how the time to completion depends on the catalyst concentration.
The theoretical time to completion determined over the linear regression with 5 mol% was 1.7 times as large as the one with 10 mol%. The observed reaction rate constant doubled when using 10 mol% of catalyst instead of 5 mol%.

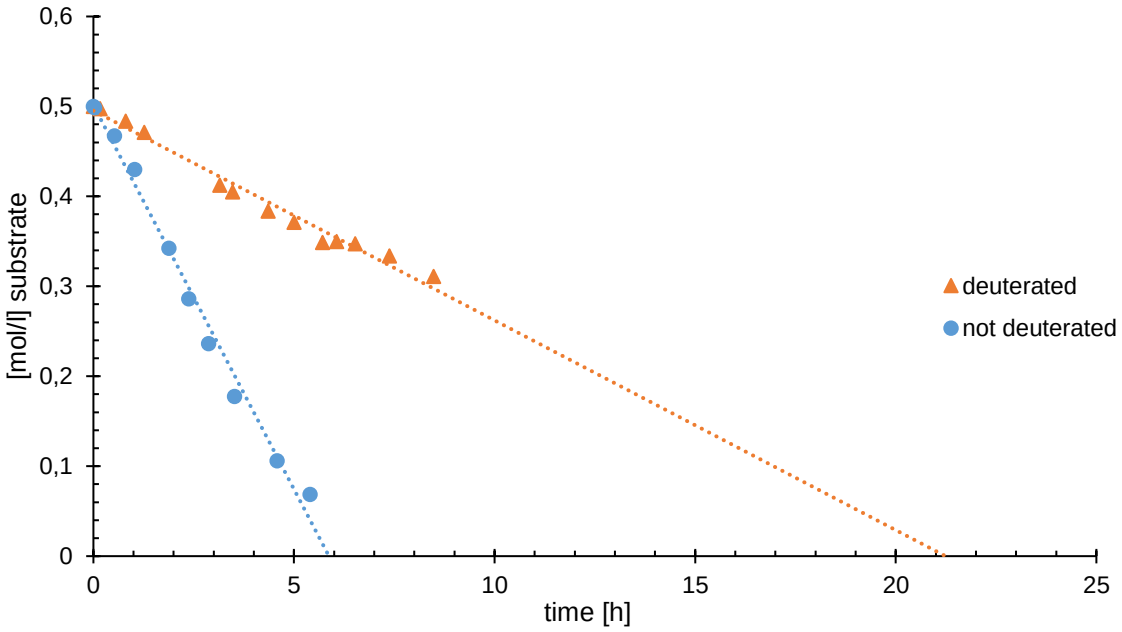

*Figure 34 – Comparison of the time dependence of substrate concentration with either N-allylpent-4-en-1-amine (**5**) or N-allylpent-4-en-1-amine-d (**5-d**) as substrate and 5 mol% Cp*$_2$SmCH(TMS)$_2$*

To determine the kinetic isotope effect, again the reaction time was compared with the reaction time of the non-deuterated amine (**5**). The reaction of (**5-*d***) with 5 mol% of Cp*$_2$SmCH(TMS)$_2$ (**1**) took 21.24 hours and had an N_t of 0.9 h^{-1} and a reaction rate constant of 0.02 mol L^{-1} h^{-1}; the reaction of (**5**) was finished after 5.55 hours and had an N_t of 3.6 h^{-1} and a reaction rate constant of 0.09 mol L^{-1} h^{-1}. Therefore, the ratio of k_H/k_D 4 indicates a significant kinetic isotope effect.

The kinetic isotope effect is a little bit smaller than the KIE of the hydroamination but still sufficiently large for a primary KIE.

Kinetic isotope effect - discussion

The reaction of *N*-allylpent-4-en-1-amine (**5**) with 5 mol% of $Cp^*_2SmCH(TMS)_2$ (**1**) was compared to the reaction of the non-deuterated amine with the same catalyst loading. Similar to the hydroamination reaction, this reaction showed a significant kinetic isotope effect. This effect is too high to result from a secondary kinetic isotope effect and therefore the data suggest a primary KIE.

Similar to the hydroamination, this is in contradiction to the proposed mechanism (shown in Figure 31), since a primary KIE means that a bond formation (or bond cleavage) should take place in the rate determining step.
Furthermore, most of the kinetic data suggest, that the RDS should be in the hydroamination step of the reaction, as proposed in Figure 31.

Therefore, the mechanism has to be concerted in the rate determining hydroamination step, but the catalytic pathway also has to undergo the carbocyclization to fullfill all requirements.

However, with the concerted mechanism, the reaction cannot undergo the carbocyclization step because the lanthanide-carbon bond would already have been broken during the hydroamination step, to form a hydrogen – carbon bond.

Therefore, it seems, like the data are in disagreement to each other. Possibly the rate determining step is not in the hydroamination step of the reaction, but in the carbocyclization step. This could also be an explanation, why the reaction with the BINO-TPS-Y(BDMA) (**2**) catalyst only undergoes the (faster) hydroamination step.

A possible concerted mechanism, with the rate determining step in the carbocyclization is shown in Figure 35.

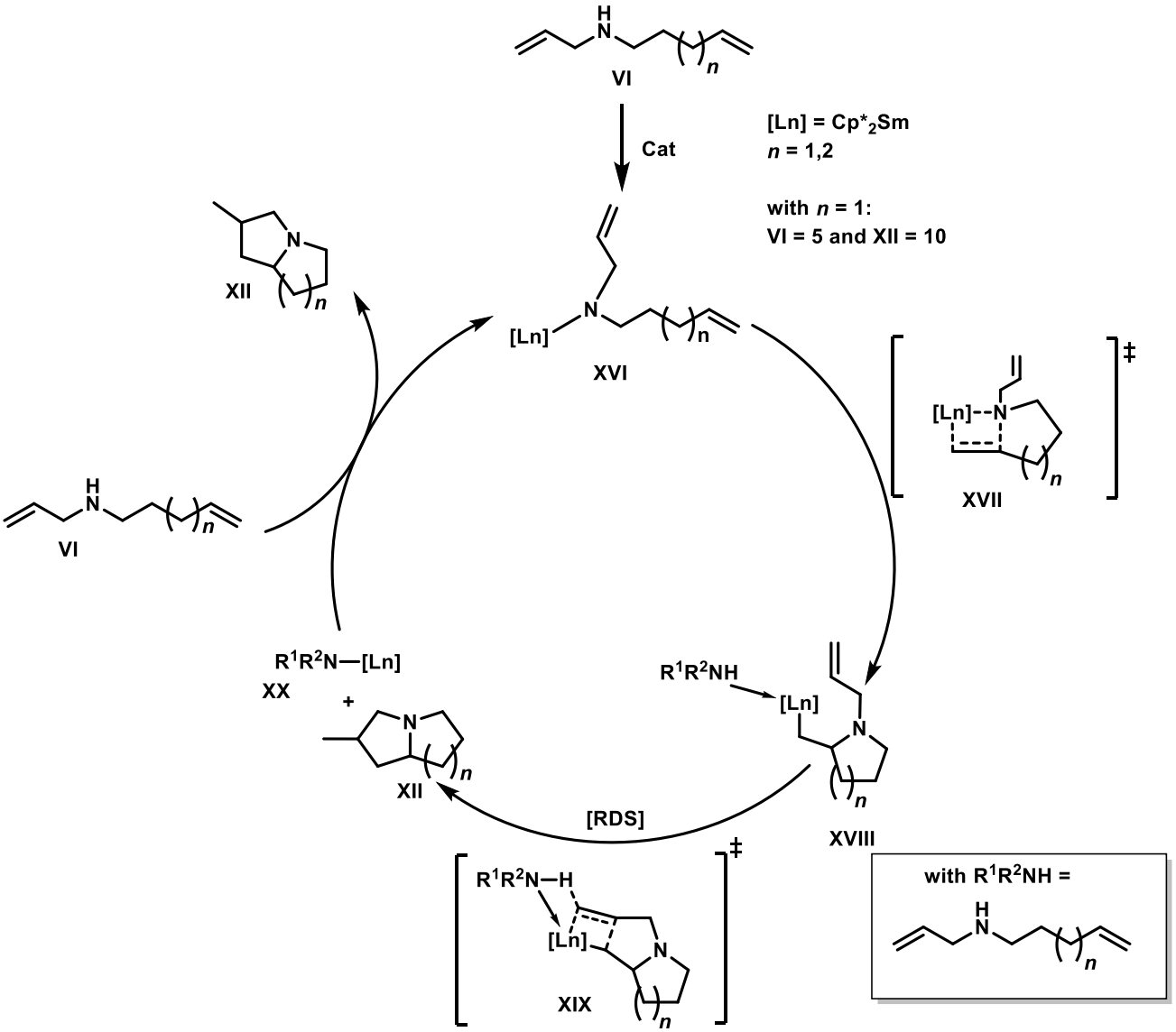

Figure 35 – Possible concerted mechanism of the hydroamination carbocyclization

In the first step of the reaction, the hydroamination leed to compound (**XVIII**). Afterwards the concerted carbocyclization takes place and the product is substituted by another substrate completing the catalytic cycle. To explain the KIE the RDS ought to be the concerted carbocyclization step.

7 Conclusion

Both the kinetics of the hydroamination cyclization as well as the hydroamination carbocyclization reaction have been measured using NMR spectroscopy. $Cp^*_2SmCH(TMS)_2$ (**1**) and BINO-TPS-Y(BDMA) $Y(BDMA)_2$ (**2**) have been used as precatalyst.

The reactions appear to be zeroth order in substrate concentration and higher order (probably first order) in catalyst concentration. Both of these observations are in agreement to the published data.[6,18,19]

Furthermore, the activation parameters of the hydroamination of *N*-methlypent-4-en-1-amine (**3**) and the activation parameters of the hydroamination/carbocyclization of *N*-allypent-4-en-1-amine (**5**) have been obtained. The activation parameters were similar to each other, suggesting that the rate determining step of the hydroamination/carbocyclization is the insertion/cyclization step of the hydroamination. The activation parameters have been obtained of the hydroamination/carbocyclization of **5** ($\Delta H^{\ddagger}$ = 49 ± 4 kJ mol^{-1} and $\Delta S^{\ddagger}$ = – 69 ± 12 J K^{-1} mol^{-1}) and of the hydroamination/cyclization of **3** ($\Delta H^{\ddagger}$ = 59 ± 7 kJ mol^{-1} and $\Delta S^{\ddagger}$ = – 34 ± 23 J K^{-1} mol^{-1}), both with 0.5 mol/L initial substrate concentration and 5 mol% of $Cp^*_2SmCH(TMS)_2$ (**1**).

The kinetic isotope effects of both reactions were measured and indicate a primary KIE for the hydroamination and the hydroamination/carbocyclization. The obtained KIE data for the hydroamination are in agreement with the obtained activation parameters. A possible mechanism for the reaction is shown in
Figure *26*.

On the other hand, the data of the KIE of the hydroamination/carbocyclization suggest, that the carbocyclization ought to be the RDS in this reaction, which is in contradiction to the activation parameters that are quite similar to the ones of the hydroamination reaction.

There are two possible explanations for this contradiction:

The first one is, that the activation parameters of the carbocyclization and the hydroamination are similar to each other and the RDS of the hydroamination/carbocyclization reaction is always the carbocyclization step leading to the mechanism shown in Figure 35.

The other possible explanation is, that the RDS of the hydroamination/carbocyclization normally is the hydroamination step, but if the deuterated substrate was used, the bond-breaking of the N-D bond is slowed down and this step would become the RDS for this reaction. This would lead to two different mechanisms, one for the non – deuterated amines (Figure 32) and one for the deuterated amines (Figure 35).

8 Experimental Part

If not stated otherwise, all reactions were carried out under inert atmosphere (argon) using either Schlenk technique or a glove box. The NMR spectra were recorded with either a Bruker AVIII 400 or a Bruker Avance III HD 700 MHz spectrometer in either $CDCl_3$ or C_6D_6. The calibration of the NMR spectra either was done over the solvent peak or by using ferrocene as internal standard during the kinetic studies.
The used chemicals were either purchased from Sigma-Aldrich and similar companies or had been prepared within the Hultzsch group before. The used solvents were dried with a MB-SPS-800 solvent purification system and stored in a flask under argon over a sodium mirror.

Synthesis of 1,2,3,4,5-pentamethylcyclopenta-2,4-dien-1-yl)lithium (Cp*-Li)[26]

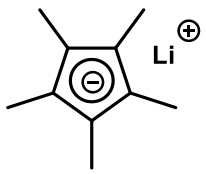

A solution of Cp*-H (1.260 g; 9.256 mmol) – which was prepared by Leonard Homberg – in hexanes (50 mL) was cooled down to –78°C. A *n*-BuLi solution (2.5 *M* in hexanes, 3.9 mL, 9.8 mmol) was added slowly dropwise and the solution was stirred at –78°C for half an hour. Afterwards it was stirred for 16 hours at room temperature. The solution was filtered and the residue was washed with hexane (2×~30 mL). Afterwards the residue was dried *in vacuo* leading to 1.081 g of product (82% yield). The product was a slightly yellowish powder.

^{1}H-NMR (C_6D_6, 400MHz): δ 0.89 (s, 5 CH_3, 15 H)

Synthesis of (bis(trimethylsilyl)methyl)lithium[27]

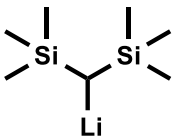

Lithium granulate with 0.5% sodium impurities (0.404 g; 58,2 mmol) was suspended in Et_2O (~50 mL) and chlorobis(trimehtylsilane)methane (1.301 g; 6.677 mmol) was added dropwise. The solution was stirred over a week at 60°C under reflux using an intensive reflux condenser. From time to time, the solution was sonicated to detach the LiCl from the Li metal. Afterwards the solution was filtered and the residue was washed with pentane (~10 mL). The solvent of the combined organic layers was

removed *in vacuo*. The residue was sublimed (120°C, 2–3×10^{-3} mbar) leading to 0.461 g of the highly pyrophoric product (42% yield). The product was a white powder.

^{1}H-NMR (C_6D_6, 400MHz): δ 0.16 (s, 6 CH_3, 18 H), –2.50 (s, CH, 1H).
The ^{1}H-NMR spectroscopic data is in agreement with the literature.[27]

Synthesis of (bis(trimethylsilyl)methyl)bis(1,2,3,4,5-pentamethylcyclopenta-2,4-dien-1-yl)samarium (Cp*Sm CH(TMS)$_2$) (1)[28]

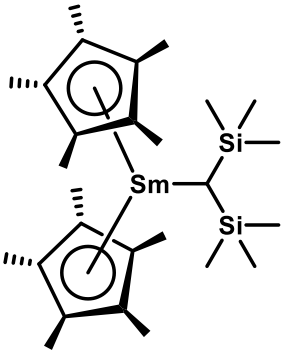

Samarium(III)chloride (0.711 g; 2.76 mmol) was suspended in THF (~35 mL) and stirred overnight at room temperature. Afterwards LiCp* was added and the mixture was stirred under reflux overnight. Then the mixture was allowed to cool down to room temperature and the solvent was removed *in vacuo*. (Bis(trimethylsilyl)lithium was added and the mixture was suspended in toluene (~35 mL) at –78°C. The reaction mixture was allowed to gradually warm up to room temperature overnight. The solvent was removed *in vacuo.* The residue was extracted with pentane (~35 mL) and filtered. The solution was cooled down to –78°C and filtered again to remove the impurities. Afterwards the solvent was removed in vacuo leading to 0.17 g of a red crystalline product (11% yield).

^{1}H-NMR (C_6D_6, 400MHz): δ 20.38 (s, CH, 1H), 0.92 (s, 5 CH_3, 15 H), 0.79 (s, 5 CH_3, 15 H), – 4.65 (s, 6 CH_3, 18 H).
The ^{1}H-NMR spectroscopic data is in agreement with the literature.[28]

Synthesis of N-methylpent-4-en-1-amine (3)[22]

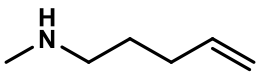

Methanamine (33% wt solution in EtOH, 60 mL; 500 mmol) and 5-bromopent-1-ene (7.548 g; 50.65 mmol) were dissolved in EtOH (30 mL). Sodium iodide (0.378 g; 2.52 mmol) was added and the mixture was stirred overnight at 60°C. Afterwards the mixture was cooled to 0°C and conc. HCl was added until pH <2 (~ 35 mL) was reached. The solvent was removed by rotary evaporation and the residue dissolved in water (50 mL), which was removed again by rotary evaporation. This procedure was repeated twice.

Afterwards the residue was dissolved in H_2O (30 mL) and the solution was extracted with Et_2O (50 mL). NaOH (15% aqueous solution, 70 mL) was added to the aqueous layer to reach pH > 12 and the solution was extracted 3 more times with Et_2O (35 mL each). The combined organic layers were dried over $MgSO_4$, filtered and the solvent removed by rotary evaporation. The residue was dried over CaH_2 and distilled (350 mbar, 75°C), leading to 2.502 g of product (50% yield). The product was a colourless liquid.

^{1}H-NMR ($CDCl_3$, 400MHz): δ 5.82–5.73 (m, CH, 1H), 4.99–4.89 (m, CH_2, 2H), 2.53 (t, *J* = 7.10 Hz, CH_2, 2H), 2.37 (s, CH_3, 3H), 2.07–2.01 (m, CH_2, 2H), 1.56–1.49 (m, CH_2, 2H), 0.79 (s, NH, 1H).
The ^{1}H-NMR spectroscopic data is in agreement with the literature.[22]

Synthesis of *N*-benzylpent-4-en-1-amine (4)[22]

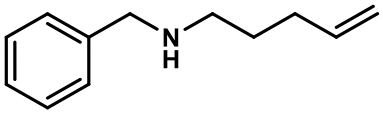

Benzylamine (29.430 g; 274.65 mmol) and 5-bromopent-1-ene (7.551 g; 50.67 mmol) were dissolved in EtOH (50 mL). Sodium iodide (0.378 g; 2.5 mmol) was added and the mixture was stirred overnight at 75°C. Afterwards the solvent was removed by rotary evaporation and the residue dissolved in H_2O (30 mL), which was removed again by rotary evaporation. This procedure was repeated twice. Afterwards the residue was dissolved in H_2O (30 mL each) and the solution was extracted 3 times with Et_2O (35 mL). The combined organic layers were dried over $MgSO_4$, filtered and the solvent removed by rotary evaporation. The residue was stirred over CaH_2 overnight and fractional distillation (9 mbar, 120°C) led to 5.328g of product (60% yield). The product was a colourless liquid.

^{1}H-NMR ($CDCl_3$, 400MHz): δ 7.29–7.17 (m, aryl-H, 4H), 5.82–5.72 (m, CH, 1H), 5.00–4.89 (m, CH_2, 2H), 3.73 (s, CH_2, 2H), 2.60 (t, *J* = 7.20 Hz, CH_2, 2H), 2.09–2.03 (m, CH_2, 2H), 1.60–1.52 (m, CH_2, 2H), 1.15 (s, NH, 1H).
The ^{1}H-NMR spectroscopic data is in agreement with the literature.[22]

Synthesis of N-allylpent-4-en-1-amine (5)[19]

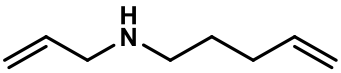

Allylamine (22.838 g; 399.99 mmol) and 5-bromopent-1-ene (15.096 g; 101.30 mmol) were heated to 70°C in a pressure tube and the mixture was stirred for 4 days at this temperature. Afterwards the solution was cooled to room temperature and H_2O (150 mL) was added. The reaction was extracted 3 times with Et_2O (50 mL).
The combined organic layers were dried over $MgSO_4$, filtered and the solvent was removed by rotary evaporation. The residue was stirred over CaH_2 for 2 hours and distilled (70°C, 30 mbar) leading to 7.352 g of the product (58% yield). The product was a colourless liquid.

^{1}H-NMR ($CDCl_3$, 400MHz): δ 5.93–5.75 (m, 2xCH, 2H), 5.17–4.91 (m, 2 CH_2, 4H), 3.24–3.21 (m, CH_2, 2H), 2.60 (t, *J* = 7.30 Hz, CH_2, 2H), 2.11–2.05 (m, CH_2, 2H), 1.61–1.54 (m, CH_2, 2H), 0.94 (s, NH, 1H).
The ^{1}H-NMR spectroscopic data is in agreement with the literature.[19]

Synthesis of 2,2-dimethylpent-4-enenitrile

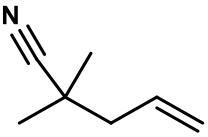

The synthesis followed a general procedure for the preparation of N-4-Pentenylurea.[23]
Diisopropylamine (1.789 g; 17.68 mmol) was dissolved in THF (150 mL) and cooled down to –78°C. n-BuLi-solution (2.5 *M* in hexane, 7.1 mL; 18 mmol) was added dropwise and the mixture was stirred one hour at –78°C and an additional hour at 0°C. Afterwards isobutyronitrile (1.222 g; 17.68 mmol) was added dropwise and the mixture was stirred for half an hour at 0°C. Allylbromide (2.244 g; 17.68 mmol) was added dropwise and the mixture was stirred for 13 hours at 0°C. Then the reaction was quenched by adding H_2O. The solution was extracted with Et_2O (3×50 ml), washed with brine (~35 mL) and dried over $MgSO_4$. The solvent was removed by rotary evaporation leading to 1.470 g of crude product (76% yield).

^{1}H-NMR ($CDCl_3$, 400MHz): δ 5.92–5.81 (m, CH, 1H), 5.24–5.16 (m, CH_2, 2H), 2.29–2.26 (dt, *J* = 7.3 Hz, 1.1 Hz, CH_2, 2H), 1.33 (s, 2 CH_3, 6H).

Synthesis of 2,2-dimethylpent-4-en-1-amine

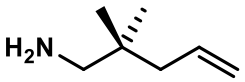

The synthesis followed a general procedure for the preparation of N-4-Pentenylurea.[23] $LiAlH_4$ (0.784 g; 20.7 mmol) was suspended in Et_2O (10 mL) and the suspension was cooled to –10°C. 2,2-Dimethylpent-4-enenitrile (1.470 g, 13.44 mmol) was dissolved in Et_2O (30 mL) and the solution was added dropwise to the suspension. Afterwards the mixture was heated to reflux and stirred for 18 h. The mixture was cooled down to –10°C and the reaction was quenched by dropwise addition of H_2O (1 mL), 15% NaOH-solution (1 mL) and H_2O (3 mL). The solution was filtered to remove LiOH and $Al(OH)_3$ and the solvent was removed by rotary evaporation. Distillation at reduced pressure (100 mbar, 70°C) led to 0.760 g (50% yield) of a colourless product.

^{1}H-NMR ($CDCl_3$, 400MHz): δ 5.76–5.70 (m, CH, 1H), 4.96–4.92 (m, CH_2, 2H), 2.36 (s, CH_2, 2H), 1.89 (d, *J* = 11.7 Hz, CH_2, 2H), 0.92 (s, NH_2, 2H), 0.77 (s, 2 CH_3, 6H).

Synthesis of *N*-(2,2-dimethylpent-4-en-1-yl)formamide

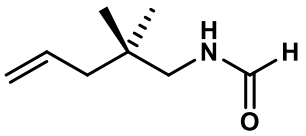

The synthesis followed a procedure for the synthesis of *N*-methyl-2,2-Diphenyl-4-penten-1-amine.[24]
2,2-Dimethylpent-4-en-1-amine (0.760 g, 6.72 mmol) and ethylformate (8.68 g, 117.2 mmol) were set to reflux for 3 days. After cooling down to room temperature, the excess of the formate was removed *via* rotary evaporation, giving 0.927 g of the crude product (99% yield).

^{1}H-NMR ($CDCl_3$, 400MHz): δ 7.45 (s, C(O)H, 1H), 5.10–4.98 (m, CH, 1H), 4.31–4.25 (m, CH_2, 2H), 2.20 (d, *J* = 6.80 Hz, NH, 1H), 1.22 (d, *J* = 7.5 Hz, CH_2, 2H), 0.53 (t, *J* = 7.20 Hz, CH_2, 2H), 0.13 (s, 2 CH_3, 6H).

Synthesis of N,2,2-trimethylpent-4-en-1-amine (6)

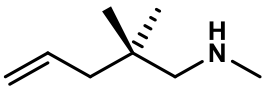

The synthesis followed a procedure for the synthesis of *N*-methyl-2,2-diphenyl-4-penten-1-amine.[24]
$LiAlH_4$ (0.930 g; 24.5 mmol) was suspended in Et_2O (15 mL) and the suspension was cooled to –10°C. *N*-(2,2-dimethylpent-4-en-1yl)formamide (0.927 g; 6.56 mmol) was

dissolved in Et_2O (30 mL) and the solution was added dropwise to the suspension. Afterwards the mixture was heated to reflux and stirred at this temperature for 9 h. The mixture was cooled down to –10°C again and the reaction was quenched by dropwise addition of H_2O (1 mL), 15% NaOH-solution (1 mL) and H_2O (3 mL). The solution was filtered and the solvent was removed by rotary evaporation. Distillation at reduced pressure (100 mbar, 70°C) led to 0.546 g of product. (65% yield). The product was a colorless liquid.

^{1}H-NMR ($CDCl_3$, 400MHz): δ 5.83–5.76 (m, CH, 1H), 5.02–4.97 (m, CH_2, 2H), 2.41 (s, CH_3, 3H), 2.31 (s, CH_2, 2H), 2.00–1.97 (m, CH_2, 2H), 0.87 (s, 2 CH_3, 6H), 0.72 (s, NH, 1H).

Synthesis of *N*-deutero-*N*-methylpent-4-en-1-amine (3-*d*)

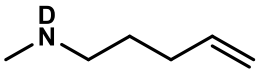

Following a procedure for the synthesis of [D_2]-1-Phenylpent-4-en-1-amine,[25] *N*-methylpent-4-en-1-amine (2.001 g; 20.2 mmol) was dissolved in pentane (5 mL) in a pressure tube and D_2O (2 mL) was added. The mixture was heated to 60°C and stirred overnight. Afterwards the mixture was allowed to cool to room temperature and the aqueous layer was discarded. This procedure was repeated twice with fresh D_2O. The organic layer was dried over $MgSO_4$, filtered and the solvent was removed by rotary evaporation (room pressure, 55°C). For both, the organic and the aqueous, solvents ^{1}H-NMR measurements were taken, to ensure that there was no product left, before they were discarded. The deuterated amine was stirred over CaH_2 overnight and distilled at reduced pressure (350 mbar, 75°C) leading to 0.301g of a colourless, liquid product (14% yield).

^{1}H-NMR ($CDCl_3$, 400MHz): δ 5.82–5.75 (m, CH, 1H), 5.02–4.91 (m, CH_2, 2H), 2.54 (t, *J* = 7.30 Hz, CH_2, 2H), 2.38 (s, CH_3, 3H), 2.09–2.03 (m, CH_2, 2H), 1.59–1.51 (m, CH_2, 2H).

Synthesis of *N*-deutero-*N*-benzylpent-4-en-1-amine (4-*d*)

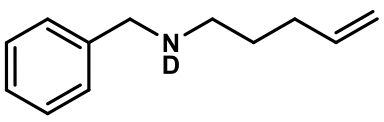

Following a procedure for the synthesis of [D_2]-1-Phenylpent-4-en-1-amine,[25] *N*-benzylpent-4-en-1-amine (1.001 g; 5.711 mmol) was dissolved in hexane (10 mL) and D_2O (5 ml) was added. The mixture was heated to 60°C and stirred overnight. Afterwards the mixture was allowed to cool to room temperature and the aqueous layer was discarded. This procedure was repeated twice with fresh D_2O. The organic layer was dried over $MgSO_4$, filtered and the solvent was removed by rotary evaporation. The deuterated amine was dried over freshly activated mole-sieves, filtered and dried over CaH_2 overnight and distilled at reduced pressure (9 mbar, 120°C), leading to 0.670 g of a colourless, liquid product (67% yield).

^{1}H-NMR ($CDCl_3$, 400MHz): δ 7.30–7.18 (m, aryl-H, 5H), 5.83–5.72 (m, CH, 1H), 5.00–4.89 (m, CH_2, 2H), 3.74 (s, CH_2, 2H), 2.60 (t, *J* = 7.10 Hz, CH_2, 2H), 2.09–2.04 (m, CH_2, 2H), 1.61–1.53 (m, CH_2, 2H).

Synthesis of *N*-deutero-*N*-allylpent-4-en-1-amine (5-*d*)

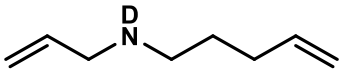

Following a procedure for the synthesis of [D_2]-1-Phenylpent-4-en-1-amine,[25] *N*-allylpent-4-en-1-amine (7.350 g; 58.70 mmol) was dissolved in hexane (10 mL) and D_2O (5 mL) was added. The mixture was heated to 60°C and stirred overnight. Afterwards the mixture was allowed to cool to room temperature and the aqueous layer was discarded. This procedure was repeated twice with fresh D_2O. The organic layer was dried over $MgSO_4$, filtered and the solvent was removed by rotary evaporation. The deuterated amine was dried over freshly activated mole-sieves, filtered and dried over CaH_2 overnight and distilled at reduced pressure (60°C, 33 mbar) leading to 5.002 g of a colourless, liquid product (67% yield).

^{1}H-NMR ($CDCl_3$, 400MHz): δ 5.93–5.75 (m, 2*CH, 2 H), 5.17–4.91 (m, 2 CH_2, 4H), 3.23-3.20 (m, CH_2, 2H), 2.59 (t, *J* = 7.10 Hz CH_2, 2H), 2.11–2.05 (m, CH_2, 2H), 1.61–1.53 (m, CH_2, 2H).

General procedure for hydroamination and hydroamination/carbocylziation

The amine was weighed into an NMR-tube and dissolved in deuterated benzene and a catalytic amount (mostly 5 or 10 mol%) of precatalyst was added. Ferrocene was added as internal standard. The reaction was monitored by ^{1}H-NMR spectroscopy either automatically with a certain time interval with the Bruker Avance III HD 700 MHz when measurements were accumulated over night or at various temperatures or with the Bruker AVIII 400 where the measurements were started manually at certain intervalls. The measurements were taken with a zg30 puls-sequence, 6.5 µsec delay and 8 pulses per measurement. Additional information on the individual measurements is provided in Table 15 in the supplementary information.

1,2-Dimethylpyrrolidine (7)

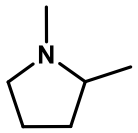

^{1}H-NMR (C_6D_6, 400MHz): δ 2.96 (td, *J* = 8.50 Hz, 2.10 Hz, CH, 1H), 2.19 (s, CH_3, 3H), 2.02–1.94 (m, CH_2, 2H), 1.77–1.64 (m, CH_2, 2H), 1.47–1.33 (m, CH_2, 2H), 1.05 (d, *J* = 5.90 Hz, CH_3, 3H); **^{13}C{^{1}H}-NMR (C_6D_6, 100MHz):** δ 61.5 (NCH), 57.5 (NCH_2), 40.2 (NCH_3), 33.6 (CH_2), 22.0 (CH_2), 19.2 (CH_3).
The NMR spectroscopic data is in agreement with the literature.[22]

2-Methyl-1-(methyl-*d*)pyrrolidine (7-*d*)

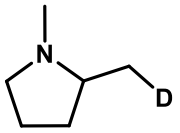

^{1}H-NMR (C_6D_6, 400MHz): δ 2.99–2.95 (td, *J* = 8.50 Hz, 2.00 Hz, CH, 1H), 2.20 (s, CH_3, 3H), 2.03–1.91 (m, CH_2, 2H), 1.75–1.67 (m, CH_2, 2H), 1.46–1.31 (m, CH_2, 2H), 1.06–1.03 (m, CH_2D, 2H); **^{13}C[^{1}H]-NMR (C_6D_6, 100MHz): δ** 61.7 (NCH), 57.7 (NCH_2), 40.5 (NCH_3), 33.8 (CH_2), 22.3 (CH_2), 19.2 (CH_2D, $J_{C,D}$ = 19.8 Hz).

1-Benzyl-2-methylpyrrolidine (8)

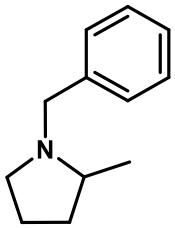

^{1}H-NMR (C_6D_6, 400MHz): δ 7.22–7.09 (m, aromatic, 5H), 3.96–3.93 (m, CH_2, 1H), 3.01–2.98 (m, CH_2, 1H), 2.93–2.88 (m, CH, 1H), 2.29–2.21 (m, CH_2, 1H), 1.98–1.91 (m, CH_2, 1H), 1.77–1.56 (m, CH_2, 2H), 1.43–1.30 (m, CH_2, 2H), 1.08 (d, *J* = 6.00 Hz, CH_3, 3H); **^{13}C{^{1}H}-NMR (C_6D_6, 100MHz):** δ

140.9 (C, aromatic), 128.9 (2 CH, aromatic), 128.4 (2 CH, aromatic), 126.9 (CH, aromatic) 59.8 (NCH), 58.6 (NCH_2), 54.3 (NCH_2), 33.3 (CH_2), 22.0 (CH_2), 19.5 (CH_3).
The NMR spectroscopic data is in agreement with the literature.[22]

1,2,4,4-Tetramethylpyrrolidine (9)

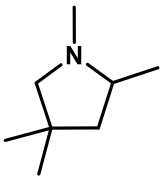

^{1}H-NMR (C_6D_6, 400MHz): δ 2.70–2.68 (m, CH_2, 1H), 2.16 (s, CH_3, 3H), 2.12–2.09 (m, CH, 1H), 1.93–1.90 (m, CH_2, 1H), 1.62–1.57 (m, CH_2, 1H), 1.27–1.22 (m, CH_2, 1H), 1.16 (s, CH_3, 3H), 1.06–1.04 (d, J = 6.10 Hz, CH_3, 3H), 0.95 (s, CH_3, 3H).

2-Methylhexahydro-1*H*-pyrrolizine (10)

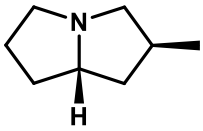

Isomer 1
"cis"

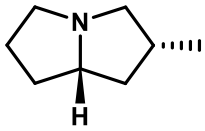

Isomer 2
"trans"

^{13}C{^{1}H}-NMR (C_6D_6, 100MHz):
Isomer 1 (“cis”): δ 64.4 (NCH), 63.1 (NCH_2), 56.6 (NCH_2), 41.3 (CH_2), 33.4 (CH_2), 32.9 (CH), 27.2 (CH_2), 18.4 (CH_3);
Isomer 2 (“trans”): δ 65.7 (NCH), 64.3 (NCH_2), 55.7 (NCH_2), 42.8 (CH_2), 37.4 (CH), 33.9 (CH_2), 26.8 (CH_2), 17.9 (CH_3).
The ^{13}C{^{1}H}-NMR spectroscopic data is in agreement with the literature.[19]

2-(Methyl-*d*)hexahydro-1*H*-pyrrolizine (10-*d*)

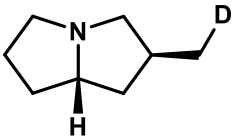

Isomer 1
"cis"

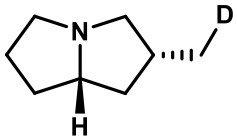

Isomer 2
"trans"

^{13}C{^{1}H}-NMR (C_6D_6, 100MHz):
Isomer 1 (“cis”): δ 64.5 (NCH), 63.28 (NCH_2), 56.65 (NCH_2), 41.40 (CH_2), 33.45 (CH_2), 32.89 (CH), 27.29 (CH_2), 18.3 (CH_2D, $J_{C,D}$ = 19.1 Hz);
Isomer 2 (“trans”): δ 65.8 (NCH), 64.5 (NCH_2), 55.8 (NCH_2), 42.8 (CH_2), 37.5 (CH); 34.0 (CH_2), 26.9 (CH_2), 17.7 (CH_2D, $J_{C,D}$ = 19.1 Hz).

1-Allyl-2-methylpyrrolidine (11)

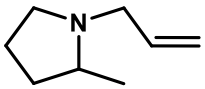

^{1}H-NMR (C_6D_6, 400MHz): δ 5.99–5.93 (m, CH, 1H), 5.20–5.01 (m, CH_2, 2H), 3.44–3.40 (m, CH, 1H), 3.11–2.99 (m, CH_2, 1H), 2.64–2.59 (m, CH_2, 1H), 2.21–2.15 + 2.04–1.97 (m, CH_2, 2H), 1.75–1.64 (m, CH_2, 2H), 1.49–1.44 (m,CH_2, 1H), 1.37–1.31 (m, CH_2, 1H), 1.04 (d, *J* = 6.00 Hz, CH_3, 3H); **^{13}C{^{1}H}-NMR (C_6D_6, 100MHz):** δ 137.3 (CH), 116.1 (CH_2), 68.6 (NCH), 57.5 (NCH_2), 54.7 (NCH_2), 33.7 (CH_2), 22.5 (CH_2), 19.9 (CH_3).

1-Allyl-2-(methyl-*d*)pyrrolidine (11-*d*)

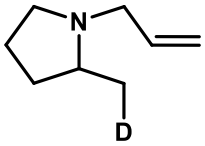

^{1}H-NMR (C_6D_6, 400MHz): δ 5.97–5.70 (m, CH, 1H), 5.20–4.97 (m, CH_2, 2H), 3.44–3.39 (m, CH, 1H), 3.09–2.99 (m,CH_2, 1H), 2.64–2.59 (m, CH_2, 1H), 2.21–2.14 (m, CH_2, 1H), 2.04–1.97 (m, CH_2, 2H), 1.76–1.60 (m, CH_2, 2H), 1.52–1.33 (m, CH_2, 2H), 1.05–1.01 (m, CH_2D, 2H); **^{13}C{^{1}H}-NMR (C_6D_6, 100MHz):** δ 137.3 (CH), 116.1 (CH_2), 68.6 (NCH), 57.5 (NCH_2), 54.7 (NCH_2), 33.7 (CH_2), 22.5 (CH_2), 19.6 (CH_2D, $J_{C,D}$ = 19.1 Hz).

9 References

(1) Gómez-Gallego, M.; Sierra, M. A. *Chem. Rev.* **2011**, *111*, 4857–4963.

(2) Gribkov, D. V; Hultzsch, K. C.; Hampel, F. *J. Am. Chem. Soc.* **2006**, *128*, 3748.

(3) Müller, T. E.; Hultzsch, K. C.; Yus, M.; Foubelo, F.; Tada, M. *Chem. Rev.* **2008**, *108*, 3795–3892.

(4) Hong, S.; Marks, T. J. *Acc. Chem. Res.* **2004**, *37*, 673–686.

(5) Reznichenko, A. L.; Hultzsch, K. C. *Org. React.* **2016**, *88*, 1–554.

(6) Gagne, M. R.; Stern, C. L.; Marks, T. J. *J. Am. Chem. Soc.* **1992**, *114*, 275–294.

(7) Motta, A.; Lanza, G.; Fragalà, I. L.; Marks, T. J. *Organometallics* **2004**, *23* (17), 4097–4104.

(8) Leitch, D. C.; Platel, R. H.; Schafer, L. L. *J. Am. Chem. Soc.* **2011**, *133* (39), 15453–15463.

(9) Manna, K.; Everett, W. C.; Schoendorff, G.; Ellern, A.; Windus, T. L.; Sadow, A. D. *J. Am. Chem. Soc.* **2013**, *135* (19), 7235–7250.

(10) Manna, K.; Xu, S.; Sadow, A. D. *Angew. Chemie - Int. Ed.* **2011**, *50* (8), 1865–1868.

(11) Manna, K.; Kruse, M. L.; Sadow, A. D. *ACS Catal.* **2011**, *1* (Iii), 1637–1642.

(12) Manna, K.; Kruse, M. L.; Sadow, A. D. *ACS Catal.* **2011**, *1* (11), 1637–1642.

(13) Tobisch, S. *Inorg. Chem.* **2012**, *51* (6), 3786–3795.

(14) Tobisch, S. *Dalt. Trans.* **2012**, *41* (30), 9182.

(15) Sven, T. *Chem. - A Eur. J.* **2015**, *21* (18), 6765–6779.

(16) Tobisch, S. *Chem. - A Eur. J.* **2011**, *17* (52), 14974–14986.

(17) Zhang, X.; Tobisch, S.; Hultzsch, K. C. *Chem. - A Eur. J.* **2015**, *21* (21), 7841–7857.

(18) Li, Y.; Marks, T. J. *J. Am. Chem. Soc.* **1996**, *118*, 707–708.

(19) Li, Y.; Marks, T. J. *J. Am. Chem. Soc.* **1998**, *120*, 1757–1771.

(20) Molander, G. A.; Pack, S. K. *Tetrahedron* **2003**, *59*, 10581–10591.

(21) Molander, G. A.; Pack, S. K. *J. Org. Chem.* **2003**, *68*, 9214–9220.

(22) Gribkov, D. V.; Hultzsch, K. C. *Angew. Chem.* **2004**, *43*, 5542–5546.

(23) Tamaru, Y.; Hojo, M.; Higashimura, H.; Yoshida, Z. *J. Am. Chem. Soc.* **1988**, *110*, 3994–4002.

(24) Stubbert, B. D.; Marks, T. J. *J. Am. Chem. Soc.* **2007**, *129*, 4253–4271.

(25) Reznichenko, A. L.; Hampel, F.; Hultzsch, K. C. *Chem. - A Eur. J.* **2009**, *15*, 12819–12827.
(26) Kortman, G. D.; Orr, M. J.; Hull, K. L. *Organometallics* **2015**, *34*, 1013–1016.
(27) Beswick, C. L.; Marks, T. J. *Organometallics* **1999**, *18*, 2410–2412.
(28) Jeske, G.; Lauke, H.; Mauermann, H.; Swepston, P. N.; Schumann, H.; Marks, T. J. *J. Am. Chem. Soc.* **1985**, *107*, 8091.

10 Appendix

Supplementary Information

Table 15 –Supplementary Information on the Kinetical Experiments

Entry	substr.	cat.	T [°C]	subst. [mg]	cat. [mg]	C_6D_6 [ml]	[subst.] [mol L^{-1}]	[cat.] [mol L^{-1}]	[cat.] [subst.]$^{-1}$ [%]	t [h]	conversion (at t [h])	measuring intervall [min]
1	(**3**)	(**1**)	21 to 60	9,9	1,7	0,6	0,17	0,005	3	24,9	50%	~60
2	(**3**)	(**1**)	25	29,8	8,7	0,6	0,50	0,025	5	3,84	95%	15
3	(**3**)	(**1**)	30	29,9	8,8	0,6	0,50	0,025	5	3,29	97%	10
4	(**3**)	(**1**)	40	29,6	8,7	0,6	0,50	0,025	5	1,22	98%	5
5	(**3**)	(**1**)	45	29,7	8,7	0,6	0,50	0,025	5	0,89	92%	2
6	(**3**)	(**1**)	21	30,1	17,6	0,6	0,51	0,051	10	0,94	66%	~30
7	(**3**)	(**2**)	21	29,9	17,3	0,6	0,50	0,025	5	6,72	40%	~60
8	(**3**)	(**2**)	25	29,9	17,4	0,6	0,50	0,025	5	9,97	62%	5
9	(**3**)	(**2**)	50	29,8	17,4	0,6	0,50	0,025	5	1,7	98%	2
10	(**4**)	(**1**)	21	53,2	17,5	0,6	0,51	0,050	10	9,39	5%	~30
11	(**4**)	(**1**)	150	53,1	17,4	0,6	0,50	0,050	10	32,5	14%	~30
12	(**4**)	(**2**)	21	53,1	34,5	0,6	0,50	0,050	10	1,68	98%	~30
13	(**4**)	(**2**)	21	53,0	34,6	0,6	0,50	0,050	10	9,93	97%	~30
14	(**5**)	(**1**)	20	31,1	7,2	0,5	0,50	0,025	5	6,07	87%	5
15	(**5**)	(**1**)	25	31,4	7,3	0,5	0,50	0,025	5	4,63	93%	5
16	(**5**)	(**1**)	30	31,2	7,2	0,5	0,50	0,025	5	4,85	95%	15
17	(**5**)	(**1**)	40	31,1	7,2	0,5	0,50	0,025	5	2,31	96%	5
18	(**5**)	(**1**)	45	31,0	7,2	0,5	0,50	0,025	5	3,07	97%	2

Entry	subst.	cat.	T [°C]	subst. [mg]	cat. [mg]	C_6D_6 [ml]	[subst.] [mol L^{-1}]	[cat.] [mol L^{-1}]	[cat.] [subst.]$^{-1}$ [%]	t [h]	conversion (at t [h])	measuring intervall [min]
19	(**5**)	(**1**)	21	31,1	14,2	0,5	0,50	0,049	10	6,18	96%	~30
20	(**5**)	(**2**)	21	38	17	1	0,50	0,025	5	9,8	80%	~30
21	(**5**)	(**2**)	21	38	35	1	0,50	0,050	10	2,1	97%	~30
22	(**6**)	(**1**)	21	32	7,3	1	0,50	0,025	5	4,8	88%	–
23	(**6**)	(**2**)	21	32	15	1	0,50	0,025	5	0,2	100%	~30
24	(**3-*d***)	(**1**)	25	29,9	8,7	0,6	0,50	0,025	5	14,63	64%	30
25	(**3-*d***)	(**1**)	40	30,0	8,7	0,6	0,50	0,025	5	7,82	85%	15
26	(**3-*d***)	(**1**)	60	30,2	8,8	0,6	0,50	0,025	5	8,58	36%	15
27	(**3-*d***)	(**1**)	21	30	17,3	0,6	0,50	0,050	10	9,22	85%	~30
28	(**4-*d***)	(**1**)	21	53	17,4	0,6	0,50	0,050	10	9,55	0%	~30
29	(**4-*d***)	(**2**)	21	53	34,5	0,6	0,50	0,050	10	8,02	0%	~30
30	(**4-*d***)	(**2**)	150	53,1	34,5	0,6	0,50	0,050	10	8,54	0%	~30
31	(**5-*d***)	(**1**)	21	38,1	8,7	0,6	0,50	0,025	5	8,49	38%	~30
32	(**5-*d***)	(**1**)	21	37,9	17,5	0,6	0,50	0,050	10	8,63	65%	~30
33	(**5-*d***)	(**2**)	21	38,0	35	0,6	0,50	0,050	10	9,79	55%	~30

NMRs

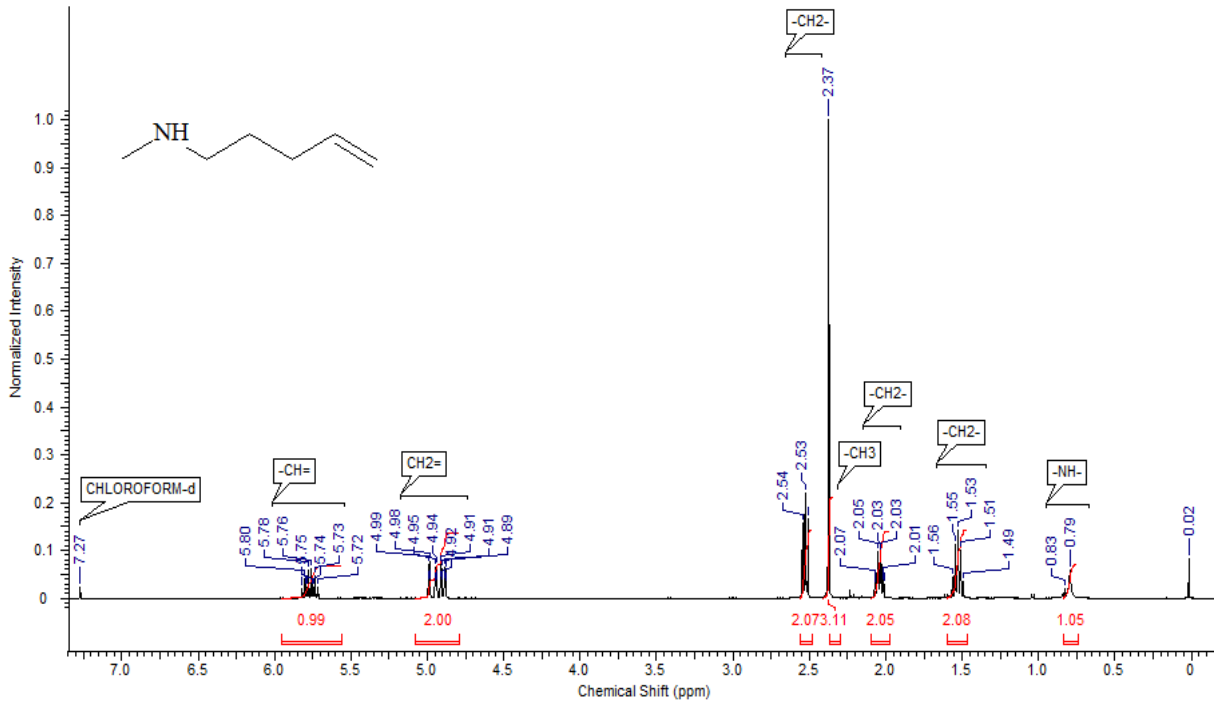

*Figure 36 – ^{1}H-NMR spectrumof N-methylpent-4-en-1-amine (**3**) in $CDCl_3$ at 25°C*

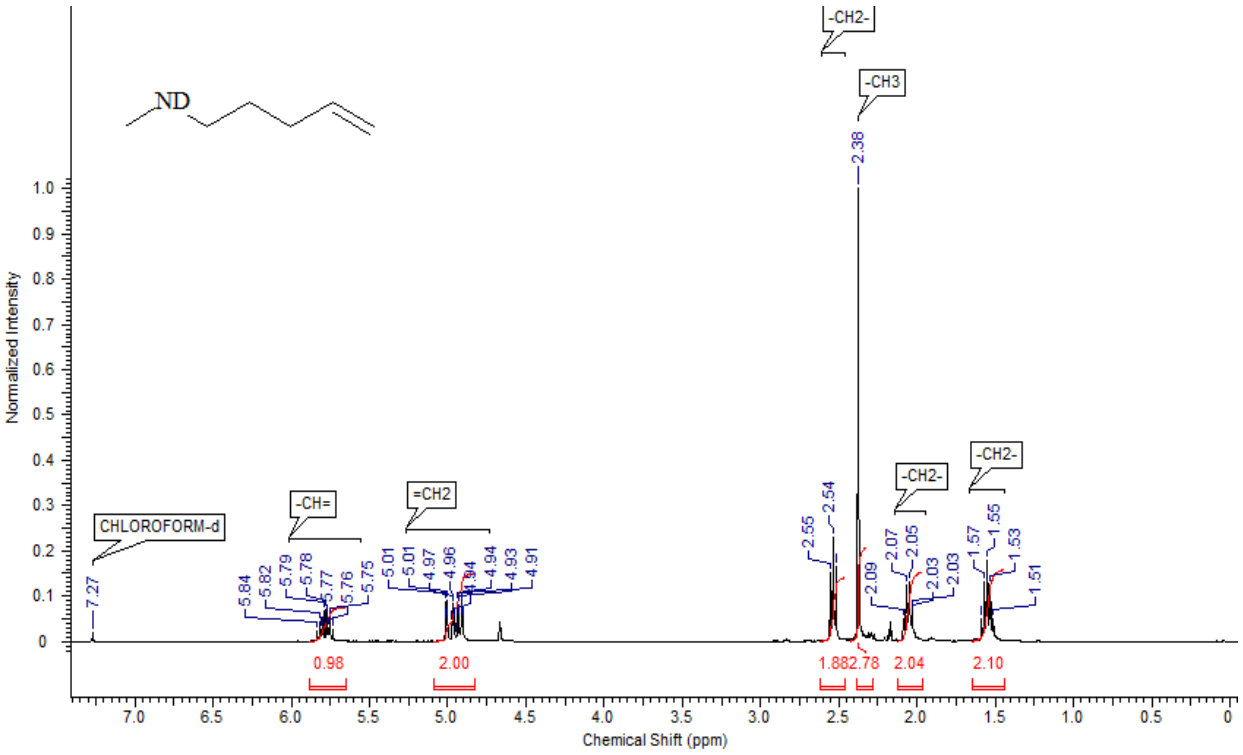

*Figure 37 – ^{1}H-NMR spectrum of N-deutero-N-methylpent-4-en-1-amine (**3-d**) in $CDCl_3$ at 25°C*

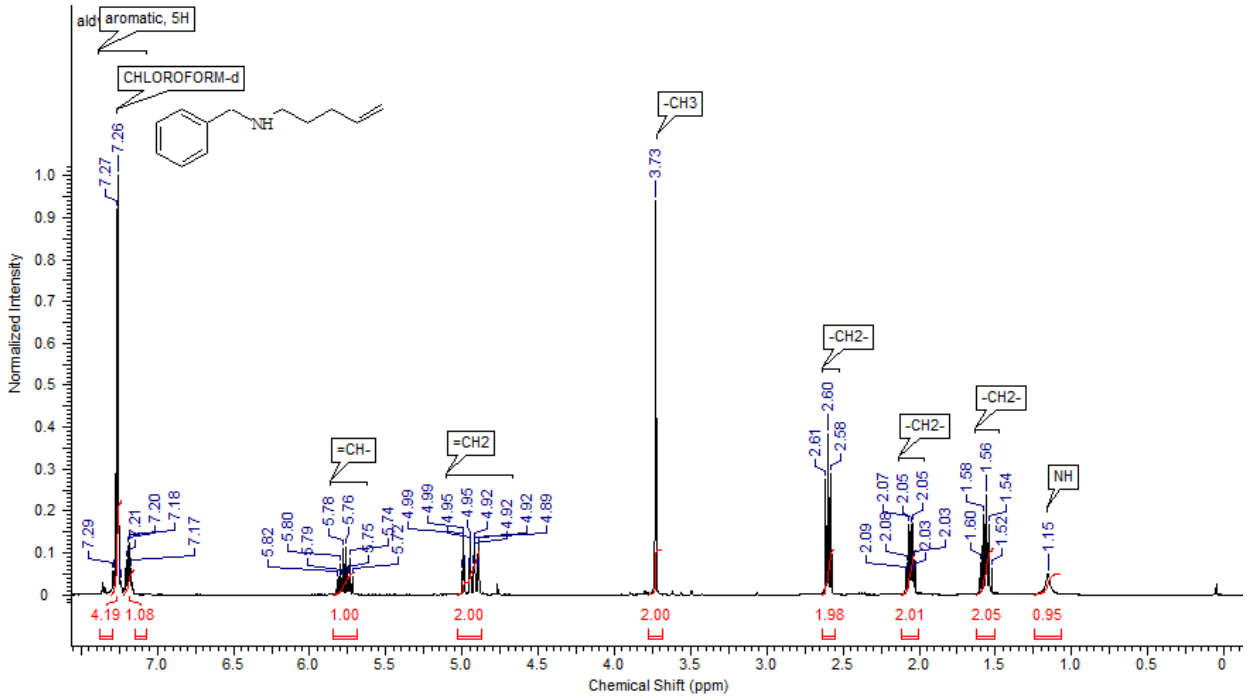

*Figure 38 – ^{1}H-NMR spectrum of N-benzylpent-4-en-1-amine (**4**) in $CDCl_3$ at 25°C*

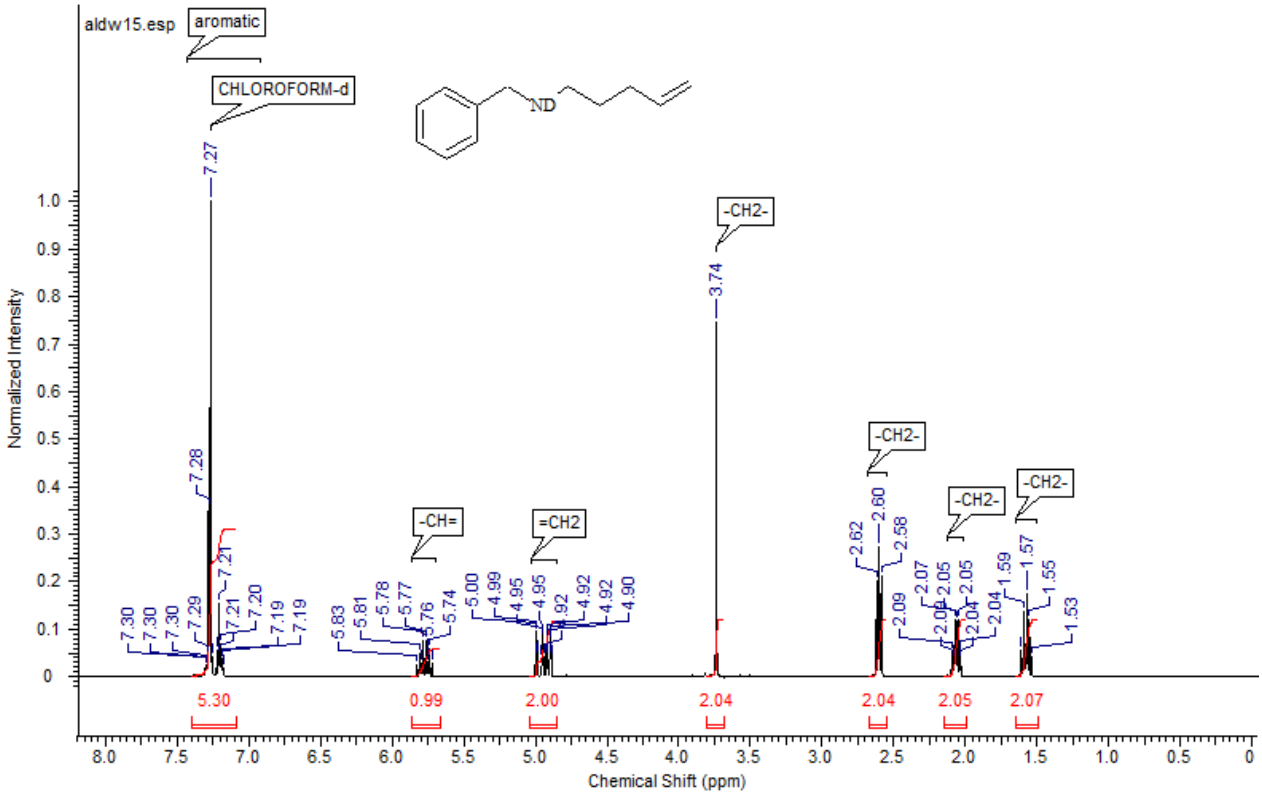

*Figure 39 – ^{1}H-NMR spectrum of N-deutero-N-benzylpent-4-en-1-amine (**4-d**) in $CDCl_3$ at 25°C*

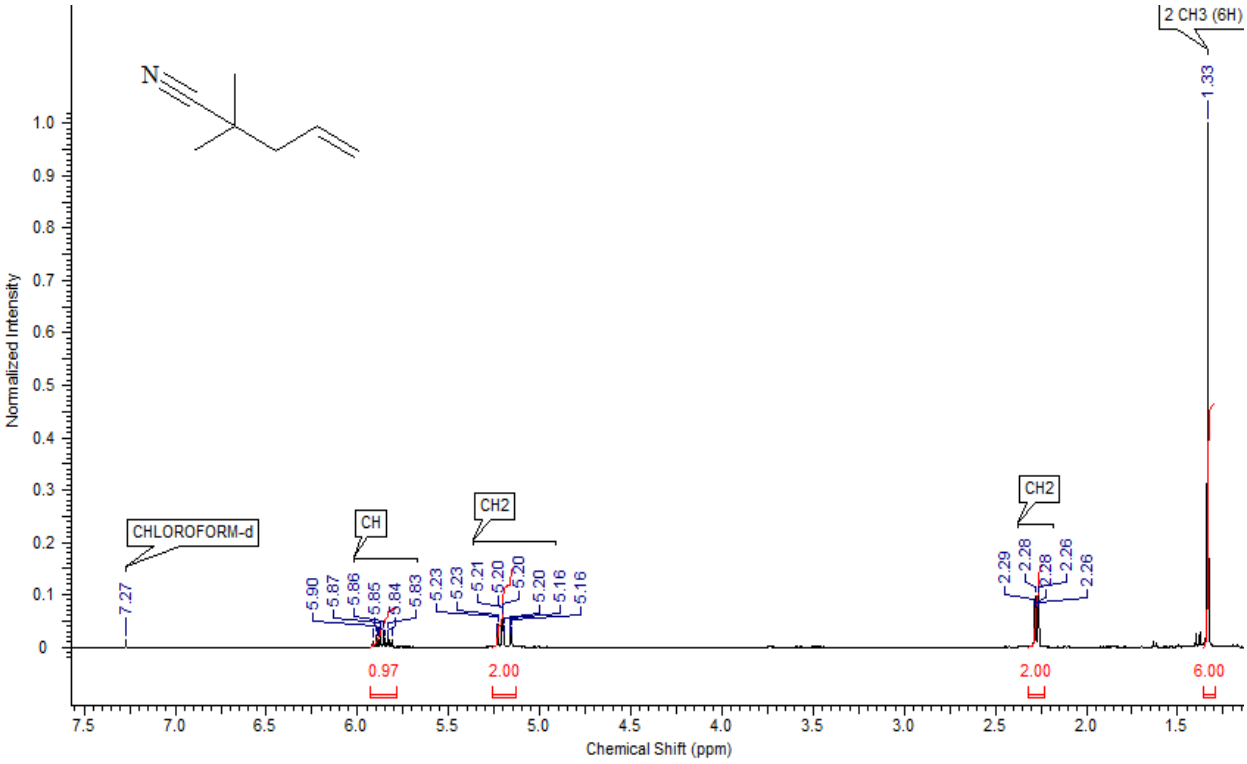

Figure 40 – ^{1}H-NMR spectrum of 2,2-dimethylpent-4-enenitrile in $CDCl_3$ at 25°C

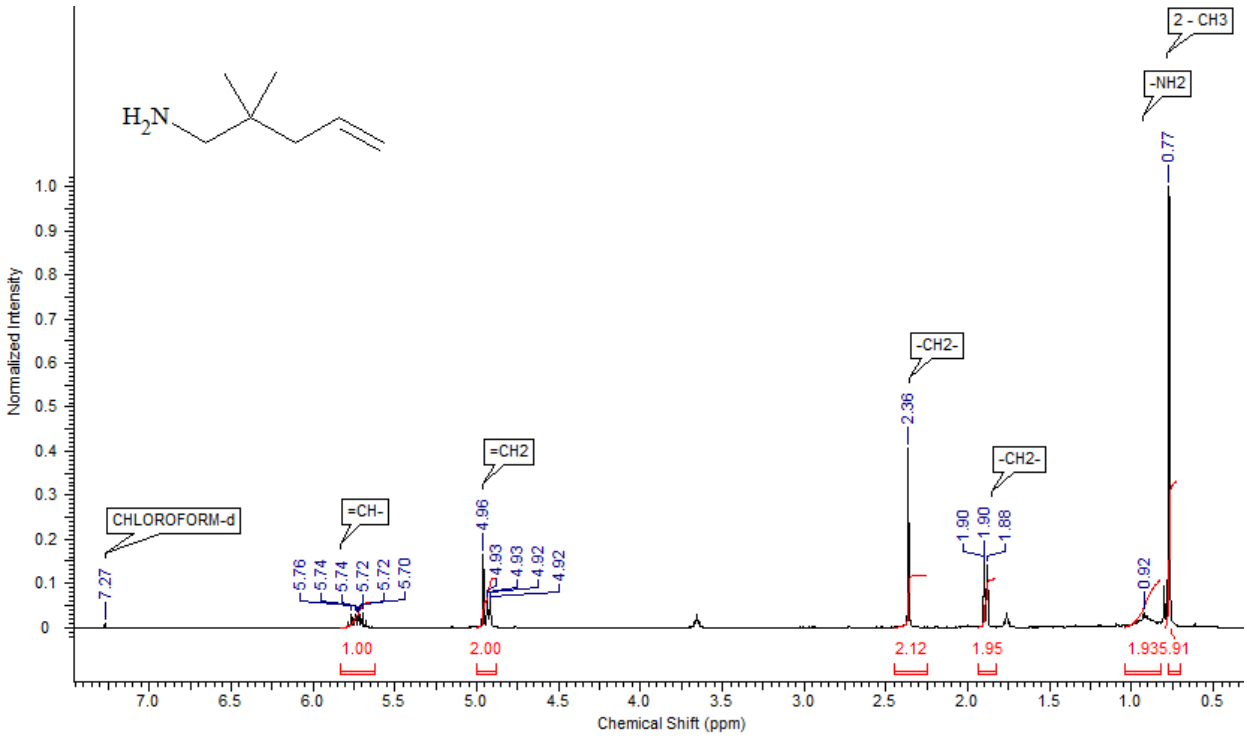

Figure 41 – ^{1}H-NMR spectrum of 2,2-dimethylpent-4-en-1-amine in $CDCl_3$ at 25°C

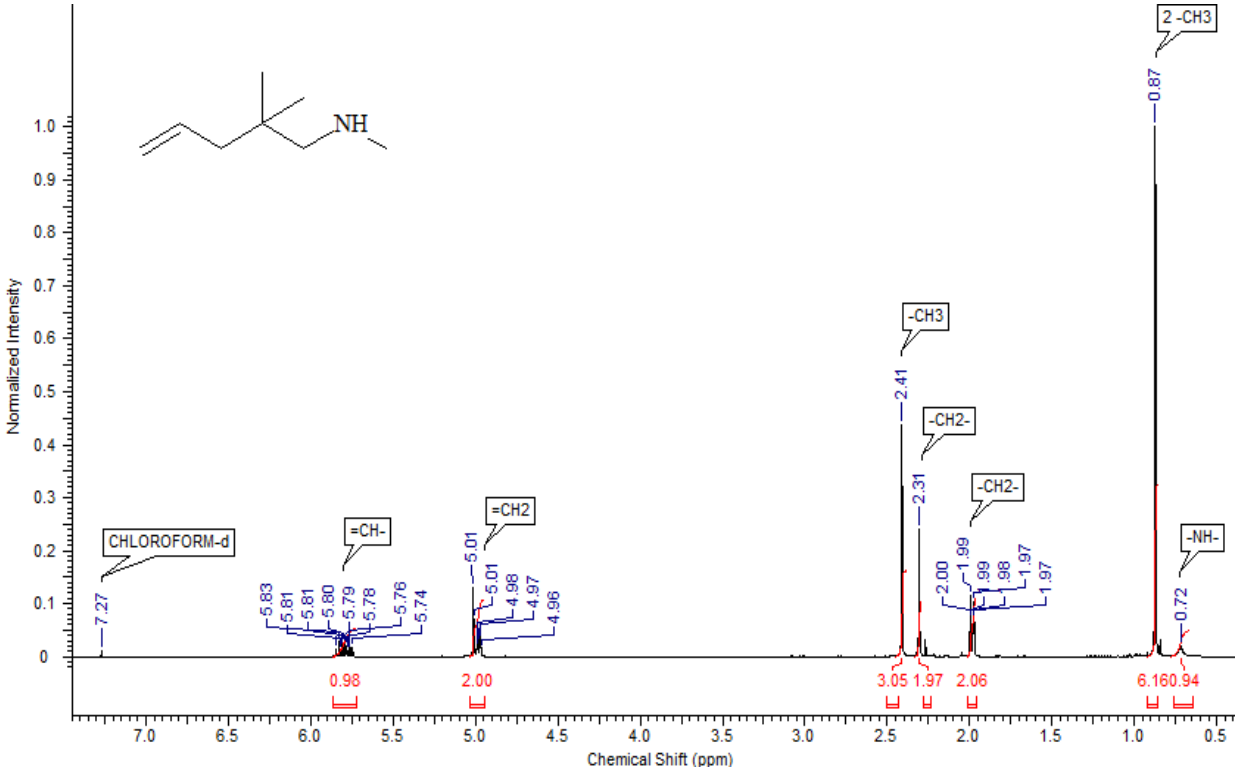

*Figure 42 – ^{1}H-NMR spectrum of N,2,2-trimethylpent-4-en-1-amine (**6**) in $CDCl_3$ at 25°C*

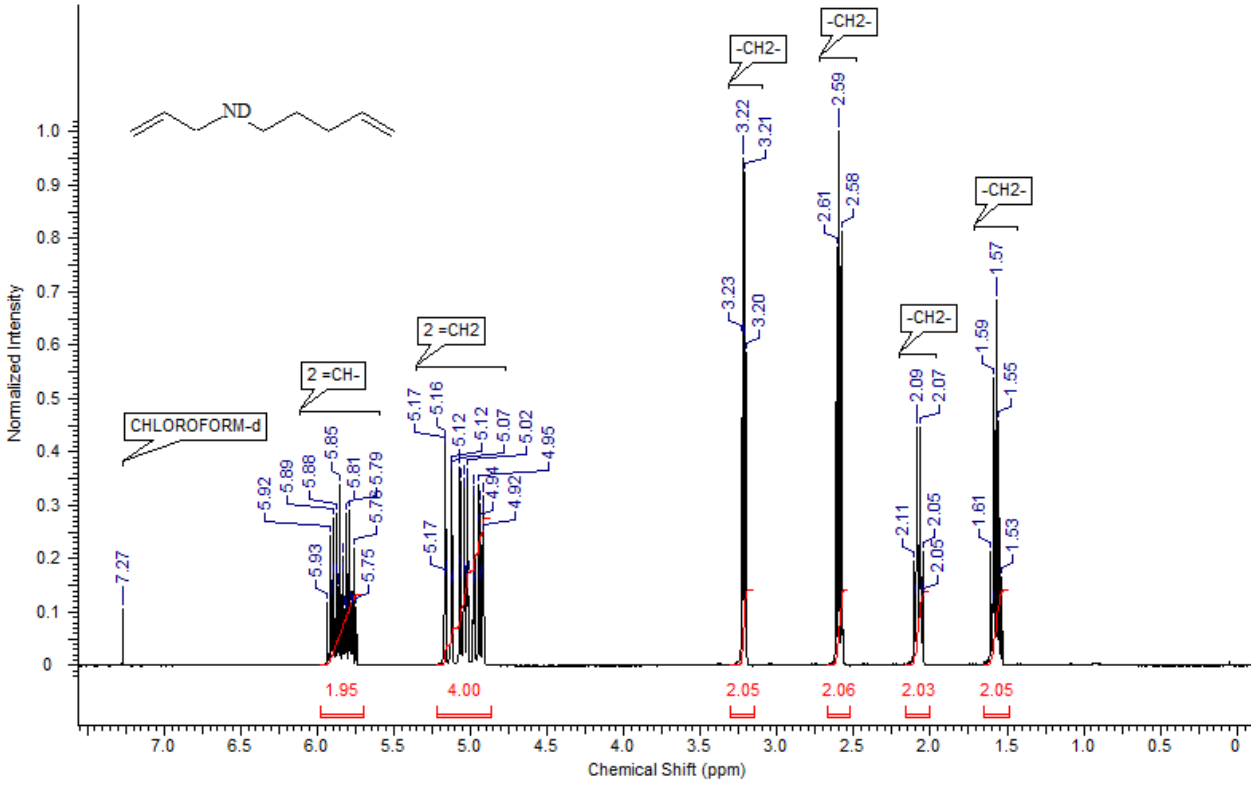

*Figure 43 – ^{1}H-NMR spectrum of N-deutero-N-allylpent-4-en-1-amine (**5-d**) in $CDCl_3$ at 25°C*

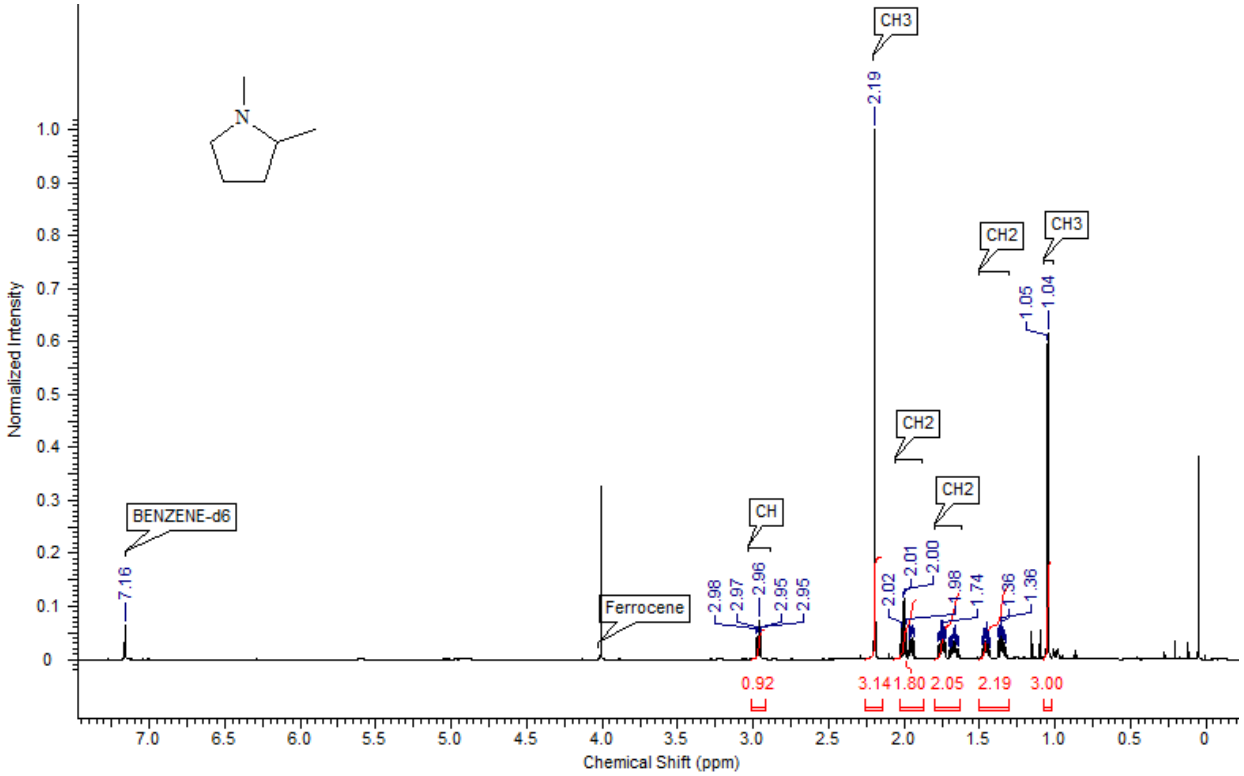

*Figure 44 – ^{1}H-NMR spectrum of 1,2-dimethylpyrrolidine (**7**) in C_6D_6 at 25°C*

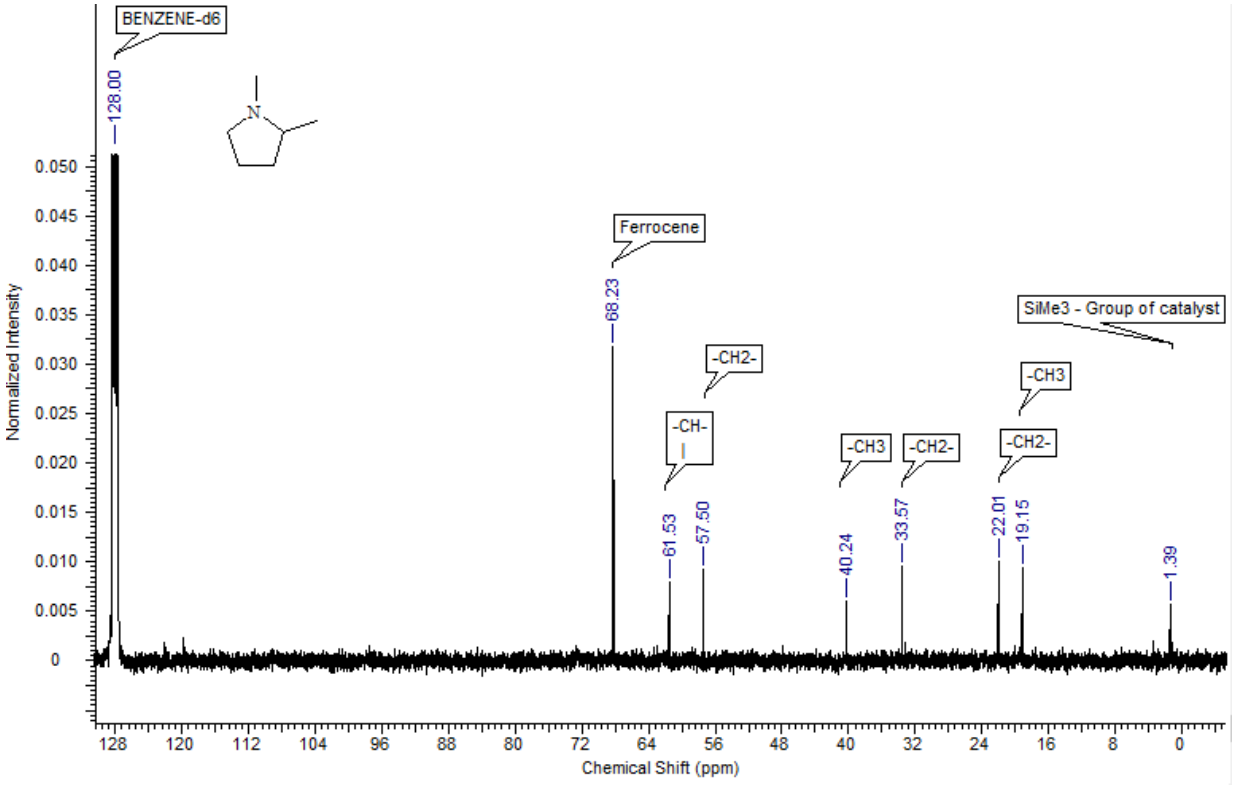

*Figure 45 – $^{13}C\{^{1}H\}$-NMR spectrum of 1,2-dimethylpyrrolidine (**7**) in C_6D_6 at 25°C*

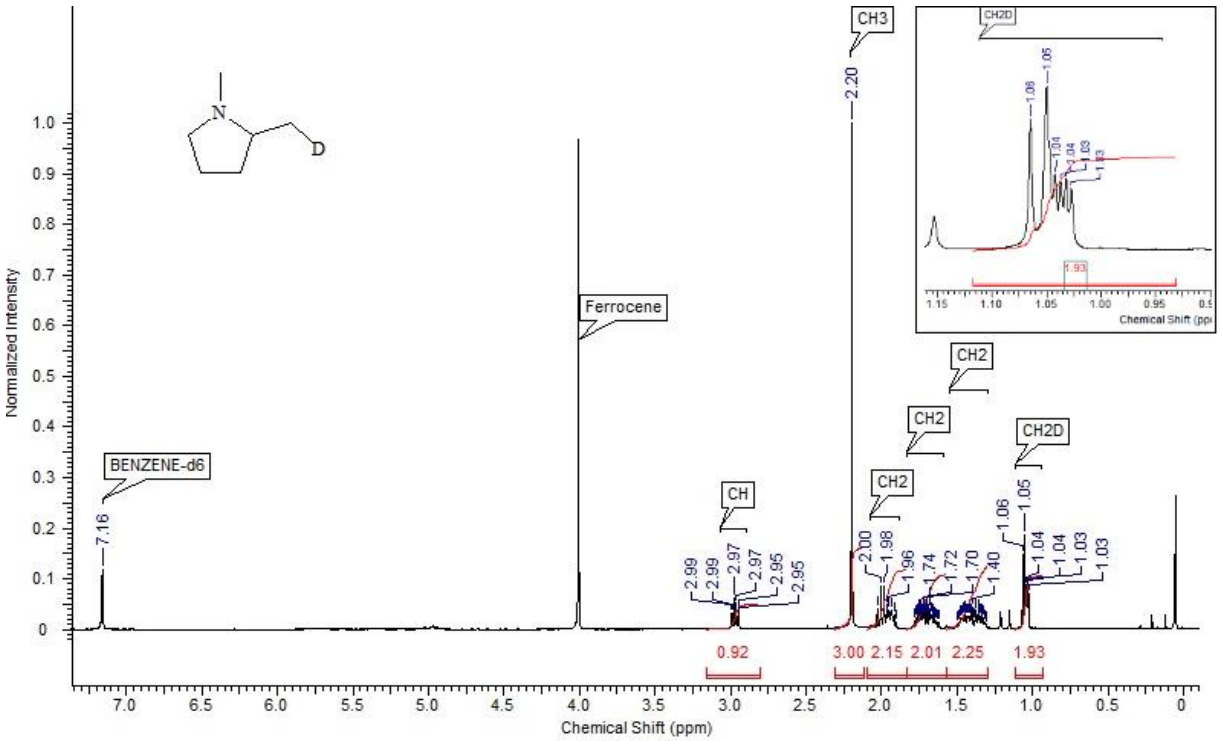

*Figure 46 – ^{1}H-NMR spectrum of 2-methyl-1-(methyl-d)pyrrolidine (**7-d**) in C_6D_6 at 25°C*

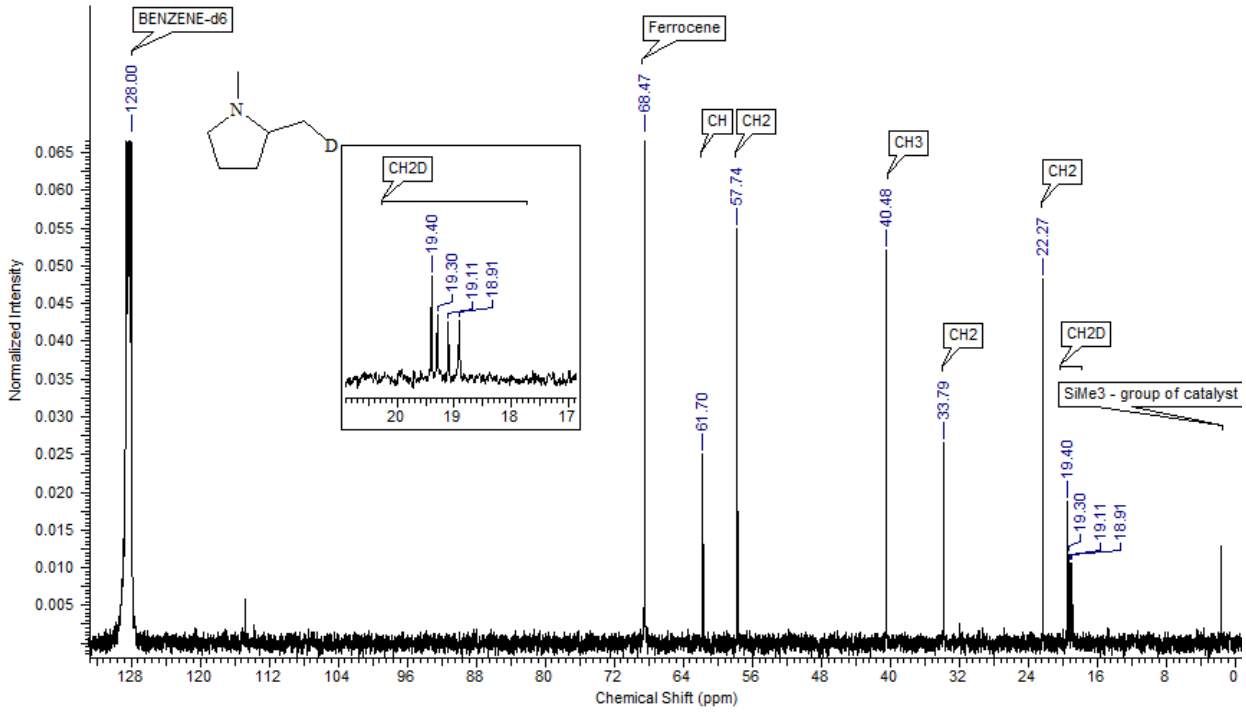

*Figure 47 – $^{13}C\{^{1}H\}$-NMR spectrum of 2-methyl-1-(methyl-d)pyrrolidine (**7-d**) in C_6D_6 at 25°C*

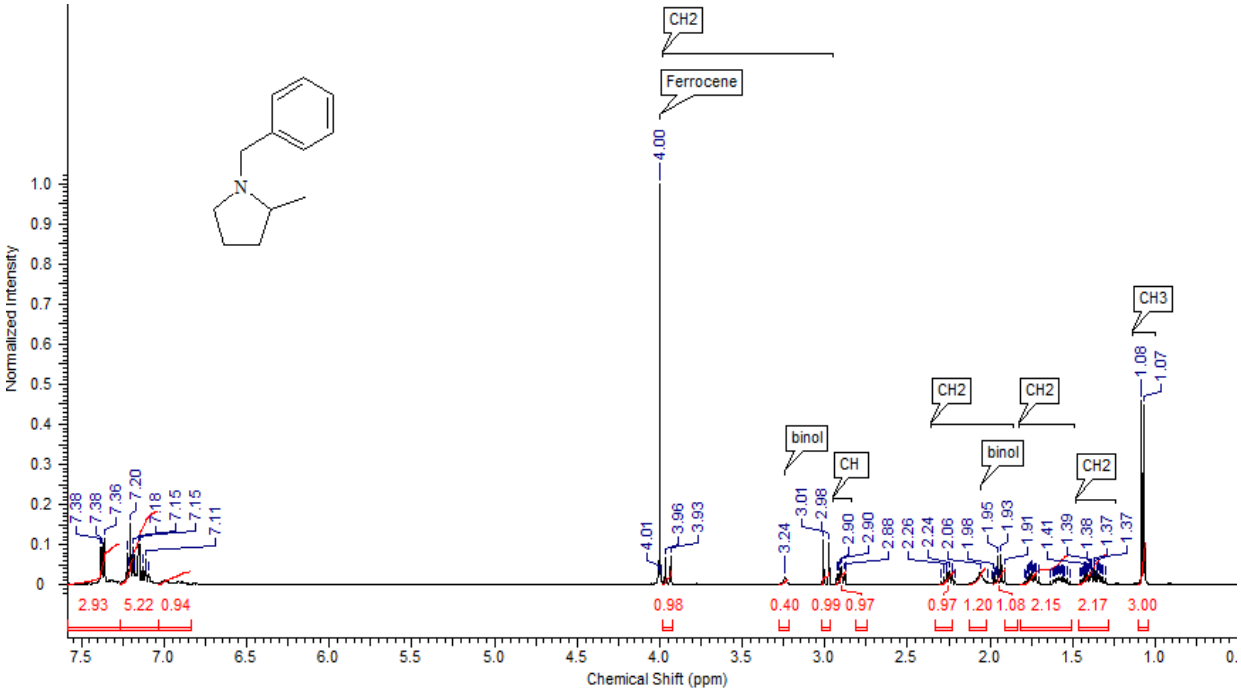

*Figure 48 – ^{1}H-NMR spectrum of 1-benzyl-2-methylpyrrolidine **(8)** in C_6D_6 at 25°C*

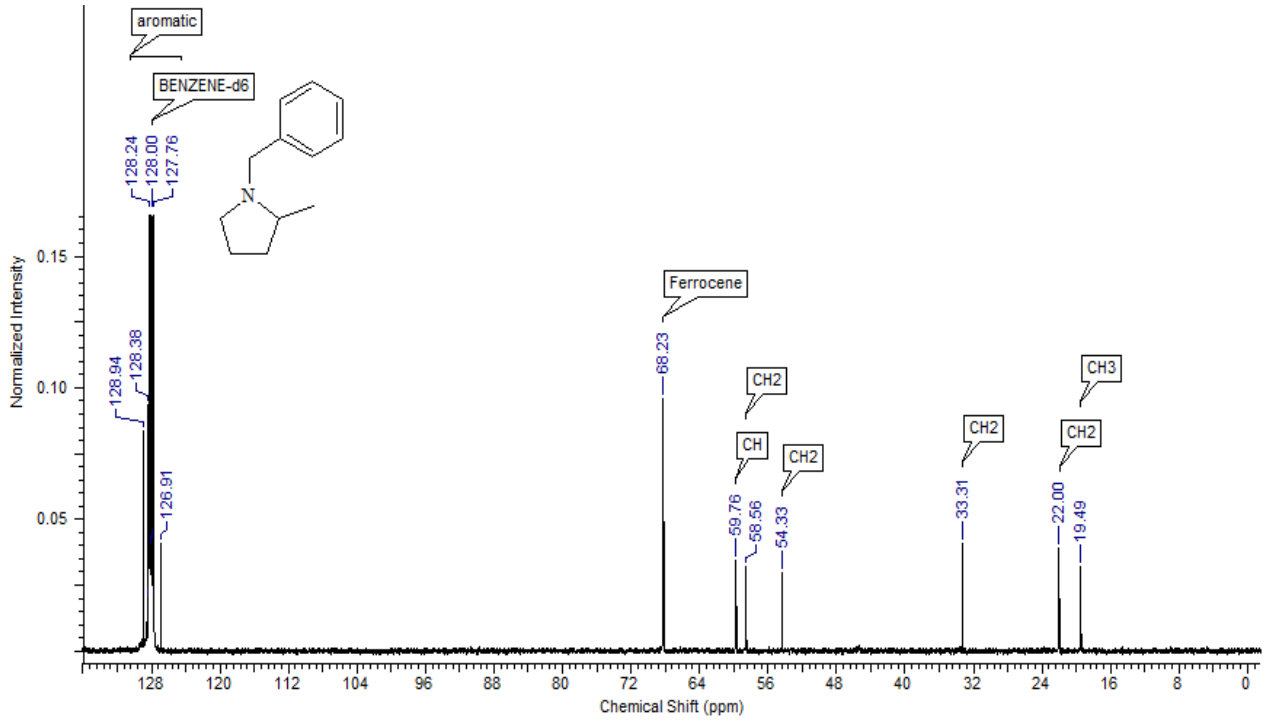

*Figure 49 – $^{13}C\{^{1}H\}$-NMR spectrum of 1-benzyl-2-methylpyrrolidine **(8)** in C_6D_6 at 25°C*

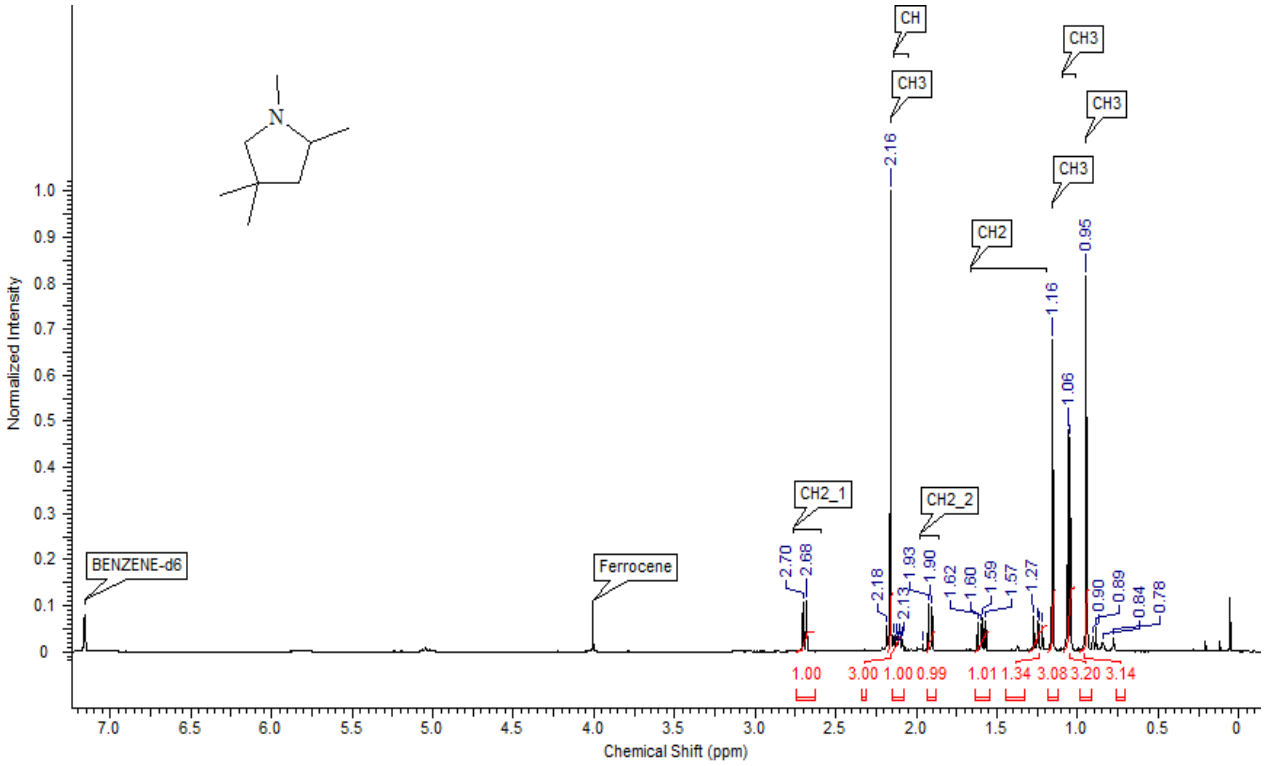

*Figure 50 – ^{1}H-NMR spectrum of 1,2,4,4-tetramethylpyrrolidine (**9**) in C_6D_6 at 25°C*

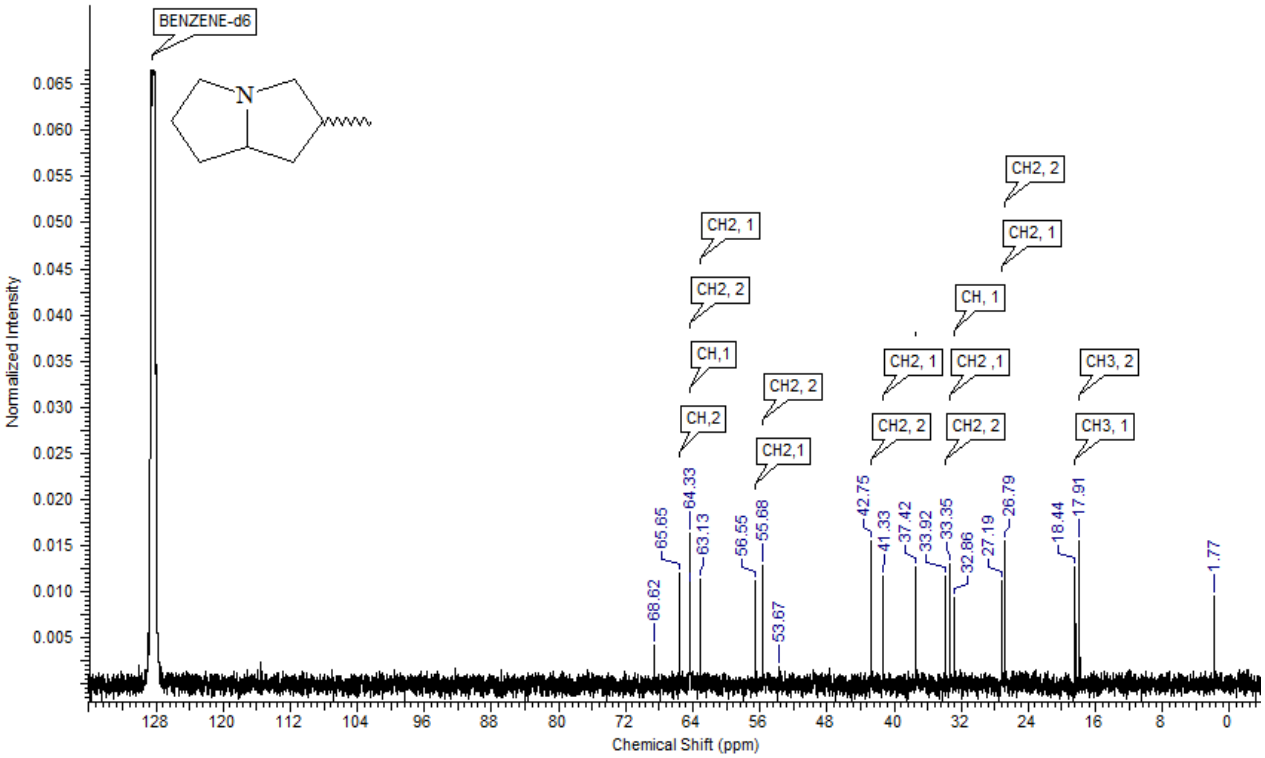

*Figure 51 – $^{13}C\{^{1}H\}$-NMR spectrum of 2-methylhexahydro-1H-pyrrolizine (**10**) in C_6D_6 at 25°C*

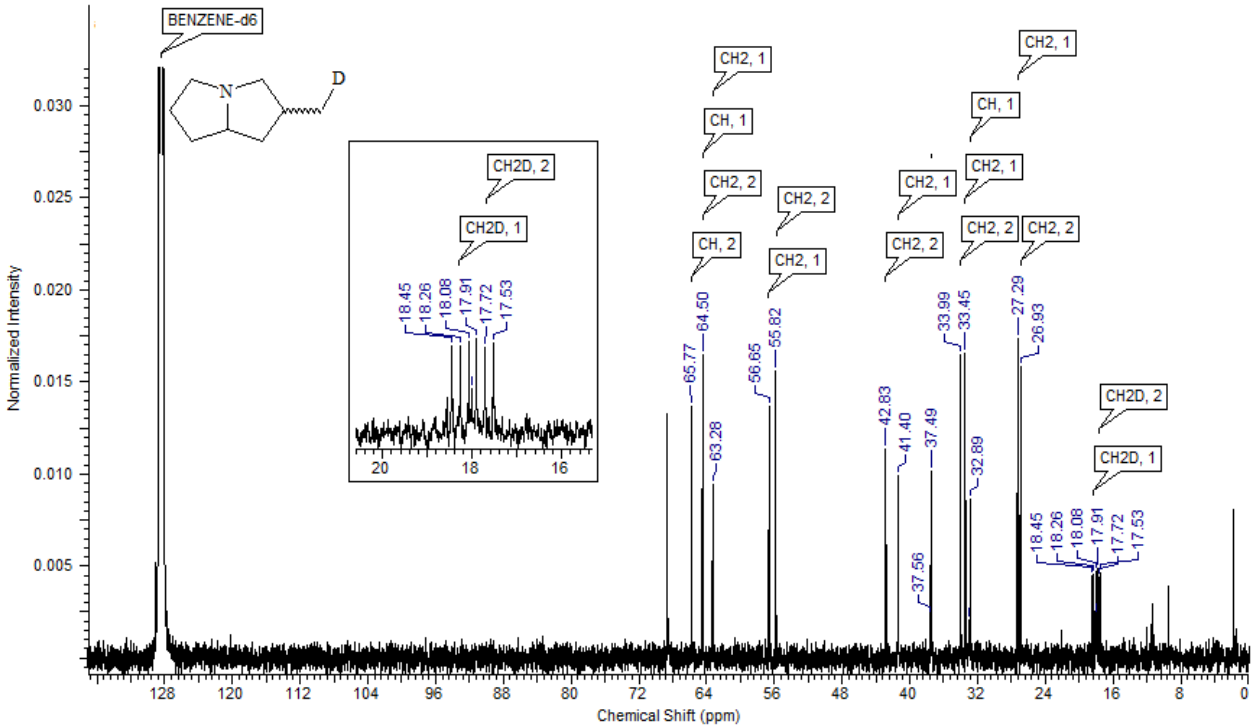

*Figure 52 – $^{13}C\{^{1}H\}$-NMR spectrum of 2-(methyl-d)hexahydro-1H-pyrrolizine (**10-d**) in C_6D_6 at 25°C*

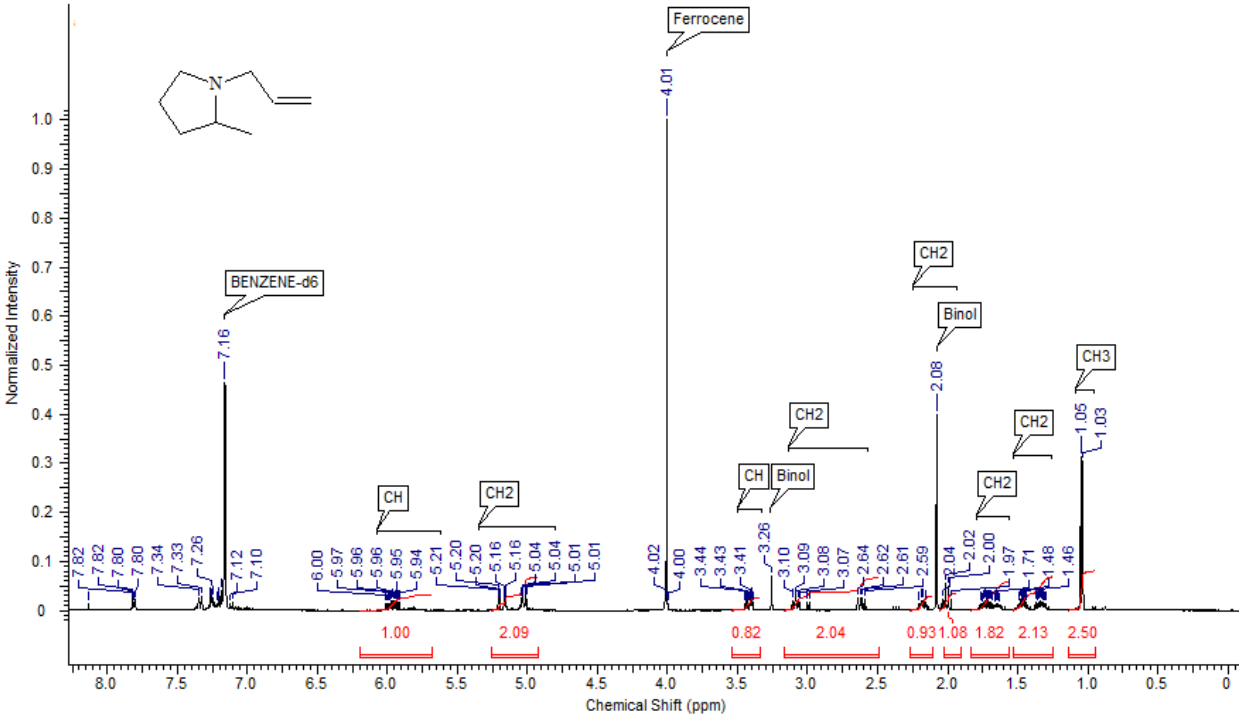

*Figure 53 – ^{1}H-NMR spectrum of 1-allyl-2-methylpyrrolidine (**11**) in C_6D_6 at 25°C*

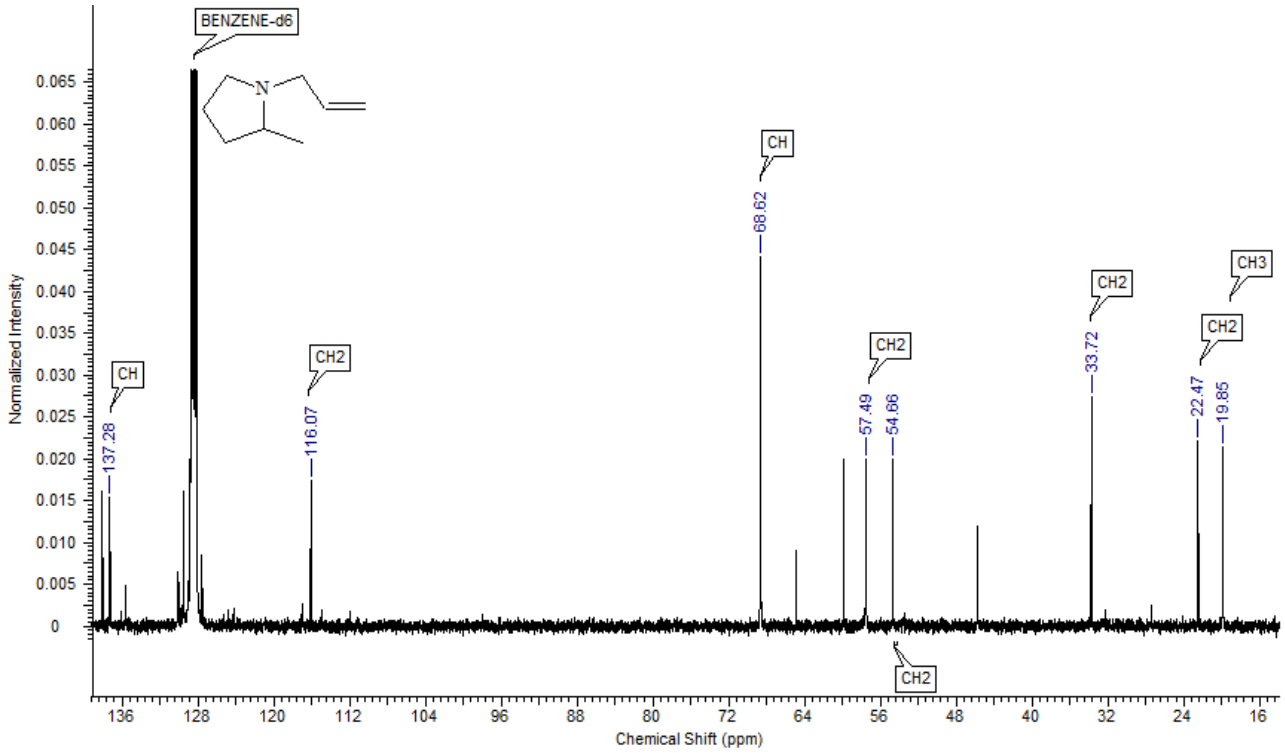

*Figure 54 – $^{13}C\{^{1}H\}$-NMR spectrum of 1-allyl-2-methylpyrrolidine (**11**) in C_6D_6 at 25°C*

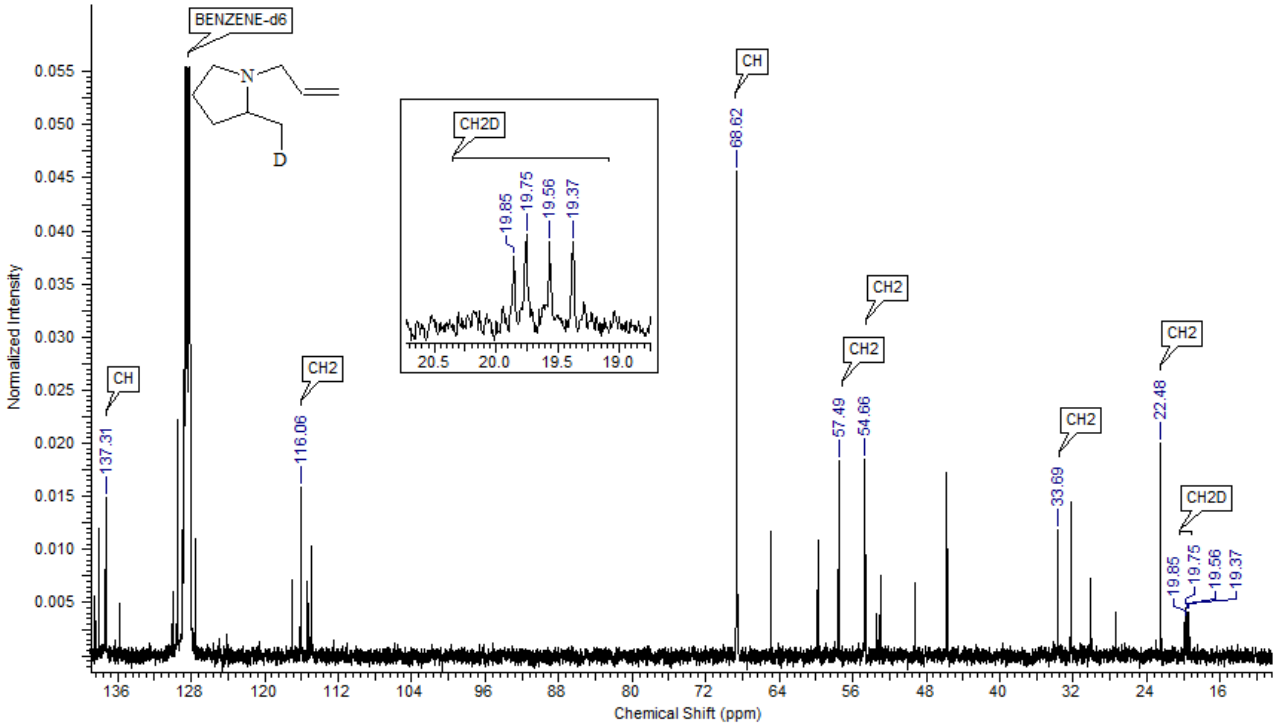

*Figure 55 – $^{13}C\{^{1}H\}$-NMR spectrum of 1-allyl-2-(methyl-d)pyrrolidine (**11-d**) in C_6D_6 at 25°C*